UNIVERSITY OF OKLAHOMA

GRADUATE COLLEGE

PRODUCTION-INDUCED CHANGES IN RESERVOIR GEOMECHANICS

A DISSERTATION

SUBMITTED TO THE GRADUATE FACULTY

in partial fulfillment of the requirements for the

Degree of

DOCTOR OF PHILOSOPHY

By

SUNDAY O. AMOYEDO
Norman, Oklahoma
2011

PRODUCTION-INDUCED CHANGES IN RESERVOIR GEOMECHANICS

A DISSERTATION APPROVED FOR THE
CONOCOPHILLIPS SCHOOL OF GEOLOGY & GEOPHYSICS

BY

_____
Dr. Roger M. Slatt, Chair

_____
Dr. Kurt J. Marfurt

_____
Dr. Shankar Mitra

_____
Dr. Deepak Devegowda

_____
Ms Martha Barnes

DEDICATION

This dissertation is dedicated to my wife Ms. Olamide O. Falade and my late brother Mr. Funsho M. Amoyedo.

ACKNOWLEDGMENTS

I wish to tender my profound gratitude to the authorities of the University of Oklahoma, ConocoPhillips School of Geology & Geophysics and the Graduate College for the opportunity given me to pass through this great institution. It's an opportunity of a life time and I am most grateful.

I am highly indebted to Dr. Roger M. Slatt and Dr. Kurt J. Marfurt for their unwavering support, supervision and guidance while this program lasted. Despite their very tight schedules, they still make time to meet students one on one. I wonder how they manage their schedules. I couldn't have asked for more from these two great supervisors. I am eternally grateful to them.

My profound appreciation also goes to other committee members- Dr. Mitra Shankar (ConocoPhillips School of Geology and Geophysics), Dr. Deepak Devegowda (Mewbourne School of Petroleum Engineering) and Ms. Martha Barnes (Marathon Oil Corporation, Houston) for their support, opinion and advice on this thesis. I am very grateful for all their contributions.

Posterity will not hold me innocent if I fail to acknowledge the effort of other faculty members of ConocoPhillips School of Geology & Geophysics and Mewbourne School of Petroleum Engineering, from whom I have received instructions towards this degree. I have learned a lot from all of them and I am grateful.

I am also grateful to my family members both immediate and extended, who have contributed in one way or the other towards my academic success. My wife, Ms.

Olamide O. Falade, has been very supportive and understanding while this program lasted. I could not have asked for more from her. I appreciate your love and care. You are indeed my world!

I wish to thank the management of Apache North Sea Ltd. for releasing their dataset for this thesis. I am particularly grateful to Klaas Koster, Gregg Barker, Phil Rose, and Jack Orman, all of Apache North Sea for their tremendous support.

All the administrative staff of ConocoPhillips School of Geology and Geophysics have been wonderful. They were always there and ready to listen and advise. I am grateful to Adrianne Fox, Teresa Hackney, Nancy Leonard and Donna Mullins. You all are great! You made life a lot easier through your friendly smile and support. God bless you real good.

My academic counselor, Mr. Donald Rodgers, was very helpful and supportive as well. He always made time to meet me even when I failed to make a prior appointment as required. I am grateful Mr. Don!

I am eternally grateful to all my friends, who have contributed in one way or the other towards this program. I appreciate your support and friendship. To AASPI members (present and alumni) and sponsors I say thank you all. I also want to say thank you to all friends and colleagues at the Reservoir Characterization Institution, University of Oklahoma.

Finally, I am full of praise to my Maker and Sustainer- the Source of life and the ultimate Consciousness for His grace.

TABLE OF CONTENTS

LIST OF TABLES

LIST OF FIGURES

CHAPTER ONE

CHAPTER TWO

CHAPTER THREE

CHAPTER FOUR

CHAPTER FIVE

ABSTRACT

Sand production remains a source of concern in both conventional and heavy oil production. Porosity increase and changes in local stress magnitude, which often enhance permeability, have been associated with severe sanding. On the other hand, sand production has been linked to a large number of field incidences involving loss of well integrity, casing collapse and corrosion of down-hole systems. It also poses problems for separators and transport facilities. Numerous factors such as reservoir consolidation, well deviation angle through the reservoir, perforation size, grain size, capillary forces associated with water cut, flow rate and most importantly reservoir strain resulting from pore pressure depletion contribute to reservoir sanding. Understanding field-specific sand production patterns in mature fields and poorly consolidated reservoirs is vital in identifying sand-prone wells and guiding remedial activities. Reservoir strain analysis of Forties Field, located in the UK sector of the North Sea, shows that the magnitude of the production-induced strain, part of which is propagated to the base of the reservoir, is of the order of 0.2 %, which is significant enough to impact the geomechanical properties of the reservoir. Sand production analysis in the field shows that in addition to poor reservoir consolidation, a combined effect of repeated perforation, high well deviation, reservoir strain and high fluid flow rate have contributed significantly to reservoir sanding.

Knowledge of reservoir saturation variation is vital for in-fill well drilling, while information on reservoir stress variation provides a useful guide for sand production management, casing design, injector placement and production management. Interpreting time-lapse difference is enhanced by decomposing time-lapse difference

into saturation, pressure effects and changes in rock properties (e.g. porosity) especially in highly compacting reservoirs. Analyzing the stress and saturation sensitivity of the reservoir and overburden shale of Forties Field, I observe that while pore pressure variations have not been significant in most parts of the field, a relatively higher decrease in pore pressure in a region of the reservoir has affected the geomechanical properties of both reservoir and overlying rock strata . I found that strain development in the field accounts, in part, for increased reservoir sand production and a negative velocity change in the overburden, which provides an indication of dilation. I use changes in the AVO intercept and gradient calibrated with laboratory measurements to decouple the time-lapse (4D) difference into saturation and pressure changes. Furthermore, I propose a new modification to time-lapse AVO inversion workflows to account for the effect of porosity change in measurements of time-lapse difference. This is particularly crucial in highly-compacting chalk and poorly consolidated clastic reservoirs.

Rock-physics-driven inversion of 3D pre-stack seismic data plays a prominent role in the characterization of both reservoir and overburden rocks. Understanding the rock physics of the overburden rock is required for efficient production of the reservoir and to safeguard wellbore, down-hole assembly and supporting surface facilities. Taking Forties Field as a case study, I observe that while instability and subsequent failure of the overburden in the field can be linked to the rapid decrease of the unconfined compressive strength (UCS) at inclinations close to 45 degrees to the bedding plan, some zones in the overburden are characterized by extreme weakness regardless of the well angle through the rock. I use the correlation between unconfined

compressive strength and elastic moduli (Young's and Bulk moduli), coupled with the results of simultaneous inversion to derive 3D elastic moduli, calibrated to laboratory measurements, to characterize the zones of extreme weakness.

Time-lapse gravimetry continues to find increasing application in reservoir monitoring, typically in gas reservoirs and reservoirs used for CO_2 sequestration. There is little or no application yet in oil-bearing reservoir monitoring, due in part to the low density contrast between oil and brine and the high acquisition cost associated with the required survey grid closely spaced. In this study, I model the 4D gravity anomaly over Forties Field. Forties Field 4D gravity model results show that a significant increase in water saturation (10-15%) is required to produce a resolvable 4D gravity anomaly. I observe that time-lapse gravity anomalies can provide vital clues to reservoir compartmentalization and by-passed oil when the saturation change is on the order of 10% or more. Reservoir subsidence can also give rise to a significant 4D gravimetric anomaly. I observe a decreasing resolution of such compaction anomalies as water saturation increases.

CHAPTER ONE

1.0 INTRODUCTION

1.1 TIME-LAPSE (4D) SEISMIC: LITERATURE REVIEW AND STATE OF THE ART

The need to optimize production and recover as much oil as possible from producing reservoirs has given rise to time-lapse (4D) seismic, one of several techniques for reservoir monitoring. Other commonly adopted reservoir monitoring technologies include: borehole surveillance, micro-seismicity, vertical seismic profiling (VSP), natural fields (gravimetry and electromagnetic) and wired fields (permanent sensors). Field economics, geology and suitability are some of the deciding factors in the selection of the monitoring technique (s). First used in the late 1990s, time-lapse seismic has quickly become the technique of choice.

The general working principle of time-lapse seismic has been known for quite some time with a number of projects being carried out each year and reported in the literature. The importance and relevance of 4D seismic varies from identifying by-passed oil to gaining a better understanding of the reservoir (as well as the surrounding non-reservoir) properties and responses to depletion (Anderson et al., 1998; Meadows, 2008; Tura and Etuk, 2006; Hawkins et al., 2007; Robinson, et al., 2005; Weisenborn and Hague 2005, etc).

Various methodologies and workflows have been implemented in different 4D seismic studies with varying degrees of success. Such procedures emphasize feasibility and repeatability in acquisition and processing for effective monitoring and interpretation. The normalized root mean square, (NRMS), which serves an index of repeatability between any two traces *b(t)* and *a(t)* within a time interval t_1 and t_2, is defined as :

$$NRMS = \frac{2 * \sqrt{[\sum_{t1}^{t2} \{(b(t) - a(t)\}^2]}}{\sqrt{[\sum_{t1}^{t2} (b(t))^2]} + \sqrt{[\sum_{t1}^{t2} (a(t))^2]}}. \quad (1)$$

Repeatability in seismic acquisition and processing and the management of the associated cost remain the sticking points in many repeat surveys, hampering successful implementation and interpretation of 4D data.

Amplitude and impedance differences between two consecutive surveys are the most commonly used attributes for 4D seismic interpretation, though several authors have reported successful use of other subtle attributes such as time-lapse (Δt), AVO attributes and self organizing waveforms. A critical component of any time-lapse study is rock physics. Detailed analysis of reservoir rock behavior is crucial to the feasibility and interpretation of time-lapse seismic.

Over the years, various authors have published the results of time-lapse seismic studies conducted in producing reservoirs around the world.

In one of the earliest time-lapse seismic case studies which was carried out over the South Timbalier 295 Field in the Gulf of Mexico, Anderson et al., (1998) used temporal changes in amplitude to identify by-passed oil and to establish sand connectivity in the

reservoir. Their workflow emphasized the importance of coupled time-lapse studies and calibrated reservoir simulation. In the same year, Johnston et al., (1998) discussed the use of time-lapse changes in acoustic impedance between 1977 and 1992 as an indication of fluid substitution in Fulmar Field, which is located in the central North Sea. The authors concluded that time-lapse seismic plays a pivotal role in guiding reservoir management decisions.

Koster et al., (2000) highlighted the importance of repeatability, modeling, history matching, uncertainty handling and the impact of reservoir depletion methods on 4D studies. Koster et al., (2000) further discussed the business impact of time-lapse and the decision-making process involved. In another publication, Fanchi (2001) showed that an integrated flow model in forward modeling of time-lapse differences helps greatly in feasibility study for reservoir monitoring and measuring sweep efficiency. Huang (2001) emphasized the role of production data coupled with time-lapse seismic in making reservoir engineering decisions.

Lumley (2001) undertook a comprehensive analysis of 4D seismic, providing a general overview of the concept as well as laying out the current workflow and predicting the road ahead. The paper gave a summary description of the 4D effect observed in the reservoir and also evaluated the potential of time-lapse seismic technology for monitoring fluid and pressure changes in Fulmar Field reservoir, located in the North Sea. Lumley (2001) further holds that with the current pace of development of permanent reservoir monitoring, time-lapse may eventually give way to micro-seismic. While micro-seismic studies continue to play a vital role in reservoir monitoring, its deployment is still limited to conventional offshore terrains and shale plays as technical

difficulties and the associated cost remain unmanageable for ultra-deep offshore reservoirs.

Olden et al., (2001) used modeling and synthetic datasets to understand the combined effect of stress and fluid changes in a producing reservoir. The paper concluded that extending modeling to a full-field 3D reservoir simulation model would lead to the possibility of directly comparing the stress sensitive simulator response with an actual time-lapse seismic survey. In the same year, Landro (2001) put forward a quantitative workflow to decouple time-lapse difference in pressure and saturation effects by combining amplitude variation with offset (AVO) attributes with laboratory measurements. The paper also demonstrated the workflow using the Magnus 4D datasets. This workflow was adopted for pore pressure detection sensitivities in Gullfaks Field by Kvam and Landro (2001).

In one of the classic papers on production-induced reservoir strain, Hatchel and Bourne (2005) implemented a workflow for seismic-derived reservoir strain. This methodology involves the use of the time shift (Δt) and the rate of change of velocity with porosity. The authors introduced the concept of the *'R'* factor, which relates the time strain ($\Delta t/t$) to reservoir uniaxial strain (ε_{zz}). For poorly consolidated rocks, the factor, *R* is expected to be less than 1.0 both in the reservoir and overburden. It must be emphasized that the formulations in their paper assumed that porosity does not change significantly during depletion, which might not hold for highly compacting reservoirs like chalks or over-pressured sands.

Several other authors have focused on predicting time-lapse stress effects using coupled geomechanical modeling (Herwangler and Horne, 2005; Sen and Settary, 2005; Dusseault et al., 2007; Staples et al., 2007; Minkoff et al., 2006).

Hodgson et al., (2007) presented another method for inverting reservoir pressure change using time strain ($\Delta t/t$) based on linear elasticity theory. The authors showed that the vertical component of the strain tensor can be written as:

$$\epsilon_{zz,M} = \sum_{n=1}^{N} \Delta p_n G_{n.M} = \Delta \mathbf{pG} \,, \tag{2}$$

where Δp is the unknown reservoir pressure and **G** is the Green's function computed to form a matrix of coefficients and M denotes the strain observation point.

Florich et al., (2005) provided another workflow to invert for both saturation and pressure changes, which involves the use of statistical analysis of depletion-sensitive seismic multi-attribute and training samples at well locations. The authors showed that the relative amplitude change of depletion-sensitive attributes is a combination of changes in saturation and pressure factors. They showed that for attributes 1....N, the coefficients C_s and C_p can be computed and used for inverting pressure and saturation changes at each training cell. This can be represented as:

For attribute 1:

$$\frac{\Delta A(x,y)}{A_b} \approx C_s \frac{\Delta S_o(x,y)}{S_{oi}} + C_p \frac{\Delta P(x,y)}{P_i} \,, \tag{3a}$$

attribute 2:

$$\frac{\Delta A'(x,y)}{A'_b} \approx C'_s \frac{\Delta S_o(x,y)}{S_{oi}} + C'_p \frac{\Delta P(x,y)}{P_i}, \quad (3b)$$

and attribute N:

$$\frac{\Delta A^n(x,y)}{A^n_b} \approx C^n_s \frac{\Delta S_o(x,y)}{S_{oi}} + C^n_p \frac{\Delta P(x,y)}{P_i}, \quad (3c)$$

where $\Delta A/A$ is relative amplitude change, while $\Delta S/S$ and $\Delta P/P$ are relative changes in saturation and pore pressure relatively. The coefficients C_s and C_p are estimated at the training cells. This workflow is strata-based and cannot be used for volumetric analysis. The procedure also assumes that time-lapse difference is induced by saturation and pressure changes only, without any changes in porosity.

Guilbot and Smith (2002) derived a 4D constrained depth method that uses time-lapse seismic measurements with a mode of reservoir compaction. The methodology accounts for velocity changes so that depth-converted seismic data and horizons give good estimates of reservoir subsidence and compaction.

Accompanying reservoir production is a decrease in pore pressure often leading to compaction in the reservoir. A significant amount of hydrocarbon production may be associated with compaction. However, instability in overburden, subsidence and local changes in stress state, which have negative effects on production, also accompany compaction. Highlighting production-induced compaction in Valhall Field, located in the Norwegian sector of the North Sea, Barkved and Kristiansen (2005), using multi-component seismic coupled with geomechanical modeling, showed that after more than 20 years of production, subsidence at the sea floor exceeded 5.4-m and increased by

about 0.25 m/yr. Landro and Stammeijer (2004) proposed workflows (near and far offset travel-time shifts and impedance changes) to estimate compaction and relative velocity change associated with increased reservoir stress. The authors showed that for NMO-corrected gathers relative change of velocity can be written as:

$$\frac{\Delta v}{v} = \frac{\frac{\Delta t_N}{t} - \frac{\Delta t_F}{t}}{tan^2\theta_F - tan^2\theta_N} \ , \qquad (4)$$

where $\Delta t_N \ and \ \Delta t_F$ represent the near and far stack travel time lags and θ_N and θ_F denote the incident angles for near far stacks.

Other authors that have focused on specific time-lapse effects in various fields include, but are not limited to, Robinson et al., (2005)- Chirac Field, Weisenborn and Hague (2005)- Gannet Field; Isaac and Lawton, (2006)- Cold Lake Canada; Tura et al., (2005)- Mars and Europa Fields. Weisenborn and Hague (2005) provided a general working principle as well as application of time-lapse seismic to well intervention programs. Robinson and Ford (2005) gave a review of the time-lapse studies conducted over Chirag Field in Apsheron Peninsula, Azerbaijan emphasizing the role of seismic acquisition and processing in effective time-lapse monitoring. They went further to report the elastic response to pressure change and fluid-front mapping from 4D seismic surveys. Rickett et al., (2007) reported some excellent 4D effects at Genesis Field. They described the concept of time strain in terms of reservoir compaction and how such a concept could be used to describe the geomechanical properties of the reservoir as well as predicting the effect of pressure changes from time strain.

Coupled simulation involving static field as well as geomechanical modeling is gradually becoming the standard petroleum industry procedure as the industry continues to deepen the knowledge of rock physics and geomechanics. Such simulations are usually focused on the reservoir section and less attention is paid to understanding the associated changes in geomechanical properties of the surrounding shale. This is especially true in the deep and ultra-deep reservoirs where available information is limited to the reservoir zone.

Time-lapse seismic continues to play a prominent role in reservoir monitoring while other technologies (such as 4D gravimetry, 4D electromagnetic, time-lapse refraction, borehole surveillance) continue to evolve. However, their application is still constrained by field economics, resolution and repeatability.

A recent innovative procedure developed by collaboration between Scripps Institute of Oceanography and Statoil Research Center has further advanced the use of gravimetric survey as a reservoir monitoring tool in the marine environment. The collaboration produced the world's first remotely operated marine gravimeter, which has been successfully deployed in Troll and Sleipner Fields, North Sea (Havard et al., 2008; Eiken et al., 2008; Zumberge et al., 2008).

A few other papers exist on the use of gravity anomalies for reservoir studies. Krahenbuhl et al., (2010) presented a multi-component feasibility study of the application of time-lapse gravity for CO_2 monitoring in Delhi Field. Model results show a strong likelihood of imaging bulk fluid movement though expected success may decrease significantly in the thinner, up-dip regions of the reservoir. Tempone and

Landro (2009) described a method for modeling 4D gravity anomaly changes for a reservoir undergoing compaction embedded in a homogenous half space with and without a rigid basement. They observed that compaction can account for as much as 30-40 μGal for a pressure depletion of 10 MPa. Stenvold et al., (2008) and Gettings et al., (2008), have also cited successes in the application of time-lapse gravimetry for reservoir monitoring.

1.2 SCOPE OF WORK AND PROBLEM DEFINITION

While all the authors mentioned above and many more have carried out a number of studies on providing the general working principle of 4D seismic, the role of rock physics and understanding the reservoir response to saturation and pressure changes, very little has been done to properly understand the response of the surrounding non-reservoir rocks (overburden and underburden) to pressure depletion and saturation change within the reservoir.

Few authors have recognized the need to understand the 4D effect on associated non-reservoir rocks. Sayers (2007) has called for a coupled understanding of both reservoir and non-reservoir responses in order to guarantee well stability and the safety of supporting surface facilities. Many of the unexpected problems encountered in the latter part of field development (sand production, overburden and well bore instability) could be traced back to a lack of proper understanding of the responses of the reservoir and overlying sediments to production effects. This knowledge gap is particularly pronounced in the ultra deep offshore environment.

This study is designed to better understand the dynamics of interaction between the reservoir and the surrounding shale. Overburden instability, occasioned by strongly varying shale fabrics, continues to account for a large number of drilling and well completion failures, especially in deepwater and poorly consolidated environments. This study will attempt to characterize overburden elastic properties and identify potentially unstable overburden using simultaneous inversion results.

There are varying degrees of in-fill well drilling problems in a depleting reservoir due to a change in reservoir stress state associated with pressure depletion and saturation change. Such difficulties are in some ways related to changes in geomechanical properties. This study investigates the link between the changing stress regime and observed drilling problems, and more importantly show how such difficulties could be predicted before selecting the location of in-fill wells. Most reservoir compaction analyses are carried out only when instability is seen to endanger the producing wells and/or the supporting surface facility. The Ekofisk, Willmington, Dan and Valhall Fields readily come to mind as typical examples. For example, remedial activities cost over $1b in the case of Ekofisk apart from lost time. As such, early detection and monitoring using time-lapse seismic coupled with well information is crucial to forestall such occurrences.

Repeatability and data balancing are crucial to successful 4D seismic reservoir monitoring. The questions remain- How repeatable are seismic surveys and what degree of repeatability is acceptable? The challenge is not only technical, with field size and production economics playing equally vital roles. Can we afford to embark on special processing and balancing of surveys when the field is barely economical? How do we handle physical structures like platforms and storage facilities already installed when embarking on a repeat survey? All these and many more issues make repeatability an eternal challenge. This study will implement a workflow to address the repeatability challenge.

Sand production remains a source of concern in both conventional and heavy oil production. Porosity increase and changes in local stress magnitude, which often

enhance permeability, have been associated with severe sanding. On the other hand, sand production has been linked to a large number of field incidences involving loss of well integrity, casing collapse and corrosion of down-hole systems. It also poses problems for separators and transport facilities. Numerous factors such as reservoir consolidation, well deviation angle through the reservoir, perforation size, grain size, capillary forces associated with water cut, flow rate and most importantly reservoir strain resulting from pore pressure depletion contribute to reservoir sanding. Understanding field-specific sand production patterns in mature fields and poorly consolidated reservoirs is vital in identifying sand-prone wells and guiding remedial activities.

Knowledge of reservoir saturation variation is vital for in-fill well drilling, while information on reservoir stress variation provides a useful guide for sand production management, casing design and injector placement. Understanding reservoir response to increase in stress and our ability to effectively use time-lapse seismic as a reservoir pressure monitoring tool derive from rock sensitivity to water saturation and pressure changes. Interpreting time-lapse differences is enhanced by discriminating between saturation and pressure effects. Decoupling time-lapse (4D) measurements into saturation and pressure effects, calibrated by well and production data, provides an additional reservoir monitoring tool. This thesis will decouples pressure and saturation changes in time-lapse differences, using changes in AVO attributes (intercept and gradient) coupled with laboratory measurements of stress sensitivity and fluid substitution models.

1.3 AIMS AND OBJECTIVES

Principal objectives of this dissertation include:

- Investigating sand production patterns in high-sand producing wells with the aim of identifying contributing factors as well as a possible link between time-lapse effects and reservoir sand production. This objective involved the computation of reservoir uniaxial strain and a detailed analysis of sand production pattern to identify other factors, in addition to more well documented factors such as grain size and perforation damage. The Forties Field, located in the UK sector of the North Sea was used as a case study.

- Simultaneously inverting for reservoir pressure and saturation changes using the Forties Field 2000 and 2005 seismic surveys. The inversion workflow involved the use of the Landro (2001) AVO attributes method coupled with laboratory measurements on core samples. The formulations were modified to account for the effect of porosity change, which could be dominant in some highly compacting reservoirs such as the Ekofisk chalk reservoir.

- Predicting overburden strength/weakness using 3D simultaneous inversion results. A case study from the Forties Field was done, where over 65% of recent wells have experienced some form of instability in the overburden associated with strongly varying and unpredictable fabrics of shale. Characterizing the overburden fabrics helped identify the zones of extreme weakness and provided a better guide for in-fill well drilling through weak zones. The workflow involved the simultaneous inversion of

reservoir and overburden elastic properties calibrated with well log and laboratory measurements.

- Forward modeling of time-lapse gravimetry signatures of an oil bearing reservoir undergoing compaction and fluid substitution. Modeling sensitivity include compaction, porosity and saturation changes.

1.4 EXPECTED CONTRIBUTION

The study will:

- Guide the understanding of field-specific sand production pattern, to help identify high-sand prone wells, thus reducing production cost (new well, clean up) and sustained production in the field and reduction in well shut-in incidences

- The study amends Landro's (2001) pressure and saturation inversion workflow to account for the effect of porosity, which could be significant in highly compacting reservoirs (chalks and other carbonates).

- Demonstrates the use of seismic-derived reservoir and non-reservoir geomechanical properties to characterize weak zones, which often account for instability and drilling failures in poorly consolidated environments.

- The study promotes the use of time-lapse gravimetry in reservoir monitoring. Forward modeling of 4D gravity anomaly provided a feasibility study for deployment of gravimetry for monitoring oil bearing reservoirs as well as possible deployment for monitoring compaction and subsidence in reservoirs.

1.5 LOCATION AND BASIC STRATIGRAPHY OF STUDY AREA

Forties Field, which is one of the early mega-fields discovered in the UK sector of the North Sea, lies approximately 120 miles north-east of Aberdeen, Scotland (Figure 1). The field was discovered in 1970 by BP with stock tank original oil in place (STOOIP) estimated at over 5 billion barrels according to recent updates. Daily production, which peaked at about 500 M barrel of oil per day (bopd) before decreasing to less than 100 M bopd, is supported mainly by water injection. About 2.6 billion barrels have been produced to date and daily production is expected to increase significantly over the next couple of years from in-fill drilling campaigns.

Forties Field reservoir comprises Late Paleocene submarine fan sands, muds and shale. The 100 to 200 m thick Forties sandstone can be divided into three units of roughly equal thickness. The initial fan advance is represented by the lowest unit, the Lower Main Sand, with the overlying Upper Main Sand being deposited as a fairly broad channel complex. Both units extend across the whole field and they have not been further subdivided. The topmost unit, the Channel Complex, consists of three major sandy channel systems, the Delta/Echo, Bravo and Alpha in order of decreasing age, together with areas of inter-channel mudstone (Thomas et al., 1974). The Charlie sand is considered a distinct unit separated from the older sands by the Charlie Shale (Figure 2 and Figure 3).

The Forties fans and channel complexes are generally very friable and characterized by excellent reservoir properties. Porosity runs as high as 35% while permeability is in the range of a few Darcys. The high recovery factor, in excess of 45%, recorded in the field

bears testimony to the excellent reservoir properties. Over 340 wells have been drilled (Figure 4), comprising 240 producers and 100 injectors since the commencement of field development. While a good number of these wells have been abandoned, some have continued to produce.

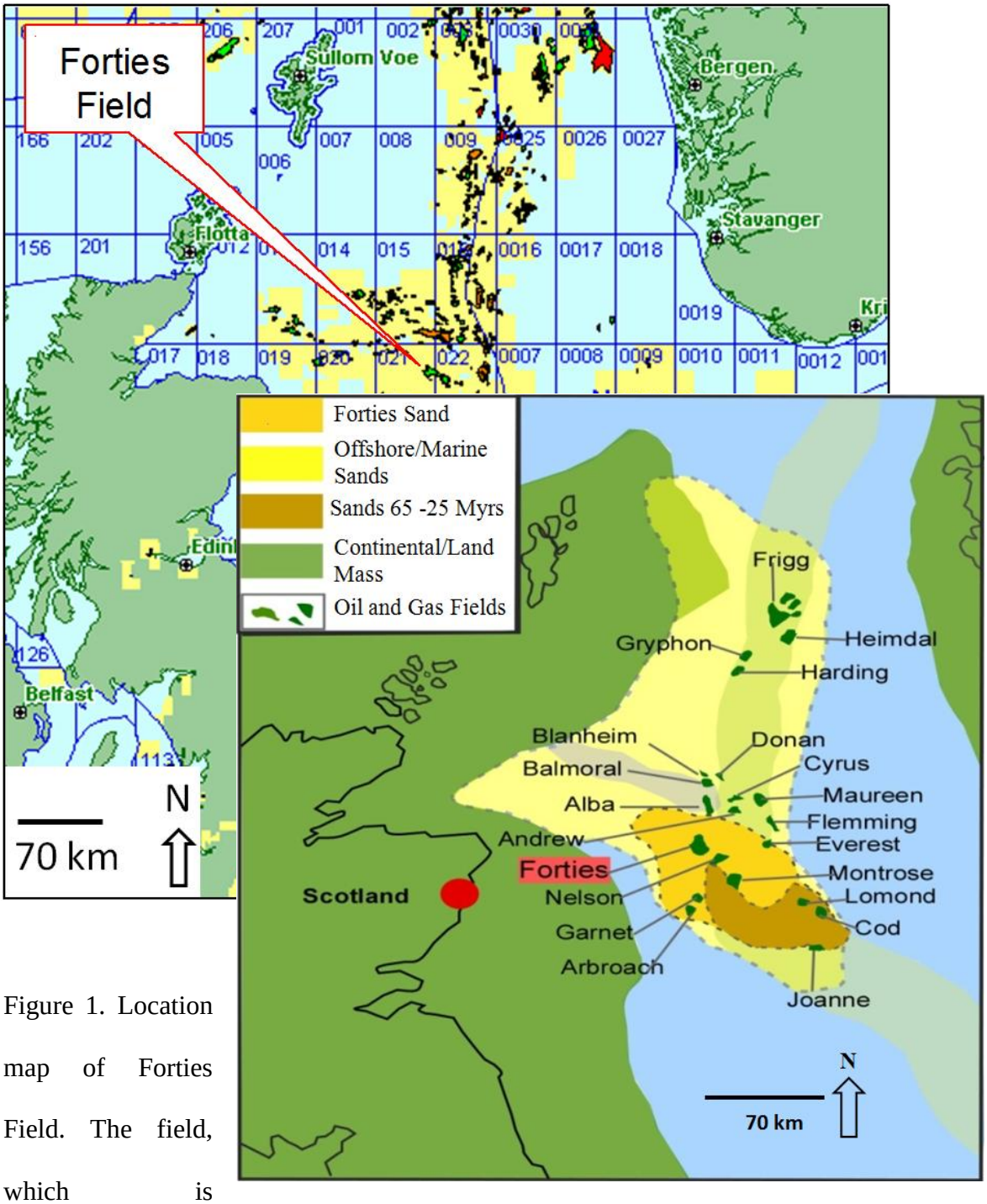

Figure 1. Location map of Forties Field. The field, which is approximately 120 miles NE of Aberdeen, Scotland, lies in the vicinity of other giant fields in the Central graben. Image is modified from an internal document of Apache North Sea Ltd.

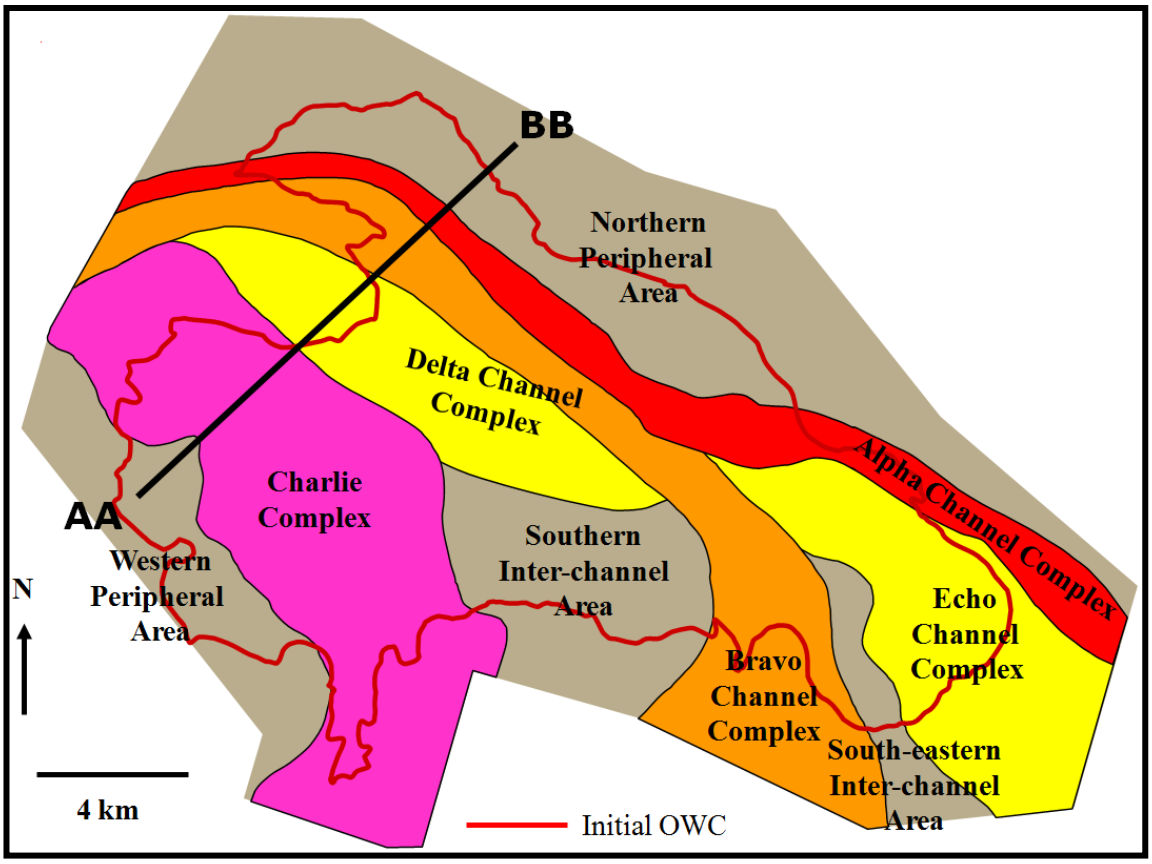

Figure 2. Schematic diagram of the various architectural elements comprising the Forties Field reservoir. Reservoir thickness varies between 200 and 300 m gross. While the other elements are inter-connected to various degrees, the Charlie complex is isolated. The cross section AA-BB on the map is shown on the litho-cube in Figure 3. Image is modified from an internal document of Apache North Sea Ltd.

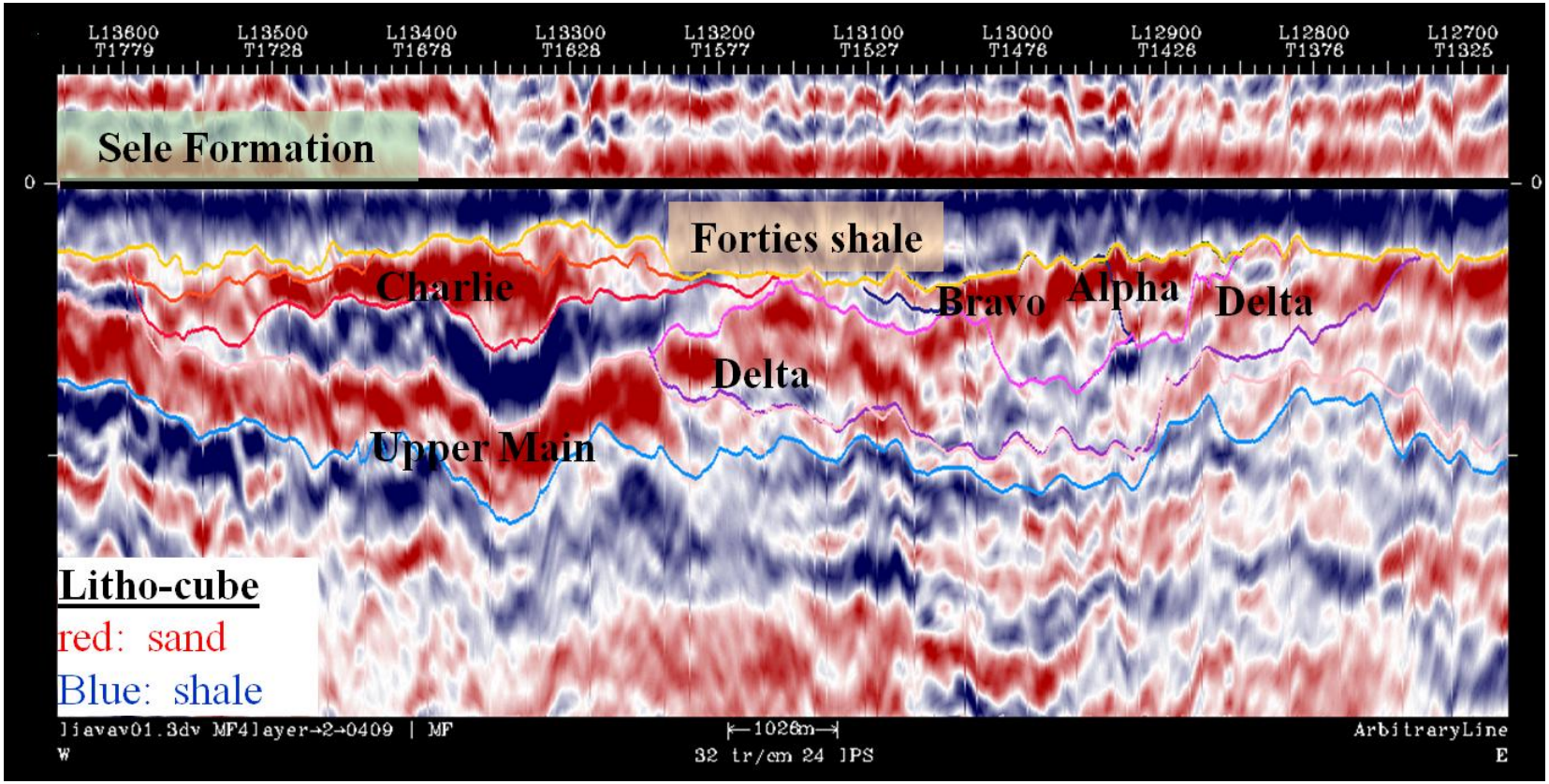

Figure 3. Forties Field cross section on a lithology-indicator volume. See Figure 2 for location. Image is modified from an internal document of Apache North Sea Ltd.

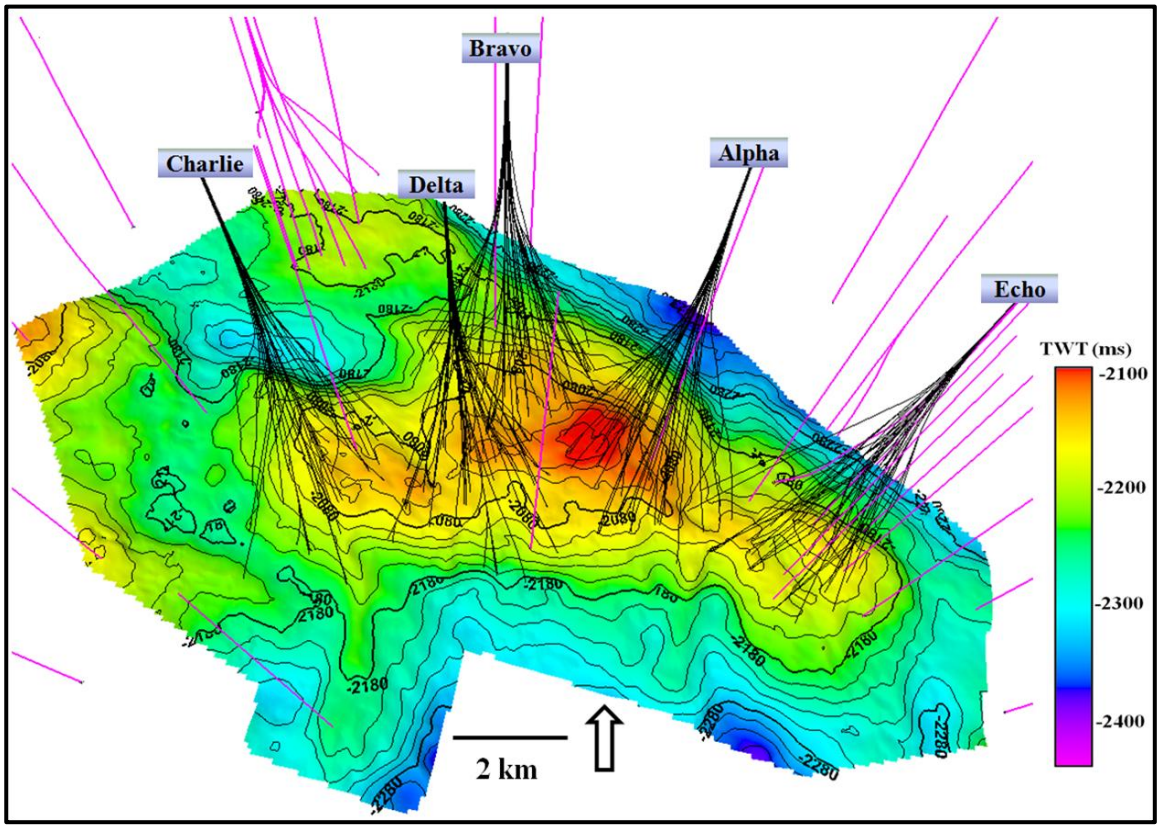

Figure 4. Time structure of the regional seal, Sele Formation, with the five production platforms, Alpha, Bravo, Charlie, Delta and Echo. In purple are the exploration wells.

REFERENCES

Anderson, N. R., G. Guerin, W. He, A. Boulanger, U. Mello, 1998, 4-D seismic reservoir simulation in a South Timbalier 295 tubidite reservoir: The Leading Edge, **17**, 1416-1417.

Barkved, O.I. and T. Kristiansen, 2005, Seismic time-lapse effects and stress changes: Examples from a compacting reservoir: The Leading Edge, **24**, 1244-1248.

Dusseault, M.B., S. Yin, L. Rothenburg, and H. Han, 2007, Seismic monitoring and geomechanics simulation: The Leading Edge, **26**, 610-620.

Eiken, O., T. Stenvold, M. Zumberge, H. Alnes, and G. Sasagawa, 2008, Gravimetric monitoring of gas production from the Troll Field: Geophysics, **73**, WA 149- 154.

Fanchi, J.R.; 2001, Time-lapse Seismic Monitoring in Reservoir Management: The Leading Edge, **20**, 1140 - 1147.

Gettings, P., D.S. Chapman, and R. Allis, 2008, Techniques, analysis and noise in a Salt Lake Valley 4D gravity experiment: Geophysics, **73**, WA 71-81.

Guilbot, J. and B. Smith, 2002, 4D constrained depth conversion for reservoir compaction estimation: Application to Ekofisk Field: The Leading Edge, **21**, 302-308.

Hatchel, P. and S. Bourne, 2005, Rocks under strain: Strain-induced time-lapse time shifts are observed from depleting reservoirs: The Leading Edge, **24**, 1222-1225.

Havard, A., O. Eiken and T. Stenvold, 2008, Monitoring gas production and CO2 injection at the Sleipner Field using time-lapse gravimetry: Geophysics, **73**, WA 155-161.

Hawkins, K., S Howe, S. Hollingworth, G. Conroy, L. Ben-Brahim, C. Tindle, N. Taylor, G. Joffroy and A. Onaisi, 2007, Production-Induced Stresses from time-lapse time shifts: A Geomechanics Case study from Franklin and Elgin Fields: The Leading Edge, **26**, 655-662.

Herwangler, J., S. Horne, 2005, Predicting time-lapse stress effects in seismic data: The Leading Edge, **24**, 1234-1242.

Huang, X., 2001, Integrating time-lapse seismic with production data: A tool for reservoir engineering: The Leading Edge, **20**, 1148-1153.

Hodgson, N., C. Macbeth, L. Ducanti, J. Rickett and K. Nihei, 2007, Inverting for reservoir pressure change using time-lapse time strain: Application to Genesis Field, Gulf of Mexico: The Leading Edge, **26**, 649- 652.

Isaac, J.H and D.C. Lawton, 2006, A case history of time-lapse 3D seismic surveys at Cold lake, Alberta, Canada: Geophysics, **71**, B93-B99.

Johnston, D. H., R.S. McKenny, J. Verbeek and J. Almond, 1998, Time-lapse seismic analysis of Fulmar Field: The Leading Edge, **17**, 1420-1428.

Koster, K, P. Gabriels, M. Hartung, J. Verbeek, G. Deinum and R. Staples, 2000, Time-lapse seismic surveys in the North Sea and their business impact: The Leading Edge, **20**, 283-293.

Krahenbuhl, R. A., Y. Li, and T. Davis, 2010, 4D gravity monitoring of fluid movement at Delhi Field, LA; A feasibility study with seismic and well data: Annual International Meeting, SEG Expanded Abstract, **30**, 4210-4214.

Kvam, O. and M. Landro, 2005, Pore-pressure detection sensitivities tested with time-lapse seismic data: Geophysics, **70**, O39-O50.

Landro, M. 2001, Discrimination between pressure and fluid saturation changes from time-lapse seismic data: Geophysics, **66**, 836-844.

Landro, M. and J. Stammeijer, 2004, Quantitative estimation of compaction and velocity changes using 4D impedance and travel-time changes: Geophysics, **69**, 949-957.

Lumley, D. 2001, Time-lapse seismic reservoir monitoring: Geophysics, **66**, 50-53.

Florich, M., C. Macbeth and R. Staples, 2005, An engineering-driven approach for separating pressure and saturation using 4D seismic: Application to a Jurassic reservoir in the UK North Sea: Annual International Meeting, SEG Expanded Abstracts, **24**, 2464-2467.

Meadows, M., 2008, Time-Lapse Seismic Modeling and Inversion of Co2 saturation for storage & Enhanced oil recovery: The Leading Edge, **27**, 506-516.

Minkoff, S. E., C.M. Stone, S. Bryant and M. Peszynska, 2006, Coupled geomechanics and flow simulation for time-lapse seismic modeling: Geophysics, **26**, 200-2011.

Olden, P., P. Corbett, R. Wetserman, J. Somerville, B. Smart and N. Koutsabeloulis, 2001, Modeling combined fluid and stress change effects in the seismic response of a producing hydrocarbon reservoir: The Leading Edge, **20**, 1154-1163.

Rickett, J., L. Duranti, T. Hudson, B. Regel, N. Hodgson, 2007, 4D Time strain and the seismic signature of Geomechanical Compaction at Genesis: The Leading Edge, **26**, 644-647.

Robinson, N., A. Ford, D. Manley, M. Riviere, S. Stewart and R. Thomas, 2005, 4D time-lapse monitoring of Chirac Field: The Leading Edge, **24**, 928-932.

Sayers, C. M. and S. Chopra, 2007: Introduction to The Leading Edge Special Edition - Rock Physics, **27**, 15-16.

Sen, V., and A. Settari, 2005, Coupled geomechanical and flow modeling of compacting reservoirs: The Leading Edge, **24**, 1284-1286.

Staples, R., J. Ita, R. Burrell and R. Nash, 2007. Monitoring pressure depletion and improving geomechanical models of the Shearwater Field using 4D seismic: The Leading Edge, **26**, 636- 642.

Stenvold, T., O. Eiken and M. Landro, 2008, Gravimetric monitoring of gas-reservoir water influx- A combined flow- and gravity-modeling approach: Geophysics, **73**, WA 123-WA 131.

Tempone, P., and M. Landro, 2009, Estimation of changes in gravity anomaly due to a compacting reservoir: Annual International Meeting, SEG Expanded Abstract, **28**, 3790-3794.

Thomas, A.N., P.J. Walmsley, and D.A.L. Jenkins, 1974, Forties Field, North Sea: The American Association of Petroleum Geologists Bulletin, **58**, No. 3, 396-406.

Tura, A., T. Barker, P. Cattiermole, C. Collins, J. Davis, P. Hatchel, K. Koster, P. Schutjens and P. Wills, 2005, Monitoring primary depletion reservoirs using amplitudes and time shifts from high-repeat seismic surveys; The Leading Edge, **24**, 1214- 1221.

Tura, A. and U. Etuk, 2006, Time-Lapse Seismic for field development at Nembe creek, Nigeria: The Leading Edge, **26**, 1142-1149.

Weisenborn, T. and P. Hague, 2005, Time-lapse Seismic in Gannet A: One more lead firmly integrated, The Leading Edge, **24**, 80-85.

Zumberge, M., H. Aines, O. Eiken G. Sasagawa and T. Stenvold, 2008, Precision of seafloor gravity and pressure measurements for monitoring: Geophysics, **73**, WA 133-141.

CHAPTER TWO

2.0 TIME LAPSE EFFECT AND PATTERN OF SAND PRODUCTION

2.1 INTRODUCTION

Sand production remains a major challenge in reservoir production , especially in poorly -consolidated reservoirs and mature fields characterized by fine grains. The domain of investigation and analysis of sand production has been in production engineering and geomechanics, however, I have looked into the problem from a geophysical perspective.

In this chapter, I investigated reservoir strain (arising from changes in reservoir stress state) and wellbore deviation angle as major factors in sand production, in addition to well known causes. A case study is taken from the Forties Field, located in the UK sector of the North Sea.

This chapter has been published in the Leading Edge September, 2011 special edition on Time Lapse Seismic.

TIME-LAPSE (4D) EFFECT AND RESERVOIR SAND PRODUCTION PATTERN IN A MATURE NORTH SEA FIELD

Sunday Amoyedo, Roger M. Slatt and Kurt J. Marfurt, The University of Oklahoma, USA

ABSTRACT

Sand production remains a source of concern in both conventional and heavy oil production. Porosity increase and changes in local stress magnitude, which often enhances permeability, have been associated with severe sanding. On the other hand, sand production has been linked to a large number of field incidences involving loss of well integrity, casing collapse and corrosion of down-hole systems. It also poses problems for separators and transport facilities.

Numerous factors such as reservoir consolidation, well deviation angle through the reservoir, perforation size, grain size, capillary forces associated with water cut, flow rate and most importantly reservoir strain resulting from pore pressure depletion contribute to reservoir sanding. Understanding field-specific sand production patterns in mature fields and poorly consolidated reservoirs is vital in identifying sanding-prone wells and guiding remedial activities.

Reservoir strain analysis of Forties Field, located in the UK sector of the North Sea, shows that the magnitude of the production-induced strain, part of which is propagated to the base of the reservoir, is of the order of 0.2%, which is significant enough to impact the geomechanical properties of the reservoir. Sand production

analysis in the field shows that in addition to poor reservoir consolidation, a combined effect of repeated perforation, high well deviation, reservoir strain and high fluid flow rate have contributed significantly to reservoir sanding.

INTRODUCTION

Sand production is not uncommon in producing fields. Its severity, however, remains a growing concern in many mature fields and in deep-water reservoirs often characterized by poor consolidation. Reservoir sand production is simultaneously a source of concern and benefit in conventional and heavy oil production. Porosity increase and changes in local stress magnitude, which often enhances permeability, have been associated with severe sanding. On the other hand, sand production has been linked to a large number of field incidences involving loss of well integrity, casing collapse and corrosion of down-hole systems. It also poses problems for separators and transport facilities. The poorly consolidated Gudao reservoir in Shengli Oilfield, China provides a typical example of casing failure (Figure 1), resulting from severe reservoir sanding (Peng et al., 2007). Sand production-induced casing problems can vary from complete shearing to contortion of well casing depending on the severity of the sand flow.

Prominent among the causes of reservoir sanding include, among others; reservoir consolidation, well deviation through the reservoir, perforation size, depth of penetration, grain size, perforation-induced damages, capillary forces associated with water cut, flow rate and most importantly in Forties Field, (UK North Sea) reservoir

time-lapse strain resulting from pore pressure depletion. Substantial strains (> 0.2%) can be induced by the effective and shear stress changes on the reservoir rock. This strain is sufficient to severely degrade the reservoir grain cohesion by breaking the small amount of brittle grain-grain mineral cements, thereby reducing the sand strength (Zhang and Dusseault, 2004).

Papamichos et al., (2001) demonstrated, using a hollow cylindrical specimen, that cumulative sand production increases linearly with fluid flow rate and effective stress. Observing the mechanism and accounting for all possible factors of sand production in a producing reservoir is difficult in practice. The task becomes harder with poor availability of field records; most sand production records are typically incomplete, when they exist.

Reservoir monitoring for pressure, temperature and fluid production has long been a critical element of field exploitation to optimize hydrocarbon recovery. Time-lapse (also called 4D) seismic has joined borehole and production-based techniques in providing a measure of changes in the reservoir between the producer and injector wells. The importance and relevance of 4D seismic varies from identifying reservoir compartmentalization, monitoring fluid fronts and identifying by-passed oil (Anderson et al., 1998; Meadows, 2008; Tura and Etuk, 2006; Robinson et al., 2005; Weisenborn and Hague, 2005). Other applications include pressure monitoring, strain analysis and perturbation of local stress in the vicinity of the well (Sayers and Schutjens, 2007; Hatchell and Bourne, 2005). Time-lapse seismic requires consecutive seismic volumes to be conformable in data acquisition and processing. Most recent 3D seismic campaigns have repeatability inconsideration, right from the acquisition design stage for

use as a base survey for later acquisition. However, such foresight has not always been the case, such that the challenge remains how best to compare two seismic volumes that are not conformable in acquisition or processing in order to compute changes in reservoir properties induced by depletion.

In this paper, we investigate sand production patterns in several high-sand producing wells in Forties Field, UK. We search for contributing factors as well as a possible link between time-lapse effect and sand production/well failures. Forties Field, which lies in the UK sector of the North Sea, is located approximately 180 km NE of Aberdeen, Scotland. We observe that the magnitude of the production-induced strain, part of which is propagated to the base of the reservoir, is of the order on 0.2%, which is significant enough to induce the weakening of grain cohesion, thereby impacting the geomechanical properties of the reservoir (Zhang and Dusseault, 2004). Our analysis of sand production in the field shows that in addition to the well-known causes of sanding (e.g. poor reservoir consolidation, high well angle of deviation through the reservoir and high flow rate), reservoir strain resulting from pore pressure depletion, also contributes significantly to reservoir sand production in Forties Field.

PRODUCTION/PRESSURE HISTORY AND WELL FAILURES

The reservoir of the Forties Field comprises Late Paleocene submarine fan sands as well as mud and channel complexes. The 100 to 200 m thick Forties Sandstone can be divided into three units of roughly equal thickness. The initial fan advance is represented by the lowest unit, the Lower Main Sand, with the overlying Upper Main Sand being deposited as a fairly broad channel complex. Both units extend across the entire field and have not been further subdivided. The topmost unit, the Channel complex, which lies beneath a thick, monotonous section of gray to brown variably calcareous and carbonaceous upper Paleocene to Holocene mudstones (Thomas et al., 1974), consists of three major sandy channel systems- the Delta/Echo, Bravo and Alpha in order of decreasing age, together with areas of inter-channel mudstone. The youngest Charlie Sand is considered a distinct unit separated from the older sands by the Charlie Shale.

The Forties fans and channel complexes are generally very friable. Porosity runs as high as 35% and permeability is in the range of a few Darcys. The high recovery factor, which is in excess of 45%, bears testimony to the excellent reservoir porosity and permeability of the Forties Field reservoir. A more comprehensive description of field geology and stratigraphy is given by Thomas et al., (1974) and Hill and Wood (1980).

Significant targets in the deeper section of the field have been identified and are currently being evaluated. The field remains very productive and still commands a significant investment from the operator. Over 350 wells have been drilled in the field

since the commencement of exploration and field development in the 1970s. While a number of these wells have been abandoned, some have continued to produce for more than 15 years.

Forties Field cumulative production, which is supported by water injection, is in excess of 2.5 billion barrels. Reservoir pressure has been generally well-maintained field-wide, though steep decreases have been recorded in the Charlie sands causing a depletion-induced stress in the production zone, especially within the time interval being studied in this paper. Figure 2 shows pressure measurements for the Charlie reservoir from 1975 to 2009. The marked interval (1988-2000) represents the time interval between the seismic surveys.

Forties Field continues to produce through a comprehensive reservoir monitoring program. This concerted effort to keep the 'giant' alive has been faced with a series of difficult drilling, well-completion and severe sand production problems. These problems result in lost production and corrosion of materials. Where possible, remedial activities cost millions of dollars per annum and often lead to the loss of wells. These losses ultimately add to production cost. The unpredictable and strongly varying fabrics of shale types in the overburden also pose a major challenge during drilling in Forties Field, where over 65% of wells drilled between 2002 and 2007 have experienced some form of instability problem (McIntyre et al., 2009).

FORTIES TIME-LAPSE (4D) SURVEYS: DATA BALANCING AND QUALITY CONTROL

Various reservoir monitoring studies on Forties Field have been published by different authors targeted at identifying and developing by-passed potentials. Ribeiro et al., (2007) reported the time-lapse (4D) effect observed between 2000 and 2005 surveys. No previous studies however, have been reported on production-induced changes in reservoir geomechanics and how such changes, when coupled with well parameters, have contributed to sanding and multiple well failures in the field. This lack of comparison is in part due to the non-conformable seismic volumes available for that period. The first 3D seismic survey was acquired in 1988, using 25 x 25 m bins, after a production of about 1.8 billion barrels of oil (Figure 3). A further 600 million barrels of oil production separates the 1988 survey and the next 3D survey in 2000, which was acquired on a smaller 12.5 x 12.5 m bins, rotated 22^0 from the initial 1988 grid.

To achieve conformity between the 1988 survey and 2000 surveys we employ a workflow that included re-gridding, de-noising, and frequency/amplitude spectral balancing (Figures 4-6). Extensive quality control is necessary to avoid signal distortion from the use of shaping filters. A comparison of the spectra before and after the application of a shaping filter is shown in Figure 7.

The normalized root mean square (NRMS), serves an index of repeatability between any two traces $b(t)$ and $a(t)$ within a time interval t_1 and t_2, is defined as

$$NRMS = \frac{2 * \sqrt{[\sum_{t1}^{t2} \{(b(t) - a(t)\}^2]}}{\sqrt{[\sum_{t1}^{t2} (b(t))^2]} + \sqrt{[\sum_{t1}^{t2} (a(t))^2]}} \quad (1)$$

Although lower values of NRMS are desirable, the NRMS at 200 ms above the regional seal (the Sele Formation), was of the order of 0.30 (Figure 8), well within the typical threshold for more modern 4D surveys (Helgerud et al., 2009). A perfectly repeated survey should have a NRMS value of 0.0 for regions devoid of production effects. Factors including weather and other random noise, differences in processing artifacts due to differences in spatial sampling, acquisition footprint and physical obstructions such as drilling rigs and production platforms contribute to higher values of NRMS.

TIME-LAPSE EFFECTS AND RESERVOIR GEOMECHANICS

Not only does time-lapse seismic have applications in fluid front monitoring, delineating reservoir compartments, analyzing fluid migration pathways in CO_2 sequestration and heavy oil development, it has also become an important tool for monitoring reservoir stress changes and the accompanying strain. Time-lapse effects include changes in amplitude (reflectivity) as well as time lags between two surveys (Δt), which in turn can be due to changes in velocity (due to pressure, saturation and porosity changes), and reservoir strain, ε_{zz}, (due to stress increase and compaction).

We cross correlated the 1988 and 2000 surveys (after estimating and removing the background time shift) to compute the time lag between them. The background time

lag was estimated at a region immediately above the regional Sele shale, which we assumed to be the seal, devoid of production effects.

The time lag, $\Delta t = T_{2000} - T_{1988}$, at the top of the regional Sele seal ranges from about +7.0 ms above the Charlie sandstone to near 0.0 ms above other complexes, conforming to the production and pressure depletion profiles. The field pressure history shows that pressure depletion is higher in the Charlie sandstone, giving rise to the observed high time lag shown in Figure 9. A decrease in pore pressure leads to an increase in stress carried by the load-bearing rock frame of the reservoir, inducing compaction within the reservoir. This compaction may be accompanied by micro-scale deformation mechanisms such as cement breakage at grain contacts, grain sliding and rotation (Sayers and Schutjens, 2007). While the reservoir compacts and subsides, the overburden shale dilates in order to maintain stability. This compaction in the reservoir and dilation in the overburden, when significant, can give rise to geomechanical problems such as wellbore instability, severe sanding, subsidence, roof cracks, and ultimately the failure of the overburden.

Hatchell and Bourne (2005) showed that fractional changes in velocity occur in proportion to fractional changes in path length, *T*. Thus, the time strain for normal incidence P-waves can be written as:

$$\tau = \partial T / T = (1 + R)\varepsilon_{zz} \qquad (2)$$

where *R* defines the ratio of 4D fractional velocity changes to fractional thickness changes and ε_{zz} is the uniaxial strain. Hatchell and Bourne (2005) found that *R* lies in the range $4 < R < 8$ for rocks undergoing extension, whereas R lies in the range $0 < R <$

2 for rocks undergoing compaction (Sayers, 2010) . In Forties Field, R = 0.75 within the reservoir while R = 0.70 in the overburden. This range of values lies outside most reported figures. Such anomalous values could be due to the high porosity and the extremely weak frame characterizing the Forties reservoir and overburden shale, suggesting a good potential for grain-on-grain contact squeezing and dilation within the reservoir and overburden, respectively. Sayers (2010) suggested that sandstone sensitivity to stress cannot be explained solely by porosity reduction but also requires grain to grain squeeze, thereby altering the grain aspect ratio. The Charlie sands and Southern inter-channel area are observed to have high strain associated with increased stress, while the other areas have experienced minimal strain, conformable with field pressure history. The analysis also shows that stress increase is not confined to the top and within the reservoir, but is also propagated to the reservoir base inducing significant velocity change and potential instability (Figure 10).

SAND PRODUCTION PATTERN

Forties Field has been plagued by severe sand production and an array of drilling and completion problems. Severe sanding in this mature UK North Sea field often leads to loss of wells, reduced production, increased cost of production (associated with clean up, drilling of side-track wells and corrosion prevention). Understanding the field-specific sand production mechanism(s) and sanding pattern in Forties Field will go a long way in identifying vulnerable wells and guiding remedial actions. Incomplete sand production records and difficulty in eliminating transitional sanding due to

extraneous factors, such as work-overs, limit the amount of available data and reliability of sand production analysis.

While poor consolidation has contributed largely to sand production in the field, we observe that other factors such as multiple completion, high well deviation angle, flow rate and increase in effective stress have contributed significantly to sanding. Specifically, we observe a gradual increase in sanding as the well deviation angle through the reservoir increases (Figure 11). The observed correlation is not unexpected. This is because of the higher perturbation of particle cohesion as deviation angle increases coupled with a potential for higher exposure areas. Furthermore, a good correlation is observed between pore pressure decrease and sand production (Figure 12). The increase in the matrix-supported load resulting from a decrease in pore pressure can lead to a displacement of grain particles within the sand matrix and thus trigger a re-alignment of grains with more sand being produced in the process. While these observations and correlation may be true, each element cannot fully account for the pattern of sanding individually. In other words, sand production is a combined effect of the afore-mentioned factors, with some factors playing more prominent roles than others.

Figure 13 shows a typical failed well due to excessive sanding from Forties Field. While increase in effective stress around the well and well deviation are less significant, the well failure can be linked directly to high fluid flow rate and the weakening of grain cohesion resulting from multiple and repeated perforations over the years. In some cases, the failures are not due primarily to fluid flow rate and repeated perforations, but to significant reservoir strain arising from pore pressure depletion. In

other cases, severe sanding have been recorded due to all these factors combined. Figure 14 is a typical case of high deviation angle, significant strain development around the well and high flow rate.

CONCLUSION

Sand production remains a source of concern in both conventional and heavy oil production. Factors such as reservoir consolidation, well deviation angle through the reservoir, perforation size, depth of penetration of perforation, grain size, capillary forces associated with water cut and flow rate and, more importantly, reservoir strain resulting from pore pressure depletion contribute to reservoir sanding. Understanding field-specific sand production patterns in mature fields and poorly consolidated reservoirs is vital in guiding remedial activities and identifying sanding-prone wells.

The Forties Field time-lapse seismic study using the 1988 and 2000 seismic surveys reveals an increased stress associated with pore pressure changes in the Charlie complex. The high time lag in the overburden shale above the Charlie sandstone suggests a significant increase in the reservoir stress. Reservoir strain analysis shows that the magnitude of the production-induced strain, part of which is propagated to the base of the reservoir, is of the order on 0.2%, which is significant enough to impact the geomechanical properties of the reservoir. We observe a correlation between sand production and time-lapse effect. Results of sand production analysis in Forties Field shows that in addition to poor reservoir consolidation, high well angle of deviation through the reservoir and high flow-rate, which are the well known factors, reservoir strain, due to pore pressure depletion, is observed to contribute significantly to sand production. For poorly-consolidated reservoirs, maintaining reservoir pressure at or close to initial condition does not only help sustain hydrocarbon production, it also serves as a sand production management tool.

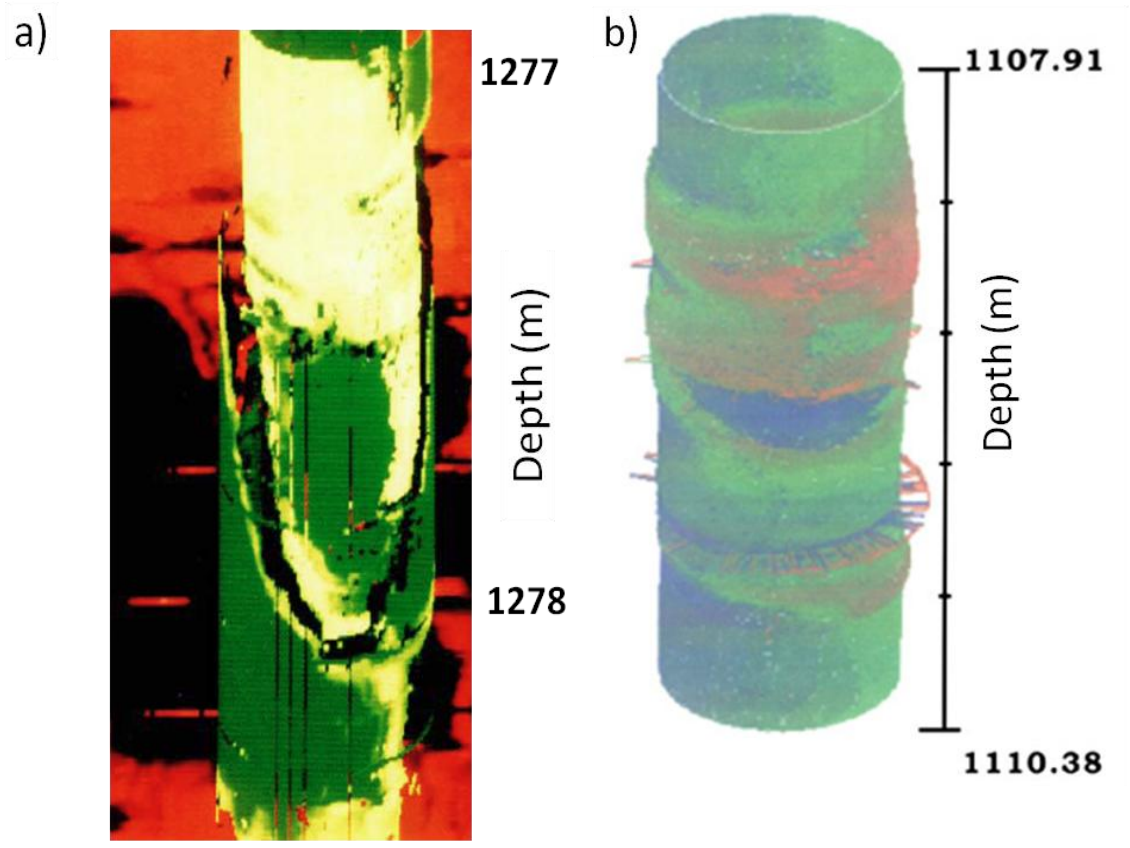

Figure 1. Examples of casing failure due to excessive sanding in the unconsolidated Gudao reservoir of the Shengli field in China using ultrasonic televiewer: (a) Three-dimensional view of shear failure and (b) Casing enlargement. Red patches in (b) shows enlarged wellbore. (After Peng et al., 2007).

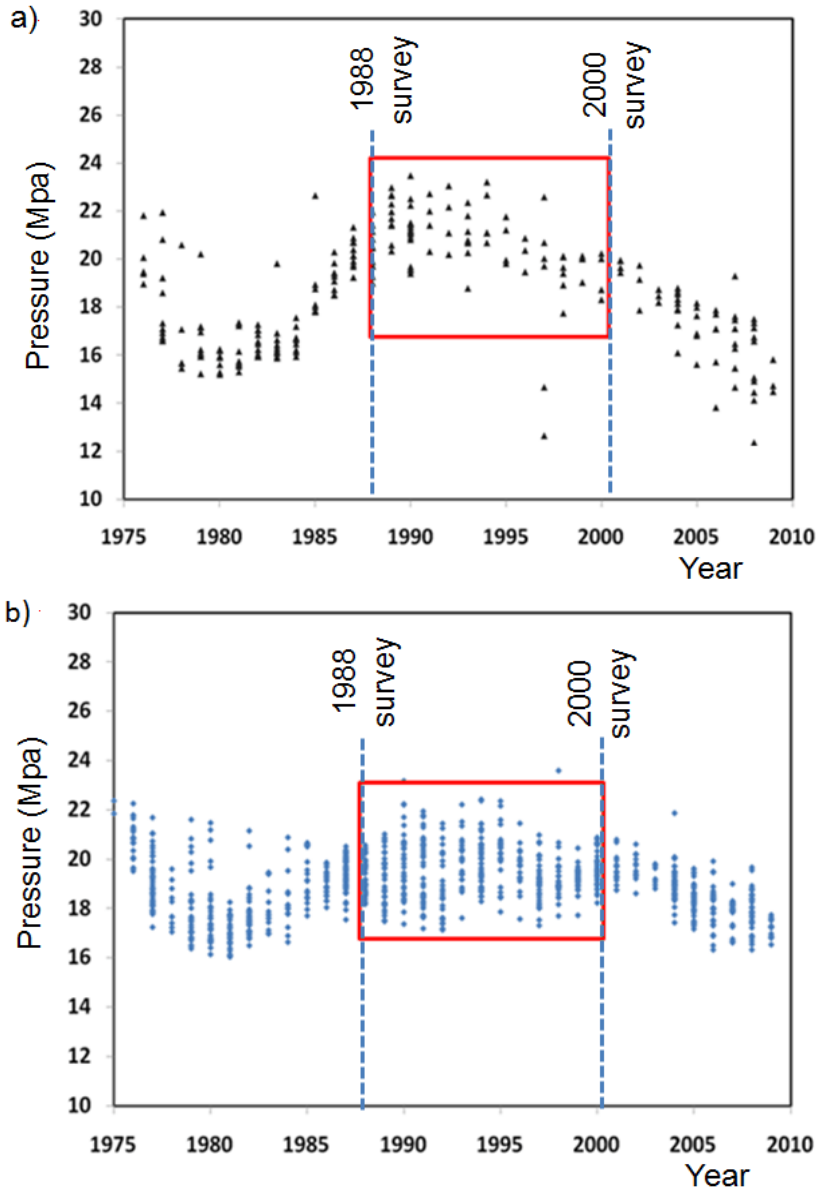

Figure 2. Historical pressure profile of (a) Charlie and (b) non-Charlie wells. Interval of interpretation in this paper is marked by the red rectangle. Observe that within the interval of study, reservoir pore pressure has been fairly steady in non-Charlie wells as opposed to a steady decrease of pressure in the Charlie wells, producing the observed higher strain around the Charlie complex. A significant increase in water injection accounts for the increase in pore pressure between 1985 and 1988.

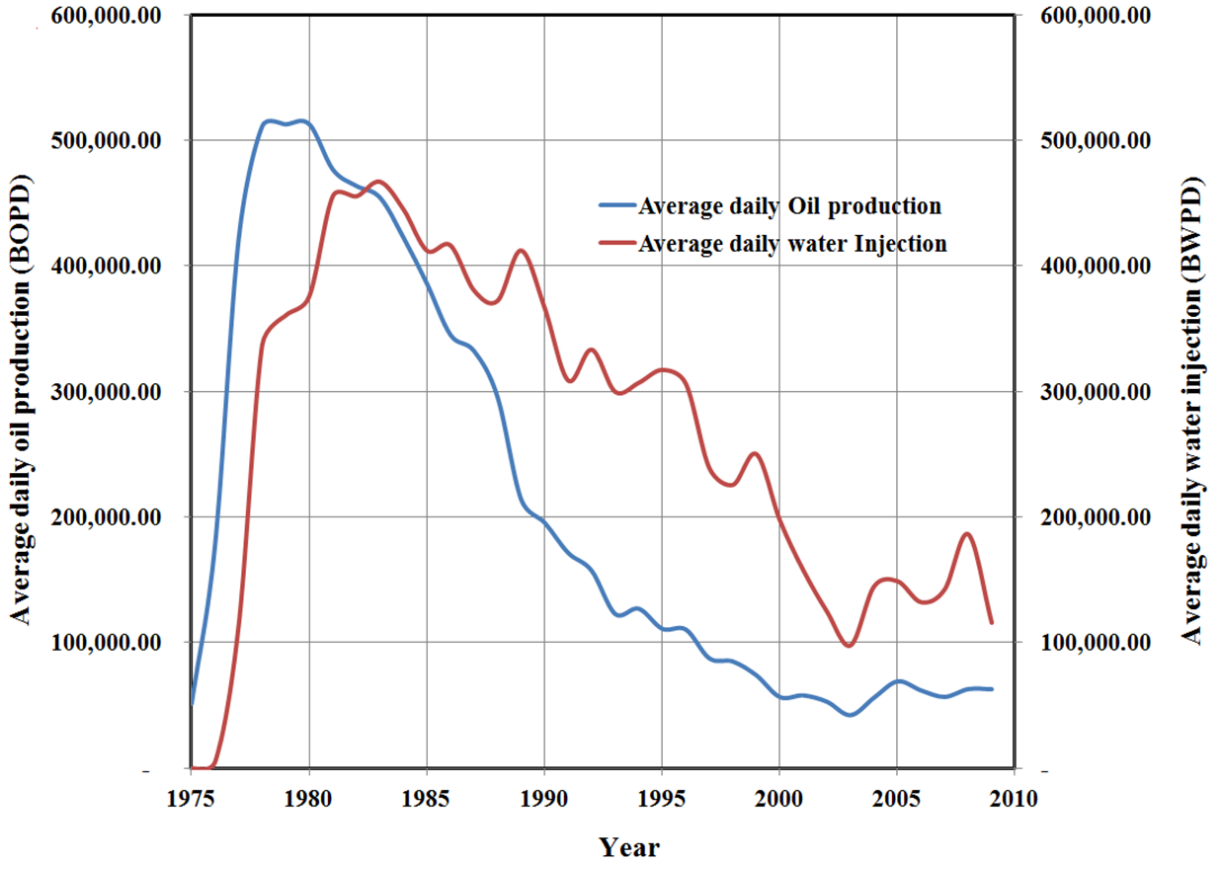

Figure 3. Profiles of average daily oil production and water injection for all wells in Forties Field.

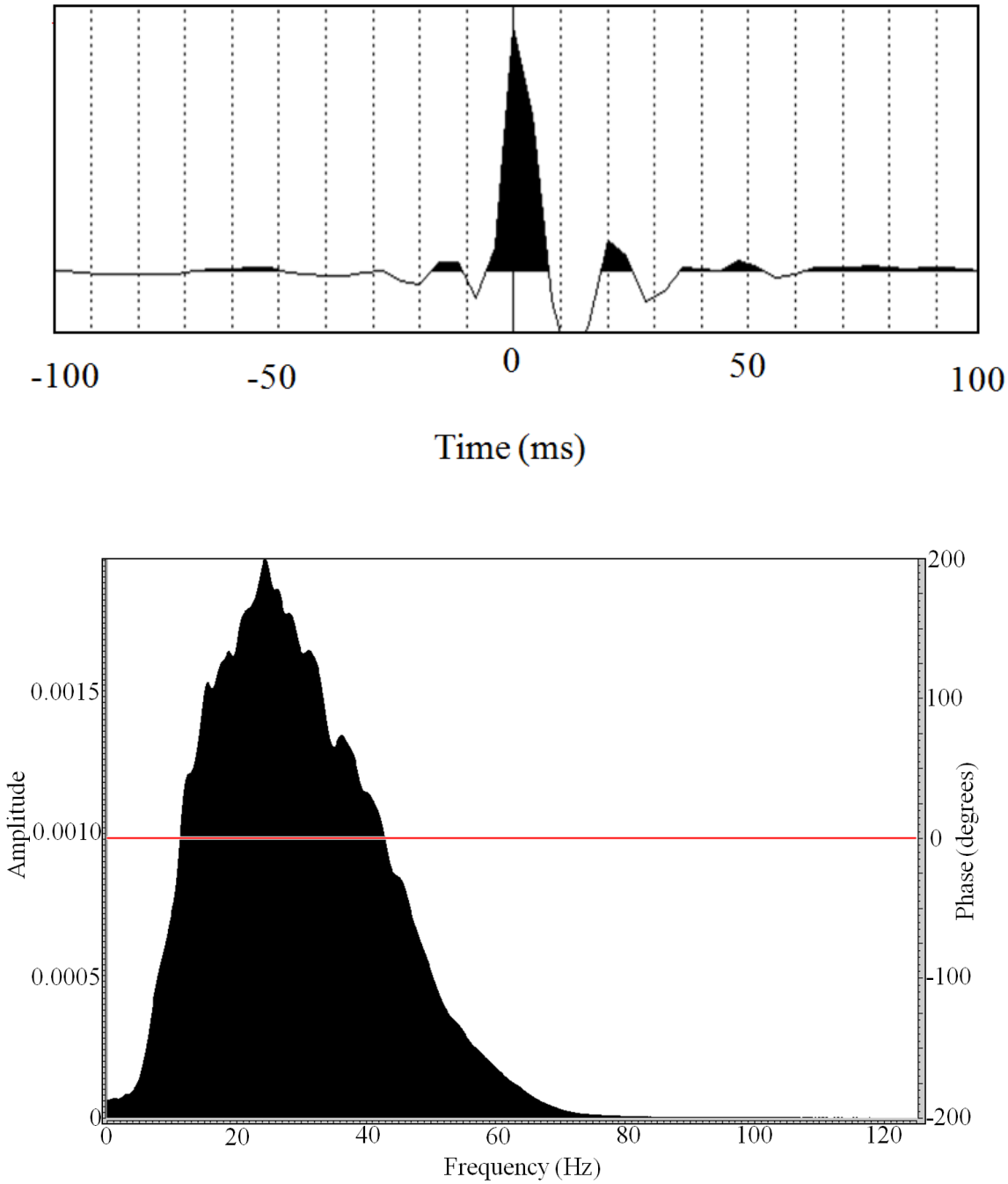

Figure 4. Shaping filter design. The above filter was used to balance the Forties Field 1988 and 2000 vintages. The frequency spectrum of the filter is the ratio of the input spectra, while the phase are subtracted from each other.

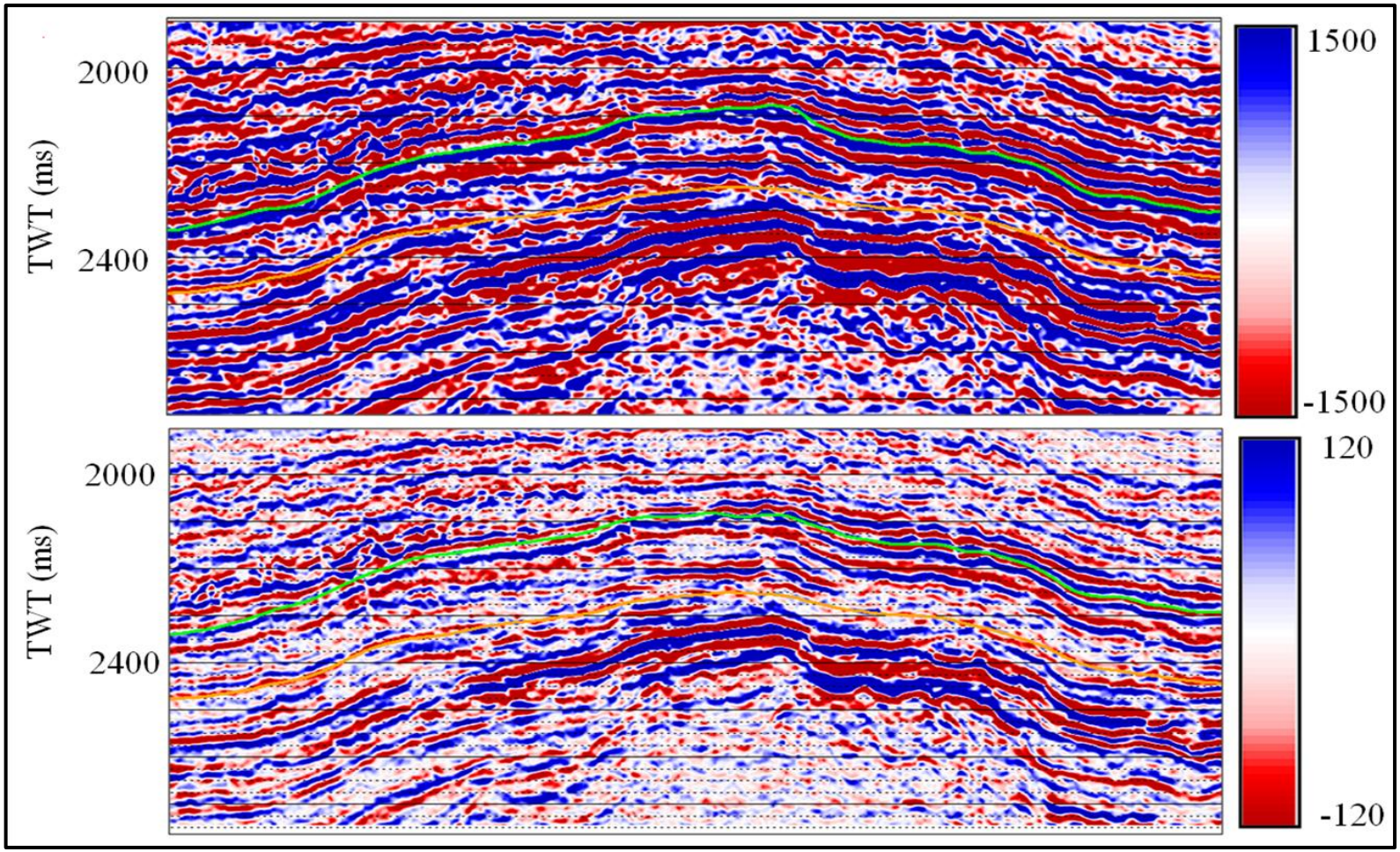

Figure 5. Spectrum balancing: Comparing Forties Field 1988 survey before (upper section) and after (lower section) the application of a shaping filter. Observe the change in amplitude scale.

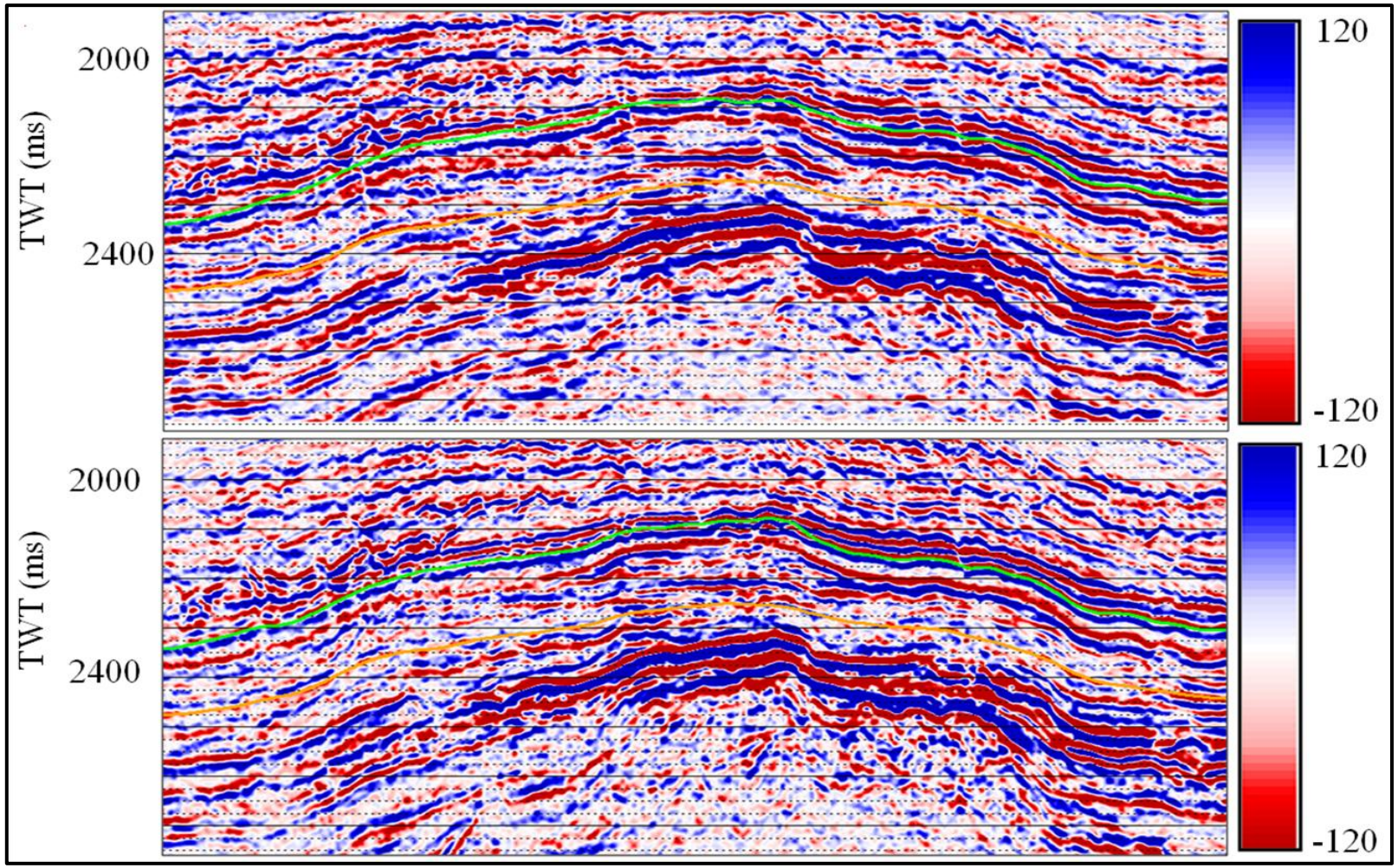

Figure 6. Comparing a section of Forties Field 1988 (upper section) and 2000 (lower section) surveys after spectrum balancing.

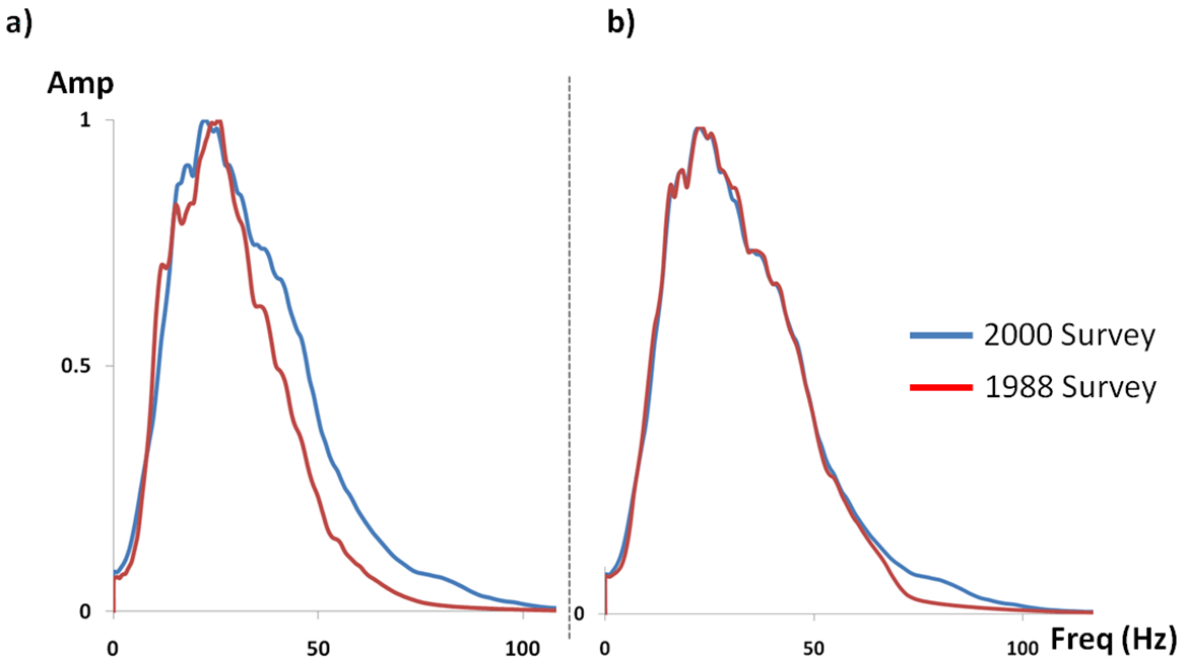

Figure 7. Frequency spectra: (a) before, and (b) after 4D balancing of 1988 and 2000 vintages.

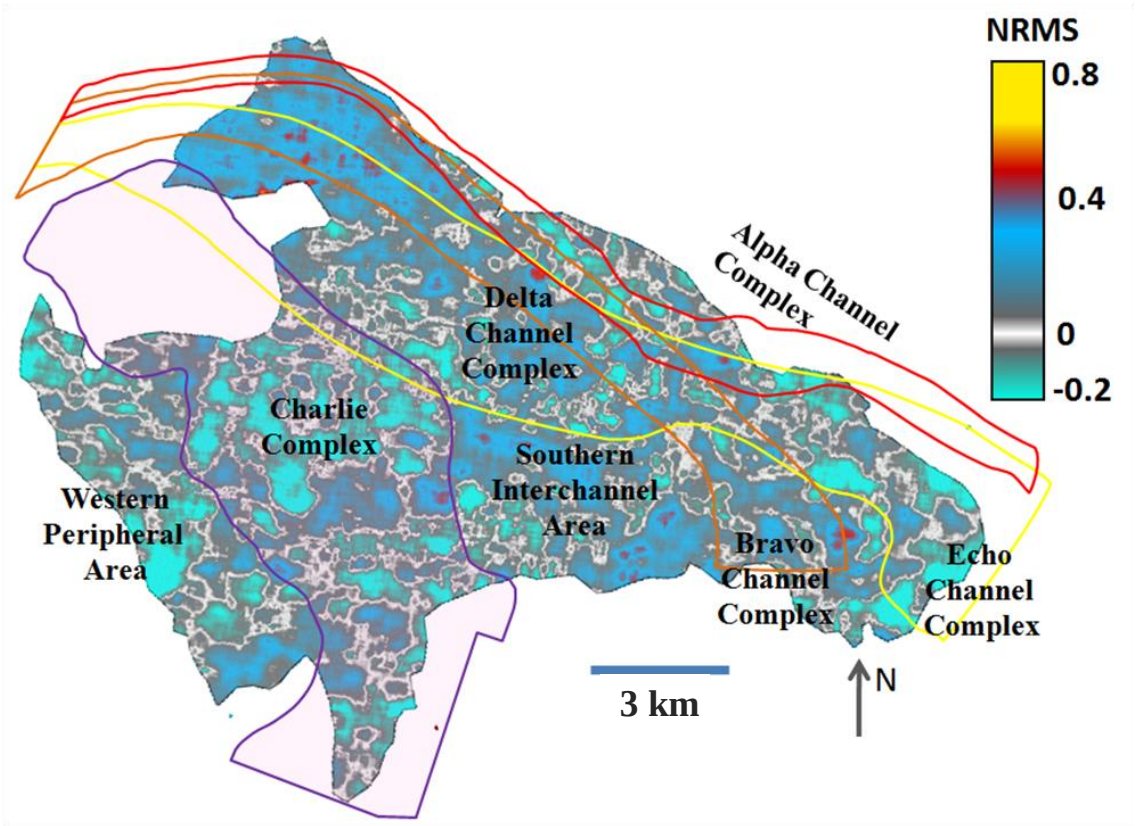

Figure 8. Normalized Root Mean square (NRMS): Index of repeatability 200ms above reservoir top.

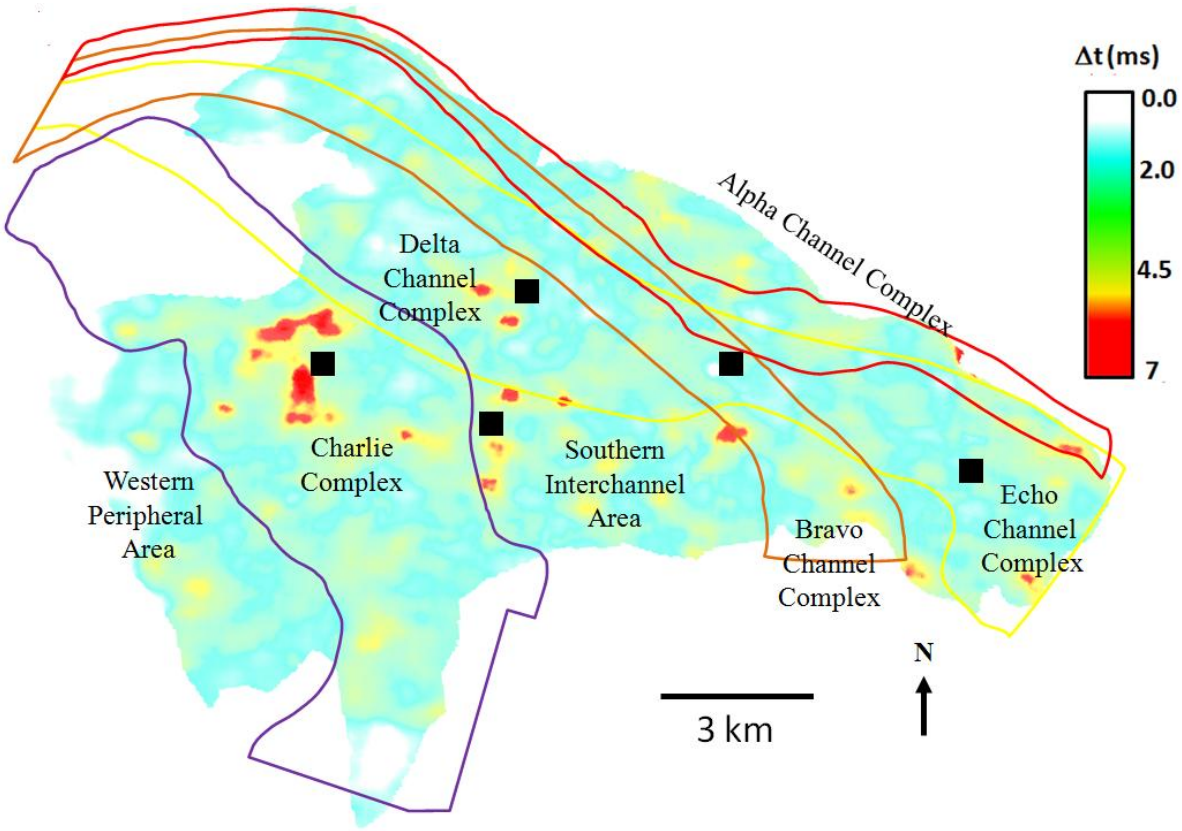

Figure 9. Time lag, Δt, at the top of regional Sele seal. The high travel time lag around the Charlie complex, due to a steady decrease in reservoir pore pressure, is an indication of compaction in the Charlie complex. Production platforms are in black squares.

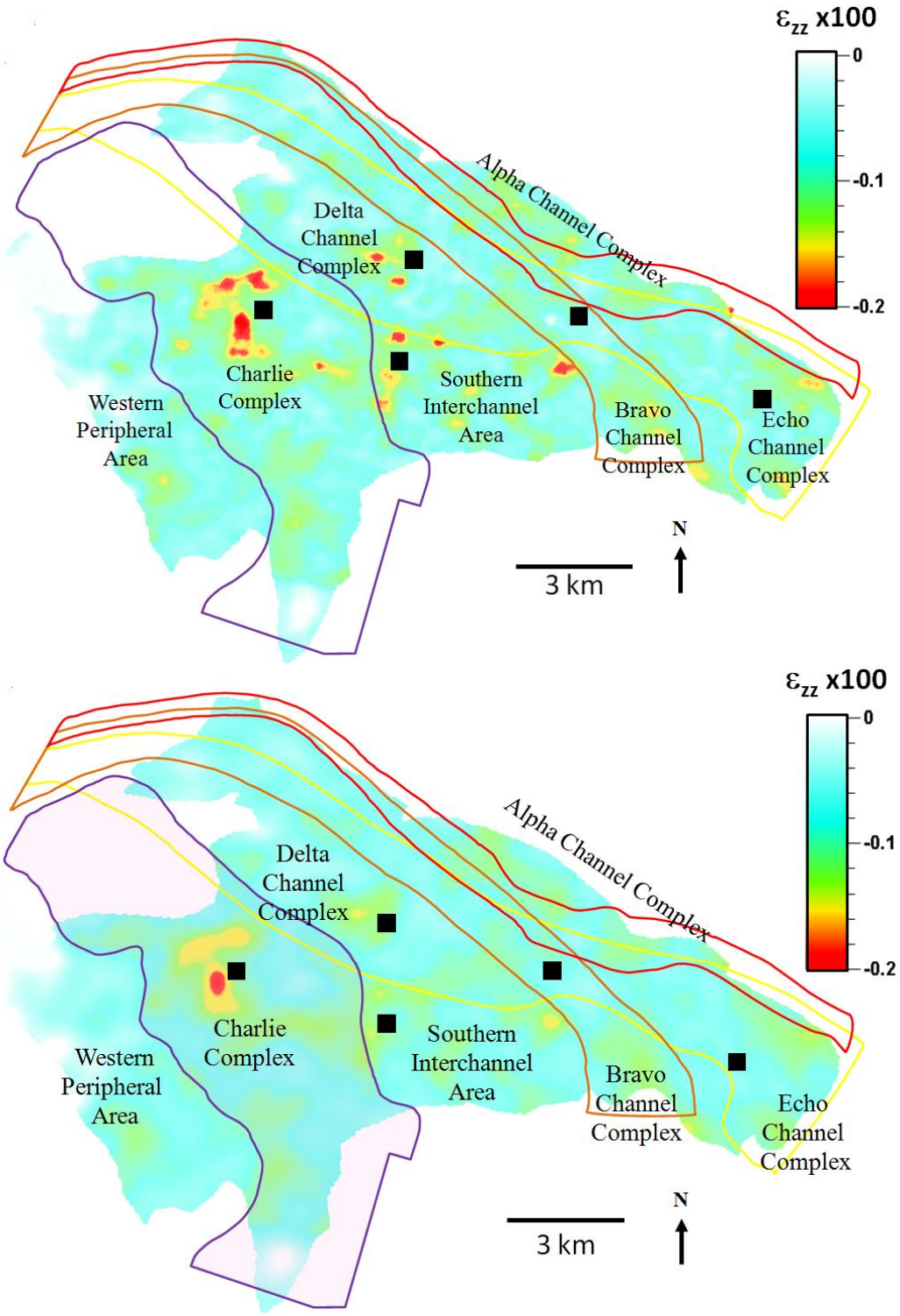

Figure 10. Computed strain, ε_{zz}, at the (a) top of the Sele regional seal, (b) base of the reservoir. The significant pore pressure decline in Charlie wells accounts for the high strain (> 0.2%) seen around the complex. Production platforms are in black squares.

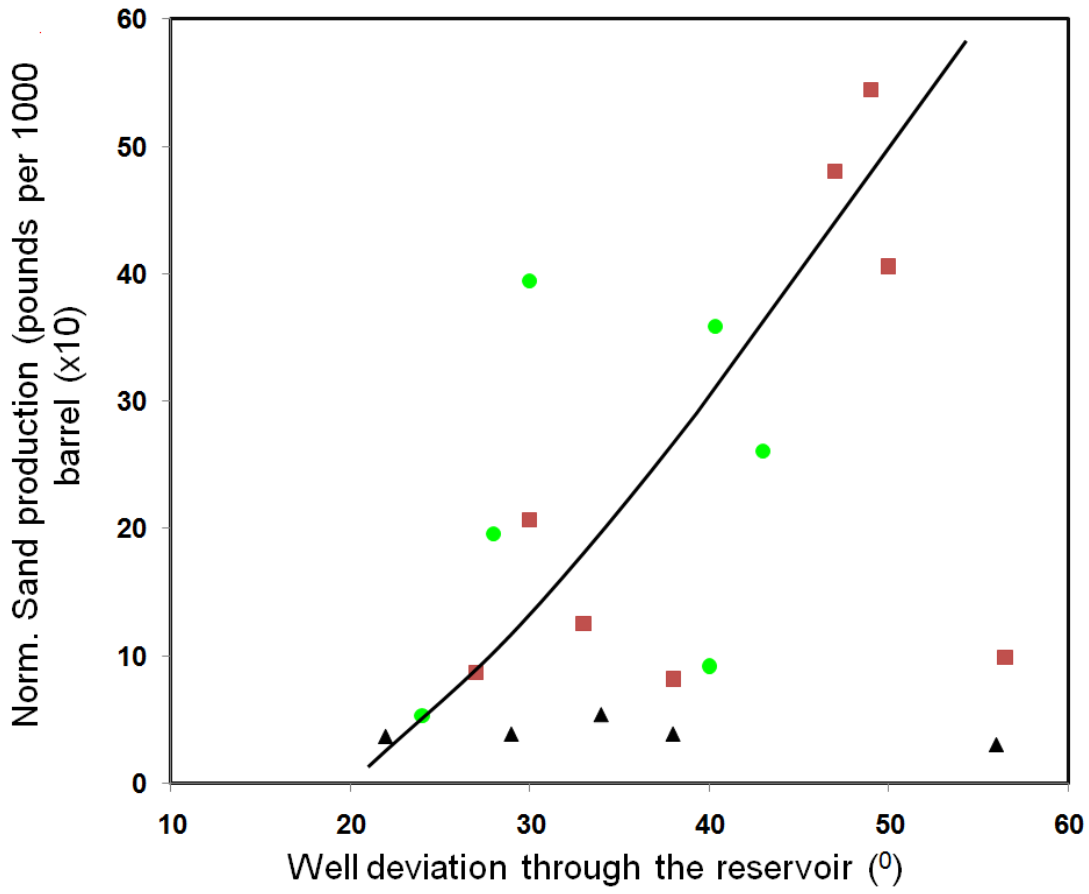

Figure 11. Sand production per unit flow as a function of well deviation angle through the reservoir. Colors represent wells from different complexes; Black triangles, green circles and red squares represent Alpha, Echo and Delta wells respectively.

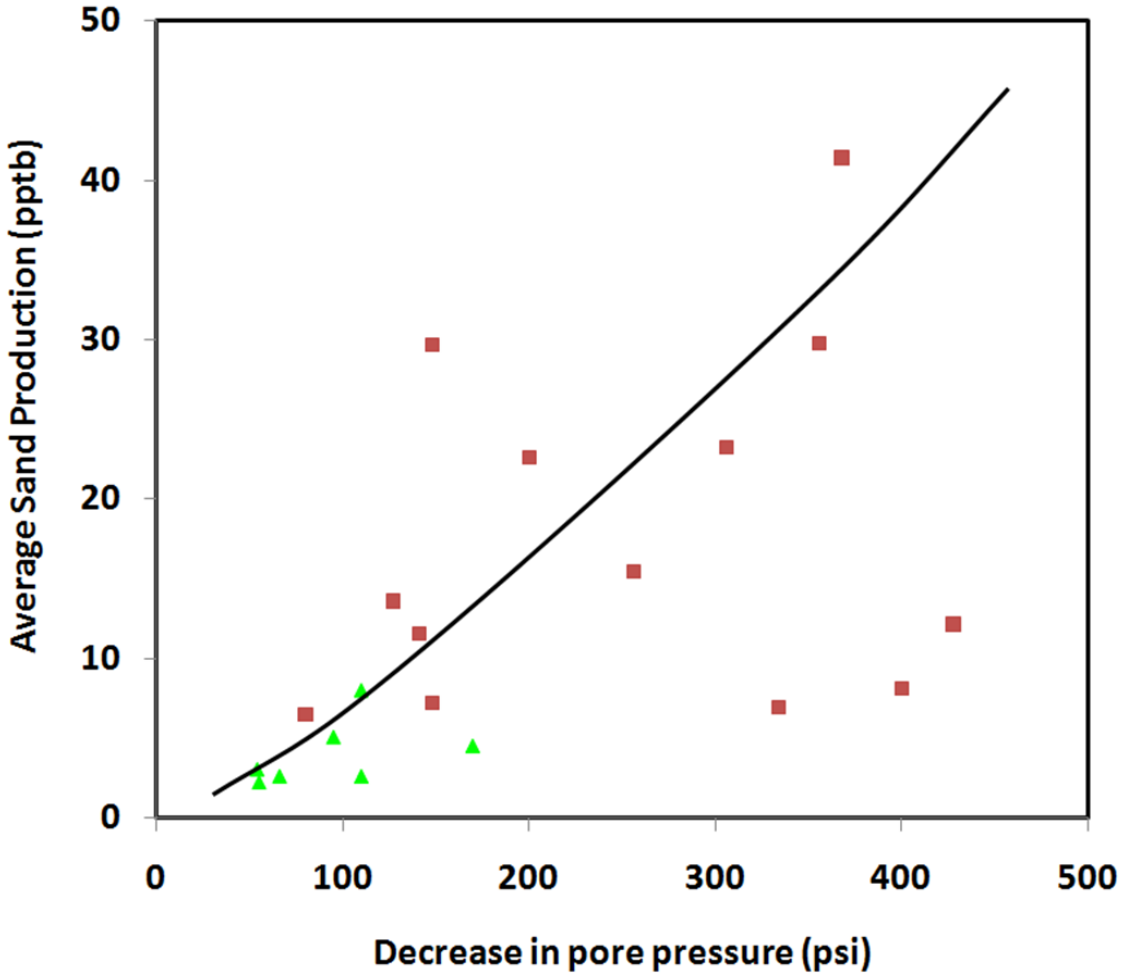

Figure 12. Crossplots showing average sand production increases with decreasing pore pressure. Colors represent wells from different complexes; Green triangles are Alpha wells while Delta wells are represented by the red squares.

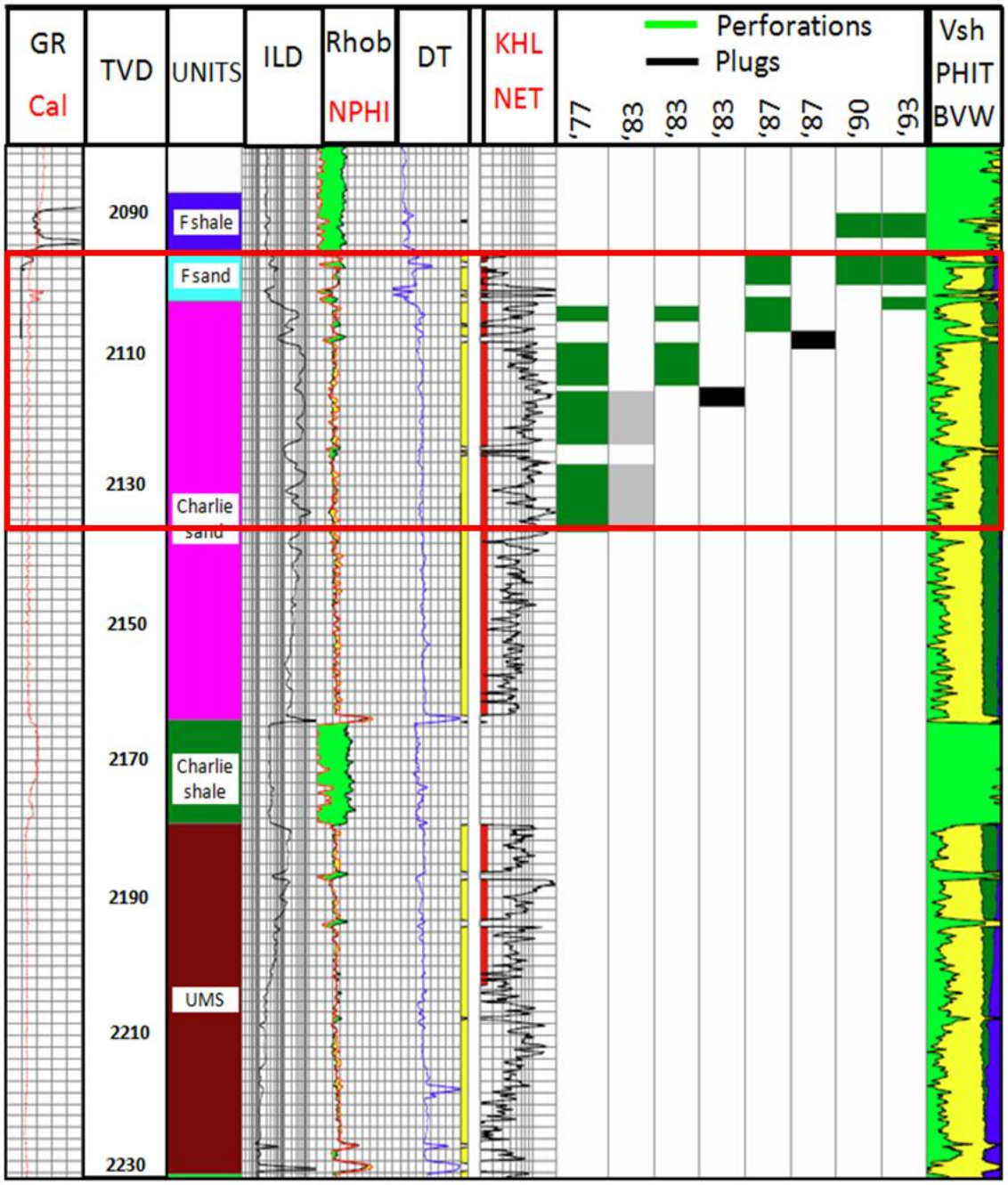

Figure 13. Logs from a high-sand producing well in Forties Field. Multiple and repeated perforation coupled with high fluid flow rate contributed significantly to the high sand production and the subsequent failure of the well. The red rectangle marks the sand producing interval. KHL refers to horizontal permeability while BVW is bulk volume of water.

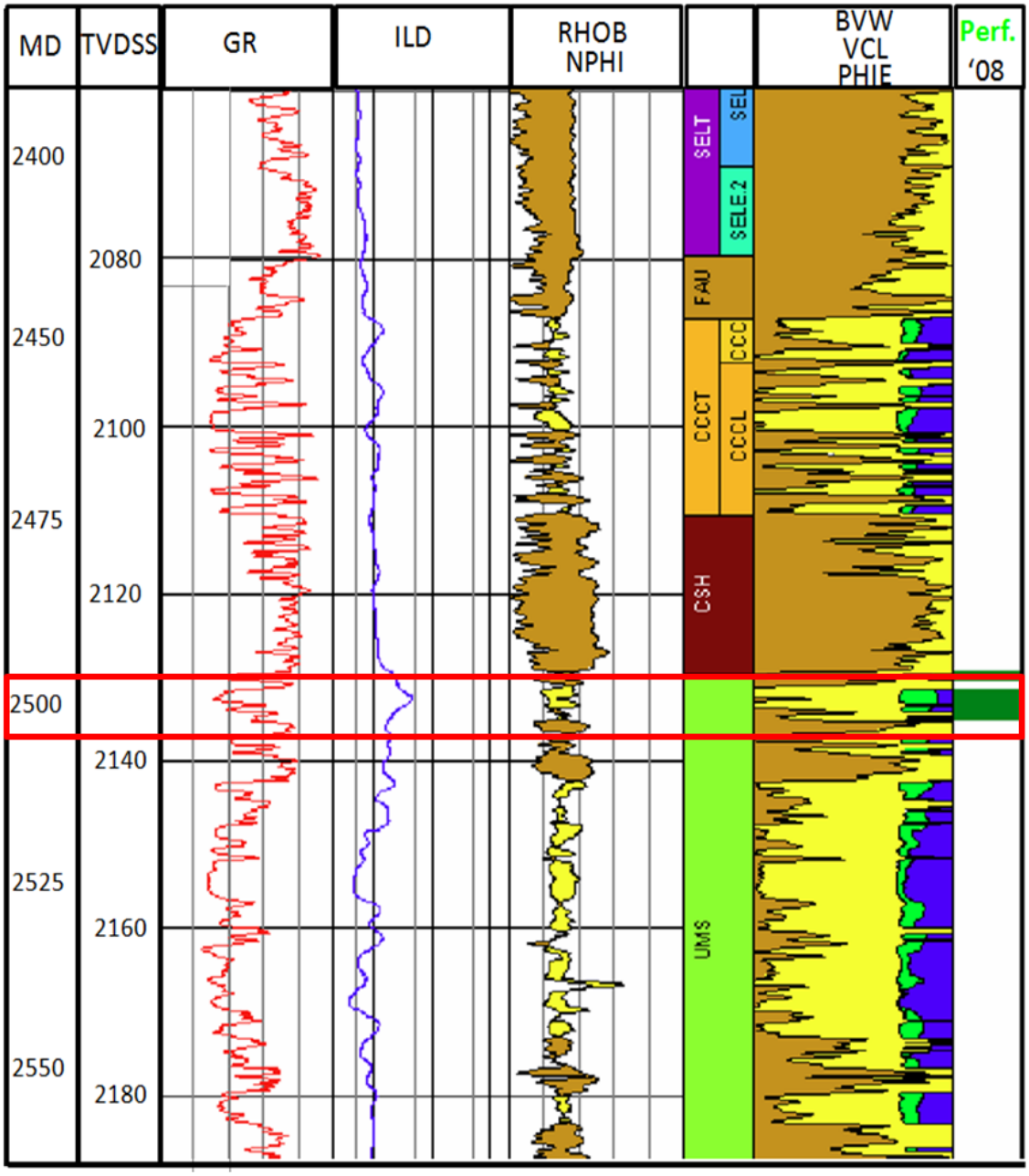

Figure 14. An example of high well sanding not attributable to only one factor but a combined effects of strain development, high flow rate and steep deviation angle through the reservoir. The red rectangle marks the sand producing interval. BVW refers to bulk volume of water, while Perf. refers to perforation.

REFERENCES

Anderson, N. R., G. Guerin, W. He, A. Boulanger and U. Mello, 1998, 4-D seismic reservoir simulation in a South Timbalier 295 tubidite reservoir: The Leading Edge, **17**, 1416-1417

Hatchell, P., and S. Bourne, 2005, Rocks under strain: Strain-induced time-lapse time shifts are observed for depleting reservoir: The Leading Edge, **24**, 1222-1225.

Helgerud, M.B., D.H. Johnston, B.G. Jardine, M.S. Udoh, N. Aubuchon, and C.Harris, 2009, 4D Case study in the Deep Water Gulf of Mexico: Hoover, Madison and Marshall, Annual international Meeting, SEG Expanded Abstract, **28**, 3949.

Hill, P.J., and G.V. Wood, 1980, Geology of the Forties Field, U.K. Continental Shelf, North Sea, in Giant oil and gas fields of the decade 1968-1978: AAPG Memoir **30**, 81-93.

Meadows, M., 2008, Time-lapse seismic modeling and inversion of C02 saturation for storage and enhanced oil recovery, The Leading Edge, **27**, 506-516.

McIntyre, B., T. Hibbert, D. Keir, R. Dixon, T. ORourke, F. Mohammed, A. Donald, L. Chang, A. Syed and V. Biran, 2009, Managing drilling risk in a mature North Sea Field; Society of Petroleum Engineers Offshore Europe Oil & Gas Conference & Exhibition, 124666.

Papamichos, E., I. Vardoulakis, J. Tronvoll, and A. Skjaerstein, 2001, Volumetric sand production model and experiment: International Journal for Numerical and Analytical methods in Geomechanics, **25**, 789-808.

Peng, S., J. Fu, and J. Zhang, 2007, Borehole casing failure analysis in unconsolidated formations: A case study: Journal of Petroleum Science and Engineering, **59**, 226-238.

Ribeiro C., C. Reiser, P. Doyen, A. Lau and S. Adiletta, 2007, Time-lapse simulator-to-seismic study- Forties Field, North Sea: Annual international Meeting, SEG Expanded Abstract, **26,** 2944-2948.

Robinson, N., A. Ford, J. Howie, D. Manley, M. Riviere, S. Stewart, and R. Thomas, 2005, Time-lapse Monitoring of Chirag Field: The Leading Edge, **24**, 928-932.

Sayers, C.M., 2010, Geophysics under stress: Geomechanical applications of seismic and Borehole acoustic waves: 2010 Distinguished Instructor Series, No. **13**, 50.

Sayers, C.M, and M.T.M. Schutjens, 2007, An introduction to reservoir geomechanics: The Leading Edge, **26**, 597-601.

Thomas, A.N., P.J. Walmsley, and D.A.L. Jenkins, 1974, Forties Field, North Sea: The American Association of Petroleum Geologists Bulletin, **58**, No. 3, 396-406.

Tura, A. and U. Etuk, 2006, Time-Lapse Seismic for field development at Nembe creek, Nigeria, The Leading Edge, **25,** 1142-1149.

Weisenborn, T. and P. Hague, 2005, Time-lapse Seismic in Gannet A; One more lead firmly integrated: The Leading Edge, **24**, 80-85.

Zhang, L., and M.B. Dusseault, 2004, Sand-production simulation in heavy-oil reservoirs: Society of Petroleum Engineers, No. 89037.

Acknowledgement: The authors will like to thank Apache North Sea Ltd for providing the data for this study and granting the permission to publish the results. We also thank Schlumberger and Hampson Russell for the use of their software for educational and research purposes. We are particularly grateful to Gregg Barker, Phil Rose, Klaas Koster and Jack Orman of Apache North Sea Ltd for their tremendous support. Funding was provided by the University of Oklahoma Attributes Assisted Seismic Processing and Interpretation (AASPI) consortium members.

CHAPTER THREE

3.0 TIME-LAPSE (4D) SEISMIC EFFECTS: RESERVOIR SENSITIVITY TO STRESS AND WATER SATURATION VARIATIONS

3.1 INTRODUCTION

The application of time-lapse seismic as a reservoir monitoring technique is not limited to fluid-front monitoring, compartmentalization studies and identifying by-passed hydrocarbons. The technique is responsive to stress changes in the reservoir. This sensitivity makes time lapse difference useful in the monitoring of pore pressure changes.

In this chapter, I studied the sensitivity of seismic velocities to changes in stress and saturation. This involved the use of laboratory measurements on rock samples and fluid substitution model. I investigated the effects of pore pressure change and the responses of horizontal and vertical components of stress to pore pressure changes.

Furthermore, I propose an amendment to the Landro (2001) time-lapse inversion method to accommodate the effect of porosity change. A case study was drawn from the Forties Field.

The chapter will be submitted to Geophysics for publication as a time-lapse inversion case study.

TIME-LAPSE (4D) SEISMIC EFFECTS: RESERVOIR SENSITIVITY TO STRESS AND WATER SATURATION VARIATIONS

Sunday Amoyedo, Kurt J. Marfurt and Roger M. Slatt, The University of Oklahoma, USA

ABSTRACT

Knowledge of reservoir saturation variation is vital for in-fill well drilling, while information on reservoir stress variation provides a useful guide for sand production management, casing design, injector placement and production management. Interpreting time-lapse difference is enhanced by decomposing time-lapse difference into saturation, pressure effects and changes in rock properties (e.g. porosity) especially in highly-compacting reservoirs.

We analyze the stress and saturation sensitivity of the reservoir and overburden shale of Forties Field, located in the UK sector of the North Sea. While pore pressure variations have not been significant in most parts of the field, a slightly high decrease in pore pressure in a region of the reservoir has had a profound effect on both reservoir and overlying rock. We find that strain development in the field accounts, in part, for increased reservoir sand production. Other effects include a negative velocity change in the overburden, which provides an indication of dilation. We use changes in the AVO intercept and gradient calibrated with laboratory measurements to invert the time-lapse (4D) difference for saturation and pressure changes.

INTRODUCTION

The need for effective reservoir monitoring is increasing in the face of diminishing reserves and a growing desire for optimized recovery. Reservoir depletion gives rise to changes in seismic amplitude, time lag between events, Δt, strain, ε_{zz}, and compaction. Knowledge of reservoir saturation variation is vital for in-fill well drilling by targeting by-passed hydrocarbons, while analysis of reservoir stress variation provides a useful guide for sand production management, casing design and injector placement. Reservoir depletion is characterized by fluid substitution and changes in effective stress resulting from variations in pore pressure. Seismic velocities in sandstone vary strongly with changes in both water saturation and stress because of differences in fluid and elastic properties as well as changes in grain boundaries, micro-cracks and fractures (Sayers, 2010).

Not only does time-lapse (4D) seismic have applications in monitoring fluid fronts, delineating reservoir compartments, and analyzing fluid migration pathways in conventional reservoirs, CO_2 sequestration and heavy oil development, it has also become an important tool for monitoring reservoir stress changes and the resulting strain.

Forties Field, composed of Late Paleocene sheet sands overlain by channel (Alpha, Bravo, Charlie, Delta, and Echo- Figure 1) complexes (Thomas et al., 1974), started production in 1977 based on a 2D seismic survey. Over 1.6 billion barrels of oil had been produced before the first 3D seismic survey was shot in 1988. Water saturation had increased by about 25-28% field-wide, while pore pressure decrease was

of the order of 5 MPa in Charlie complex between 1988 and 2005 (Figure 2). Seismic time lag, Δt, provides a direct indication of a change in seismic propagation velocity, induced by stress and saturation changes. The magnitude of the lag is related to the degree of change in stress and saturation.

Sand production, which constitutes a major source of well failure, can be linked to a number of factors including well deviation through the reservoir, grain size, poor reservoir consolidation, perforation-induced damages, capillary forces associated with water cut, flow rate, and most importantly reservoir stress resulting from pore pressure depletion. Substantial strains (> 0.2%), which can be induced by the effective stress and shear stress changes on the reservoir rock, are sufficient to severely degrade cohesion by breaking the small amounts of brittle grain-to-grain mineral cements as the pore pressure decreases. (Zhang and Dusseault, 2004).

Primary objectives of this study include: understanding the impact of changes in pore pressure on reservoir stress state in a poorly consolidated reservoir, AVO sensitivity analysis to production effect, establishing a link, if any, between reservoir sand production and time-lapse effects and to invert for saturation and pressure variations using changes in AVO volumes.

We begin by estimating and removing the background (non-production related) time shift between the 1988 and 2005 seismic surveys. The background time lag was estimated at a region above the producing interval devoid of production effects. We compute the production-induced time lag by the cross correlation of the two surveys (1988 and 2000). We observe a velocity slowdown (negative velocity change) in the

overburden directly above the Charlie complex, where there has been a significant variation in pore pressure. Elsewhere, the time lag was insignificant.

Our workflow involves a combination of laboratory measurements, fluid substitution models, AVO analysis and modifying an earlier published workflow (Landro, 2001; Landro, et al; 1999) for pressure and saturation inversion. We observe that the pore pressure-induced change in the reservoir stress state impacts mainly the total horizontal stress while the vertical stress remains largely unchanged as pore pressure decreases. This is because the vertical stress greatly exceeds the horizontal stress. Our laboratory measurements and fluid substitution model show strong amplitude variation with offset (AVO) attributes to changes in reservoir stress and water saturation. Extending the workflow described by Landro, (2001) to account for porosity change, we decouple the seismic time-lapse difference into pressure and saturation effects.

TIME-LAPSE EFFECTS: ROCK SENSITIVITY TO STRESS AND WATER SATURATION CHANGES

Time-lapse seismic difference (amplitude, impedance difference and time lag) is a combined effect of fluid substitution and stress increase accompanying a decrease in pore pressure. Figure 3 shows a vertical slice through acoustic impedance difference section across part of the reservoir after a production period of over 12 years. The associated linear relation between effective and pore pressure is expressed as

$$P_e = P_o - \alpha P_p, \quad (1)$$

where P_e, P_o, α and P_p represent effective pressure, overburden pressure, Biot's constant and pore pressure respectively. While fluid substitution is effectively handled by Gassmann's model, understanding sandstone sensitivity to stress is far more complex and requires a good knowledge of the geomechanical behavior of the reservoir rock.

Forties Field, which is composed of sheet sands overlain by channel complexes (Thomas et al; 1974; Hill and Wood, 1980), is broadly divided into the "Charlie" and the "non-Charlie" sandstone complexes. Reservoir pressure has been fairly stable in the non-Charlie complexes, with a steeper decrease in formation pressure recorded in Charlie wells within the 1988-2005 interval of study. For consolidated rocks, a formation pressure decline of 5 MPa may not have a significant impact on the reservoir geomechanical properties; however, the effects could be more pronounced on weak and unconsolidated sediments such as the Forties Field reservoir. Not only is the reservoir unconsolidated, the overburden is equally weak in many parts of the field making the Forties sediments particularly sensitive to stress changes. Figure 4 shows images of core samples of both weak and competent shales belonging to the Sele formation, which forms the seal. The unpredictable and strongly varying fabrics of shale types in the overburden pose a major drilling challenge in Forties Field, where over 65% of wells drilled between 2002 and 2007 have experienced some form of instability problem (McIntyre et al; 2009).

Velocities vary considerably in sandstones as stress increases because of stress-sensitive discontinuities within the rock, such as grain boundaries, micro-cracks, and fractures (Sayers, 2010). Laboratory measurements on dry samples of Forties Field sandstone from depths ranging between 2229 and 2256 m show remarkable sensitivity

of p-wave and s-wave velocities to an increase in confining stress (Figure 5a). Specifically, compressional velocity increases from 2560 to over 3400 m/s while shear velocity increases from under 1600 to 2180 m/s corresponding to an increase in confining stress approaching 30 MPa. A similar velocity sensitivity is observed in the Forties shale when a slow tri-axial compressional stress is applied. Both compressional and shear velocities increase almost linearly until rock failure occurs. (Figure 5b). This velocity sensitivity can be explained by grain-to-grain squeezing, closure of micro-cracks, and a slight porosity loss. Sensitivity to stress cannot be explained solely by porosity reduction but also requires grain-to-grain squeeze, and the altering of the grain aspect ratio (Sayers, 2010).

A direct effect of reservoir production is compaction and sometimes subsidence in the production area. These effects are due to changes in both total vertical and horizontal components of stress, which produces an increase in velocity within the reservoir in addition to any changes due to fluid substitution. In order to maintain stability, the overburden is stretched (dilated), resulting in a velocity slow down (or a negative change in velocity).

Landro and Jansen (2002) and Landro and Stammeijer (2004) showed that for NMO-corrected traces, keeping leading orders only, the relative change in velocity is given by

$$\frac{\Delta v_p}{v_p} = \frac{\frac{\Delta t_N}{t} - \frac{\Delta t_F}{t}}{tan^2\theta_F - tan^2\theta_N}, \qquad (2)$$

where $\Delta t_N \; and \; \Delta t_F$ represent the near and far stack travel time lags respectively, θ represents the seismic ray angle through the layer and *t* the two-way travel time after NMO correction.

We balance Forties Field sub-stacks and extract travel time lags for both near and far stacks between the base (1988) and monitor (2005) surveys. The observed residual spectra difference in the far stack is due largely to anisotropy, resulting from the different acquisition geometries. The computed relative velocity change over the Charlie sandstone shows an expected velocity increase with a corresponding velocity decrease in the overburden shale, indicating stretching (Figure 6). Reservoir pore pressure depletion can alter the minimum and maximum horizontal stress as well as the vertical effective stress. Micro-seismic events inside or close to the reservoir zone provide direct evidence of the changing stress regime induced by production (Hettema et al., 1998). The geomechanical response of rocks to increasing stress can vary significantly depending on the stress path. The stress path is defined in terms of the ratio of changes in stress values as they deviate from their initial reservoir values (Sayers, 2010 and Hettema et al., 1998).

For a laterally extensive reservoir, we define the parameter γ_v as the change of the total vertical stress, $\Delta\sigma_v$, over the change in pore pressure, Δp, expressed as:

$$\gamma_v = \frac{\Delta\sigma_v}{\Delta p} = \frac{GC_u h}{R} f\left(\frac{D}{R}\right), \tag{3}$$

where *G* is the shear modulus, C_u is the compaction coefficient, *h* is the reservoir average thickness, *R* is the average lateral extent of the reservoir, while the function $f\left(\frac{D}{R}\right)$ depends on the ratio of reservoir depth to its radius (Hettema et al., 1998).

The change in total horizontal stress, $\Delta\sigma_h$, gives rise to a parameter γ_h (for an isotropic state) as pore pressure changes is

$$\gamma_h = \frac{\Delta\sigma_h}{\Delta p}. \quad (4)$$

The change in total horizontal stress, $\Delta\sigma_h$, is defined as

$$\Delta\sigma_h = \left(\frac{v}{1-v}\right)\Delta\sigma_v + \alpha\Delta p\left(1 - \frac{v}{1-v}\right), \quad (5)$$

where v is the Poisson's ratio.

With these definitions, equation 6 can therefore be written as:

$$\gamma_h = \frac{\Delta\sigma_h}{\Delta p} = \left(\frac{v}{1-v}\right)\gamma_v + \alpha\left(1 - \frac{v}{1-v}\right). \quad (6)$$

Using the values in Table 1 in equations 3 and 6, we observe that γ_v is on the order of 6.58 x10^{-3}, which is insignificant when compared with γ_h which is on the order of 0.72. This observation allows us to link the velocity changes within the reservoir and overburden directly to changes in the total horizontal stress and saturation. The decrease in total horizontal stress, which in this case is of the order of the pore pressure change, might be significant enough to induce fault slippage in the overburden.

Table 1:Rock and fluid properties

Porosity	Depth	Thickness	Compaction Coefficient	Shear Modulus	Bulk Modulus	Poisson's ratio	Oil density
28	2480	300	0.001	7555	9667	0.2119	0.7465
%	m	m	MPa^{-1}	MPa	MPa	-	g/cm^3

TIME-LAPSE EFFECTS AND RESERVOIR GEOMECHANICS

Time-lapse effects include changes in amplitude (reflectivity) as well as time lags between two events, Δt, which can be due to changes in velocity and rock strain.

We cross correlated the 1988 and 2000 surveys (after estimating and removing the background time shift) to compute the time lag between them. The background time lag was estimated at a region immediately above the regional Sele shale, which is devoid of production effects. A decrease in pore pressure leads to an increase in stress carried by the load-bearing rock frame of the reservoir, inducing compaction within the reservoir and dilation in the overburden. These changes may be accompanied by micro-scale deformation mechanisms such as cement breakage at grain contacts, grain sliding, rotation and significant alteration of reservoir geomechanical properties (Sayers and Schutjens, 2007).

Hatchell and Bourne (2005) showed that fractional changes in velocity occur in proportion to fractional changes in path length, T. Thus, the time strain for normal incidence P-waves can be written as:

$$\tau = \partial T/T = (1+R)\varepsilon_{zz} \ , \qquad (7)$$

where R defines the ratio of 4D fractional velocity changes to fractional thickness changes and ε_{zz} is the uniaxial strain. Hatchell and Bourne (2005) found that R lies in the range $4 < R < 8$ for rocks undergoing extension, whereas R lies in the range $0 < R < 2$ for rocks undergoing compaction (Sayers, 2010) . In Forties Field, we found $R = 0.75$ within the reservoir while $R = 0.70$ in the overburden. This range of values lies outside most reported figures. Such anomalous values could be due to the high porosity and the

extremely weak frame characterizing the Forties reservoir and overburden shale, suggesting a good potential for grain-on-grain contact squeezing within the reservoir and dilation in the overburden. The Charlie sands and southern inter-channel area of Forties Field are observed to have high strain associated with increased stress, while the other areas have experienced minimal strain. The analysis also shows that stress increase is not confined to the top and within the reservoir, but is also propagated to the reservoir base inducing significant velocity change and potential instability (Figure 7).

DEPLETION AND SAND PRODUCTION PATTERN

Forties Field has been plagued by severe sand production and an array of drilling and completion problems. Severe sanding in this mature UK North Sea field has led to the loss of wells, reduced production and consequently increased cost of production (associated with well clean up operations, drilling of side-track wells and corrosion prevention). Understanding the field-specific sand production mechanism(s) and sanding pattern in Forties Field can significantly aid in identifying vulnerable wells and guiding the remedial actions. Incomplete sand production records and difficulty in eliminating transitional sanding due to extraneous factors such as workovers limit the amount of available data and reliability of sand production analysis.

While poor consolidation has contributed largely to sand production in the field, we observe that other factors such as multiple completions, high well deviation angle, flow rate and increase in effective stress have contributed significantly to sanding. Specifically, we observe a gradual increase in sanding as the well deviation angle through the reservoir increases (Figure 8a). The observed correlation is not unexpected.

This is because of the higher perturbation of particle cohesion as deviation angle increases coupled with a potential for higher exposure areas. Furthermore, a correlation is observed between pore pressure decrease and sand production (Figure 8b). The increase in the matrix-supported load resulting from a decrease in pore pressure can lead to a displacement of grain particles within the sand matrix and thus trigger a re-alignment of grains with more sand being produced in the process. While these observations and correlations may be true, each element cannot fully account for the pattern of sanding individually. In other words, sand production is a combined effect of the afore-mentioned factors, with some factors playing more prominent roles than others.

Figure 9 shows typical failed wells due to excessive sanding from Forties Field. While increase in effective stress around the well and well deviation are less significant, the well failure can be linked directly to high fluid flow rate and the weakening of grain cohesion resulting from multiple and repeated perforations over the years. In some cases, the failures are not due primarily to fluid flow rate and repeated perforations, but to significant reservoir strain arising from pore pressure depletion. In other cases, severe sanding have been recorded on the account of all these factors combined.

AVO SENSITIVITY TO CHANGES IN WATER SATURATION AND STRESS

Reservoir production gives rise not only to changes in travel time but also changes in amplitude variation with offset (AVO) response within the producing interval. Changes in stress state and fluid replacement result in changes in velocity, which in turn gives rise to changes in the compressional and shear wave reflectivities. Following Shuey (1985), the linearized reflection coefficient for PP reflections , R_{pp}, is

$$R_{pp}(\theta) = b_0 + b_1 sin^2\theta + b_2 [tan^2\theta - sin^2\theta], \quad (8a)$$

the AVO intercept b_0, gradient b_1, and curvature b_2 are

$$b_0 = \frac{1}{2}\left[\frac{\Delta V_p}{V_p} + \frac{\Delta\rho}{\rho}\right], \quad (8b)$$

$$b_1 = \left[\frac{1}{2}\frac{\Delta V_p}{V_p} - 2\frac{V_s^2}{V_p^2}\left(\frac{\Delta\rho}{\rho} + 2\frac{\Delta V_s}{V_s}\right)\right], \quad (8c)$$

$$b_2 = \frac{1}{2}\frac{\Delta V_p}{V_p}, \quad (8d)$$

where $\Delta V_p, \Delta V_s, \Delta\rho$ indicate changes in P-wave velocity, S wave velocity and density, and $V_p, V_s \; and \; \rho$ indicate average compressional velocity, shear velocity and density.

Examining equations 8b-d and Figure 10, we observe the sensitivity of AVO intercept to fluid replacement and stress variation. The gradient and curvature, while being sensitive to stress changes, are less sensitive to fluid substitution. This is because the s-wave velocity does not respond to fluid types. The gradual decrease in the variation of amplitude with offset as water saturation and stress increase is attributable to the loss of velocity sensitivity at high values of stress and water saturation changes. The sensitivity

curves shows that AVO gradient and curvature do not contribute significantly to time-lapse effect, while the intercept changes account for the observed variation. This observation is also confirmed by the results of simultaneous inversion of the 4D-processed seismic cubes for the interval of study. The observed sensitivity of AVO intercept and gradient to changes in water saturation and reservoir pore pressure provides a useful strategy to decouple the two effects.

TIME-LAPSE DIFFERENCE: DECOUPLING SATURATION AND PRESSURE CHANGES

Reservoir monitoring is a vital tool in field development as a source of information on changes in reservoir fluid saturation, drainage pattern and stress changes. Time-lapse seismic experiments measure the combined effect of saturation and pressure changes. Our ability to interpret time-lapse differences effectively is enhanced by decoupling them into their components saturation and pressure effects. Knowledge of reservoir saturation variation is vital for in-fill well drilling and fluid front movement, while reservoir stress variation provides useful information for sand production management, casing design, carbon storage management and injector well placement.

Time-lapse seismic effects are sometimes pressure dominated, such as Magnus Field, (Watts et al., 1996), or saturation dominated, such as Gullfaks Field, (Landro et al., 1999), and the Draugen Field, (Gabriels et al., 1999, Veire et al., 2007). In other cases, time-lapse differences are a combined effect of both pressure and saturation

changes. In such cases it is necessary to decouple production related differences (Tura and Lumley, 1999; Landro, 2001; Lumley et al., 2003).

Recalling the linearized PP reflectivity as a function of angle in equation 8, Landro (2001) assumed that the shear modulus remains unchanged and found that the change in reflectivity associated with fluid substitution can be written as :

$$\Delta R^F(\theta) \approx \frac{1}{2}\left(\frac{\Delta\rho^F}{\rho} + \frac{\Delta\alpha^F}{\alpha}\right) + \frac{\Delta\alpha^F}{2\alpha}\, tan^2\theta, \tag{9a}$$

while the change in reflectivity attributable to pressure change, assuming that density remains the same, can be written as

$$\Delta R^P(\theta) \approx \frac{1}{2}\frac{\Delta\alpha^P}{\alpha} - \frac{4\beta^2}{\alpha^2}\frac{\Delta\beta^P}{\beta}\, sin^2\theta + \frac{\Delta\alpha^F}{2\alpha}\, tan^2, \tag{9b}$$

where the P-velocity, S-velocity, change in P-velocity (due to pressure, $\Delta\boldsymbol{P}$, and saturation change, $\Delta\boldsymbol{S}$), and change in S-velocity (due to pressure change) are denoted as α, β, $\Delta\alpha^P$, $\Delta\alpha^F$ and $\Delta\beta^P$. Modifying Landro's (2001) equation, we can write that the relative changes in compressional, shear velocities and density as:

$$\frac{\Delta\alpha}{\alpha} \approx n_\alpha\Delta S + j_\alpha\Delta P + m_\alpha\Delta P^2 + k_\alpha\Delta\Phi\,, \tag{10a}$$

$$\frac{\Delta\beta}{\beta} \approx n_\beta\Delta S + j_\beta\Delta P + m_\beta\Delta P^2 + k_\beta\Delta\Phi, \text{ and} \tag{10b}$$

$$\frac{\Delta\rho}{\rho} \approx n_\rho\Delta S + j_\rho\Delta P + k_\rho\Delta\Phi\,, \tag{10c}$$

where $\Delta\Phi$ represents the change in porosity as the reservoir stress state changes.

Substituting equations 10 a - c into equations 8 a-d, we can write that the changes in AVO intercept, gradient and curvature as :

$$\Delta b_0 = \left[\frac{n_\propto + n_\rho}{2}\right]\Delta S + \left[\frac{j_\propto + j_\rho}{2}\right]\Delta \boldsymbol{P} + m_\propto \boldsymbol{\Delta P^2} + \left[\frac{k_\propto + k_\rho}{2}\right]\Delta \boldsymbol{\Phi}, \quad (11a)$$

$$\Delta b_1 = \left[\frac{n_\propto - 8\delta n_\beta}{2}\right]\Delta \boldsymbol{S} + \left[\frac{j_\propto - 8\delta\, j_\beta}{2}\right]\Delta \boldsymbol{P} + \left[\frac{m_\propto - 8\delta m_\beta}{2}\right]\boldsymbol{\Delta P^2} + \left[\frac{k_\propto - 8\delta k_\beta}{2}\right]\Delta \boldsymbol{\Phi}, \text{ and} \quad (11b)$$

$$\Delta b_2 = \left[\frac{n_\propto}{2}\right]\Delta \boldsymbol{S} + \left[\frac{j_\propto}{2}\right]\Delta \boldsymbol{P} + m_\propto \boldsymbol{\Delta P^2} + \left[\frac{k_\propto}{2}\right]\Delta \boldsymbol{\Phi}. \quad (11c)$$

Solving equations 11 a- c by recursive substitution, we can show that for a highly compacting reservoir,

$$\left[m_\propto - nc_7 + k\left(\frac{n_\propto}{k_\propto}c_7 - \frac{m_\propto}{k_\propto}\right)\right]\boldsymbol{\Delta P^2} + \left[j - nc_6 + k\left(\frac{n_\propto}{k_\propto}c_6 - \frac{j_\propto}{k_\propto}\right)\right]\boldsymbol{\Delta P}$$

$$+\left[nc_5 + k\left(\frac{2\,\Delta b_2}{k_\alpha} + \frac{n_\propto}{k_\propto}c_5\right)\right] - \Delta b_0 = 0 \quad (12a)$$

Given a change in pressure, ΔP, computed from the quadratic solution of equation (12a), we can further show that the change in water saturation

$$\boldsymbol{\Delta S_w} = c_5 - c_6\boldsymbol{\Delta P} - c_7\,\boldsymbol{\Delta P^2}, \quad (12b)$$

while the change in porosity can be written as:

$$\boldsymbol{\Delta \Phi} = \frac{2}{k_\propto}\Delta b_2 - \frac{n_\alpha}{k_\alpha}\boldsymbol{\Delta S} - \frac{j_\alpha}{k_\alpha}\boldsymbol{\Delta P} - \frac{m_\alpha}{k_\alpha}\boldsymbol{\Delta P^2}, \quad (12c)$$

where:

$$n = \frac{n_\propto + n_\rho}{2}, \quad (12d)$$

$$j = \frac{j_\propto + j_\rho}{2}, \quad (12e)$$

$$k = \frac{k_{\propto} + k_{\rho}}{2}, \tag{12f}$$

$$\delta = \frac{{v_s}^2}{{v_p}^2}, \tag{12g}$$

$$c_1 = \frac{n_{\propto} - 8\delta n_{\beta}}{2}, \tag{12h}$$

$$c_2 = \frac{j_{\propto} - 8\delta j_{\beta}}{2}, \tag{12i}$$

$$c_3 = \frac{m_{\propto} - 8\delta m_{\beta}}{2}, \tag{12j}$$

$$c_4 = \frac{k_{\propto} - 8\delta k_{\beta}}{2}, \tag{12k}$$

$$c_5 = \frac{\Delta b_1 k_{\alpha} - 2c_4 \Delta b_2}{c_1 k_{\alpha} - c_4 n_{\alpha}}, \tag{12l}$$

$$c_6 = \frac{c_2 k_{\alpha} - c_4 j_{\alpha}}{c_1 k_{\alpha} - c_4 n_{\alpha}}, \text{ and} \tag{12m}$$

$$c_7 = \frac{c_3 k_{\alpha} - c_4 m_{\alpha}}{c_1 k_{\alpha} - c_4 n_{\alpha}}. \tag{12n}$$

The scalar quantities n_{α}, n_{β}, n_{ρ}, m_{α} j_{α}, j_{β}, j_{ρ}, and m_{β} are determined from laboratory measurements and the fluid substitution model (Figure 11), while k_{α}, k_{β} and k_{ρ} can be determined from coupled reservoir simulation and geomechanical model.

For highly compacting reservoirs (e.g. chalk reservoirs where saline water interaction with carbonate weakens the reservoir matrix) the 4D difference could be dominated principally by changes in porosity, $\Delta\Phi$. Therefore, accounting for this effect in reservoir elastic properties becomes necessary in the interpretation of time-lapse difference.

We adopted the above methodology to invert for pressure and saturation changes in Forties Field between 1988 and 2005. However, we assumed that the quantities k_α, k_β and k_ρ are negligible i.e. stress-porosity sensitivity is low within the range of pore pressure changes in the interval of study). This assumption, however, will fail when pore pressure variation is much stronger or in chalk reservoirs.

Figure 12 shows the pressure and saturation change maps at the top of the reservoir. Significant variation in saturation is observed at the various well locations across the field. Production records show that over 600 million barrels of oil were produced across the field during this interval of investigation, which accounts for the observed variation. On the other hand, the pressure map reveals little or no change in reservoir pressure in the non-Charlie complexes but a higher variation of pressure in the Charlie complex. This result is validated by the reservoir pressure measurements, which indicates a 5 MPa decrease in pore pressure in the Charlie complex.

CONCLUSION

Knowledge of reservoir saturation variation is vital for in-fill well drilling, while reservoir stress variation provides a useful guide for sand production management, casing design, injector placement and production management. We show that the reservoir response to increase in stress and our ability to effectively use time-lapse seismic as a reservoir pressure monitoring tool derive from rock sensitivity to water saturation and pressure changes.

Forties Field reservoir rock and overburden shale are stress and water saturation sensitive. The weak rock frame characterizing the field provides room for grain-grain contact squeezing. A velocity decrease in the overburden, which is associated with stretching (dilation), is a direct consequence of increasing reservoir stress. Results of sand production analysis in Forties Field shows that in addition to the well-known factors, poor reservoir consolidation, high well angle of deviation through the reservoir and high flow rate, reservoir strain due to pore pressure depletion also contributes significantly to sand production. The AVO intercept provides an indication of reservoir sensitivity to changing stress and water saturation. For these reasons, time-lapse (4D) differences inverted for saturation and pressure effects and calibrated by well and production data, provide an additional tool for reservoir pressure monitoring.

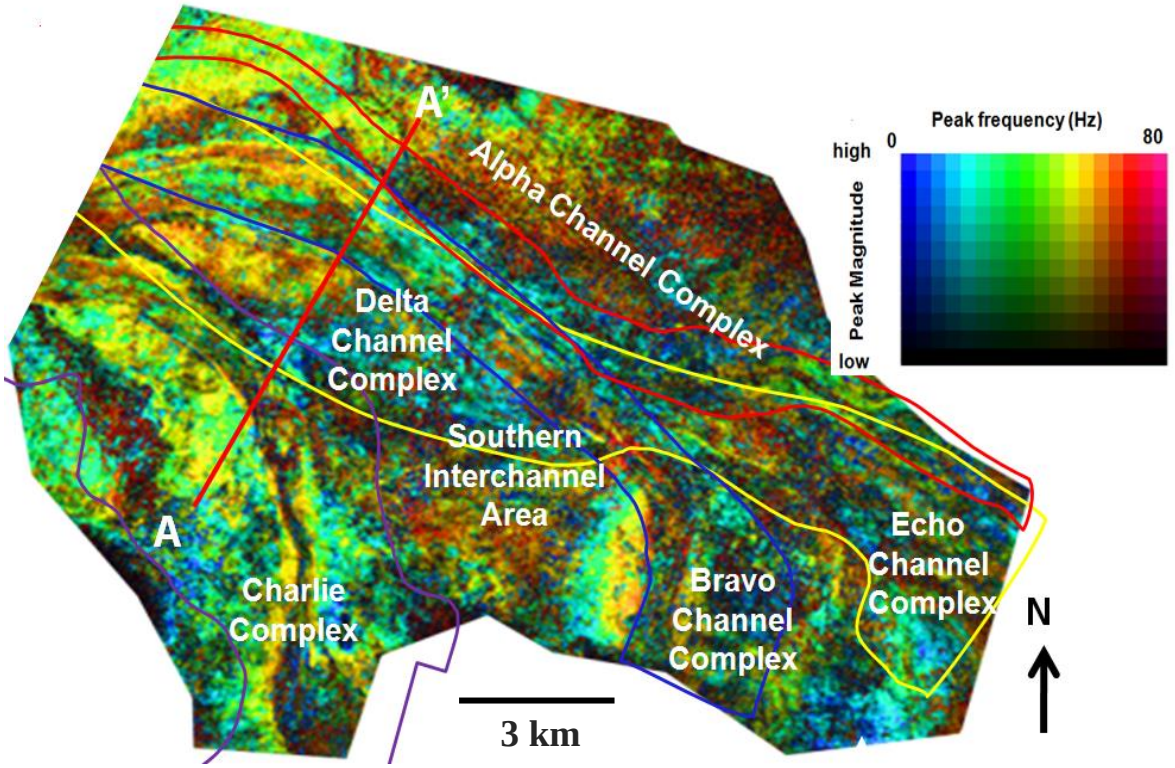

Figure 1. Forties Field channel sands- Alpha, Bravo, Charlie, Delta and Echo. Profile A-A' on the acoustic impedance difference cube is shown in Figure 3. Underlying the channel complexes are the Upper and Lower Main sheet sands. Total thickness varies between 200 and 250 m.

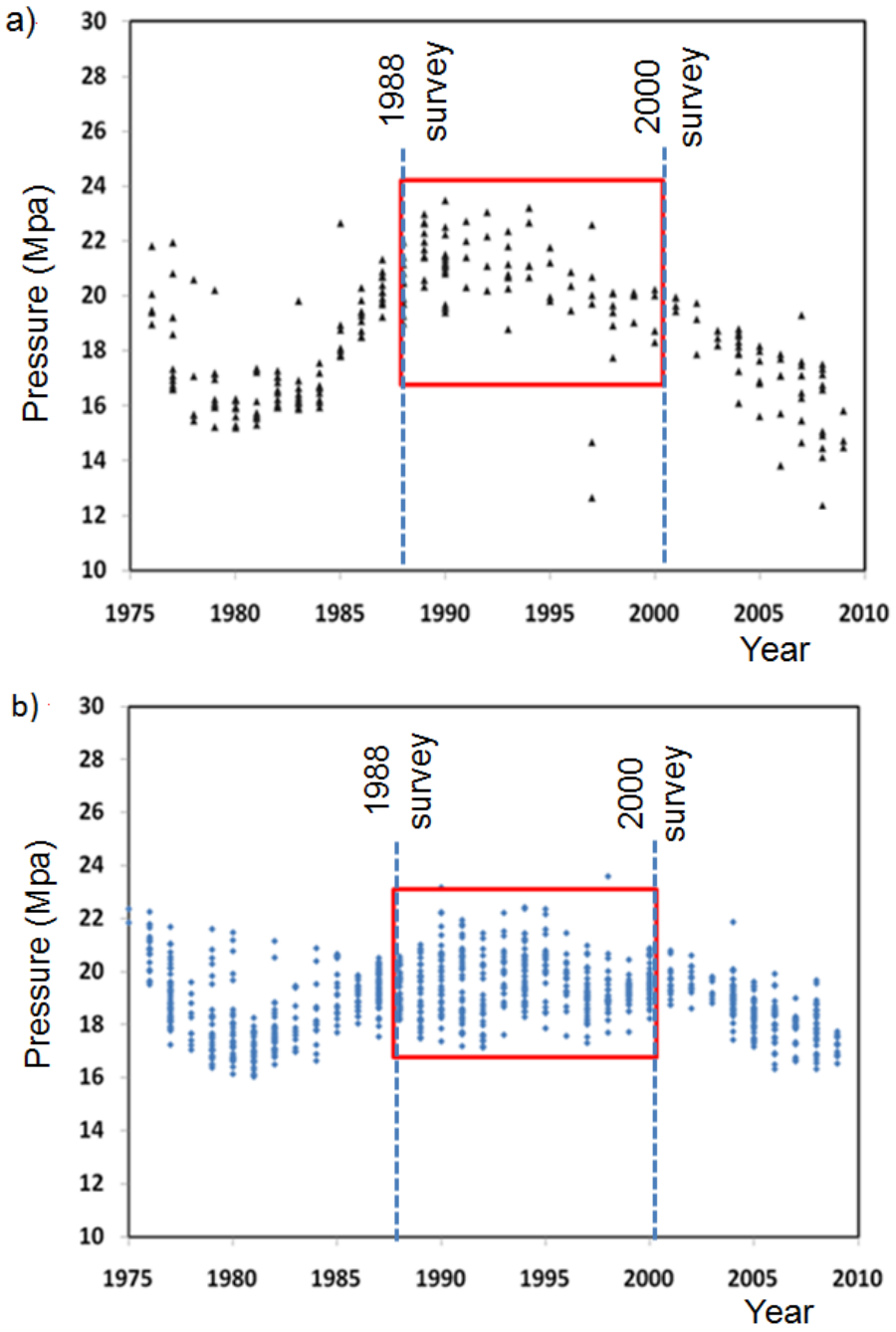

Figure 2. Forties Field pore pressure history: (a) Charlie and (b) Non-Charlie wells. The interval of interest between the two seismic surveys is marked by the red rectangle.

Pressure support in the field is through water injection.

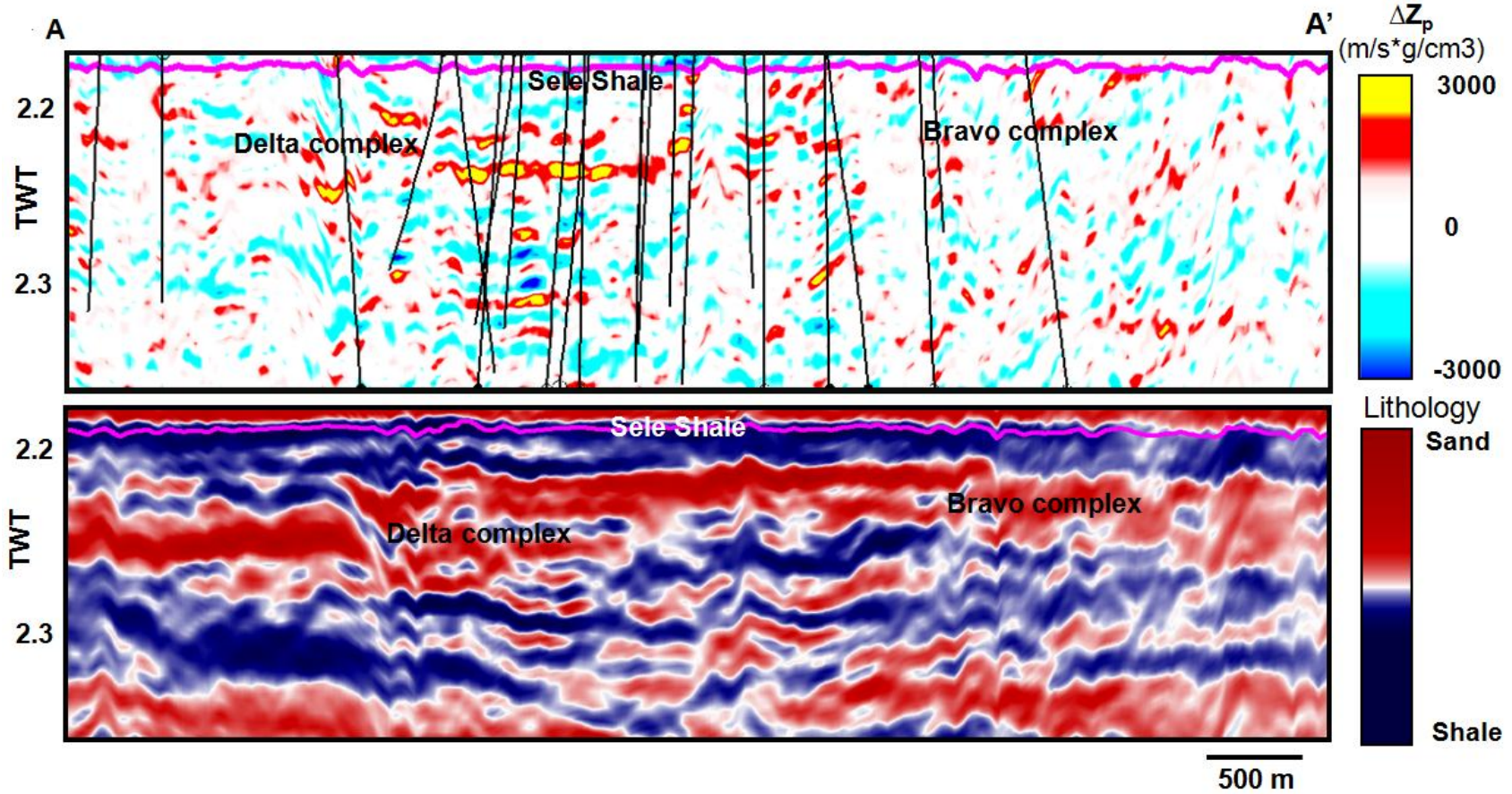

Figure 3. (a) Difference in Acoustic impedance, $\Delta Z_{p.}$ (b) The corresponding litho-cube section. The Delta complex is observed to have significant depletion in this section of the reservoir. The location of the line is shown in Figure 1.

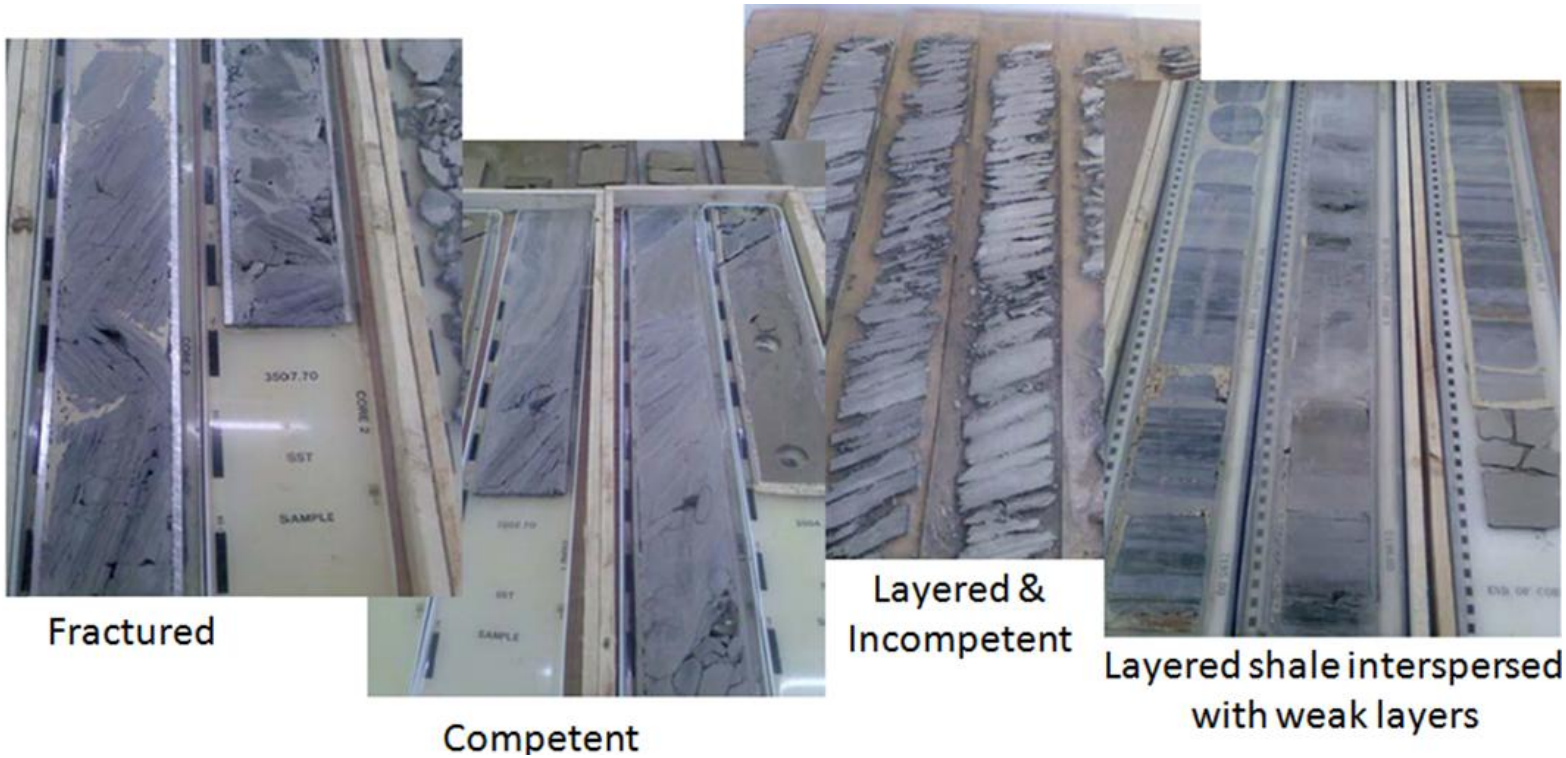

Figure 4. Images of core samples showing different overburden shale fabrics varying from competent, fractured and layered to incompetent shale. Core photos from McIntyre et al., (2009).

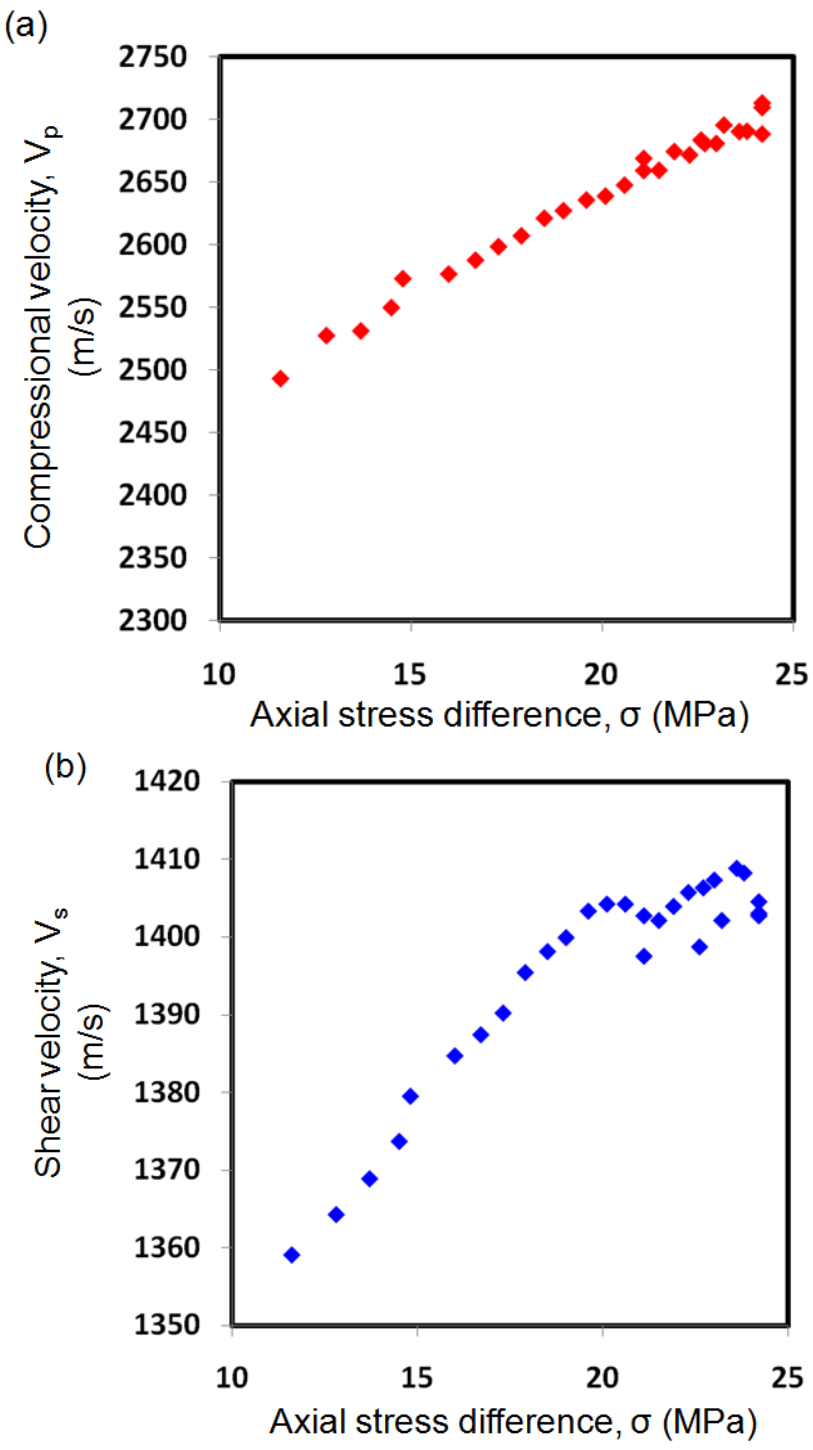

Figure 5. Overburden shale sensitivity to an increasing axial stress difference, σ, while keeping the confining pressure constant. Increase in (a) compressional and (b) shear wave velocities.

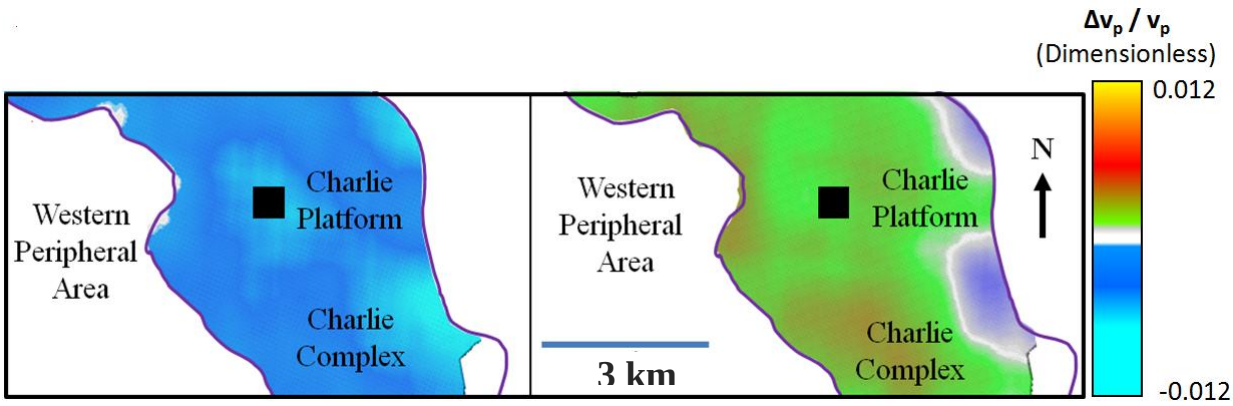

Figure 6: Decrease in velocity at the top of Sele shale (Left) and increase in velocity within the reservoir (right)

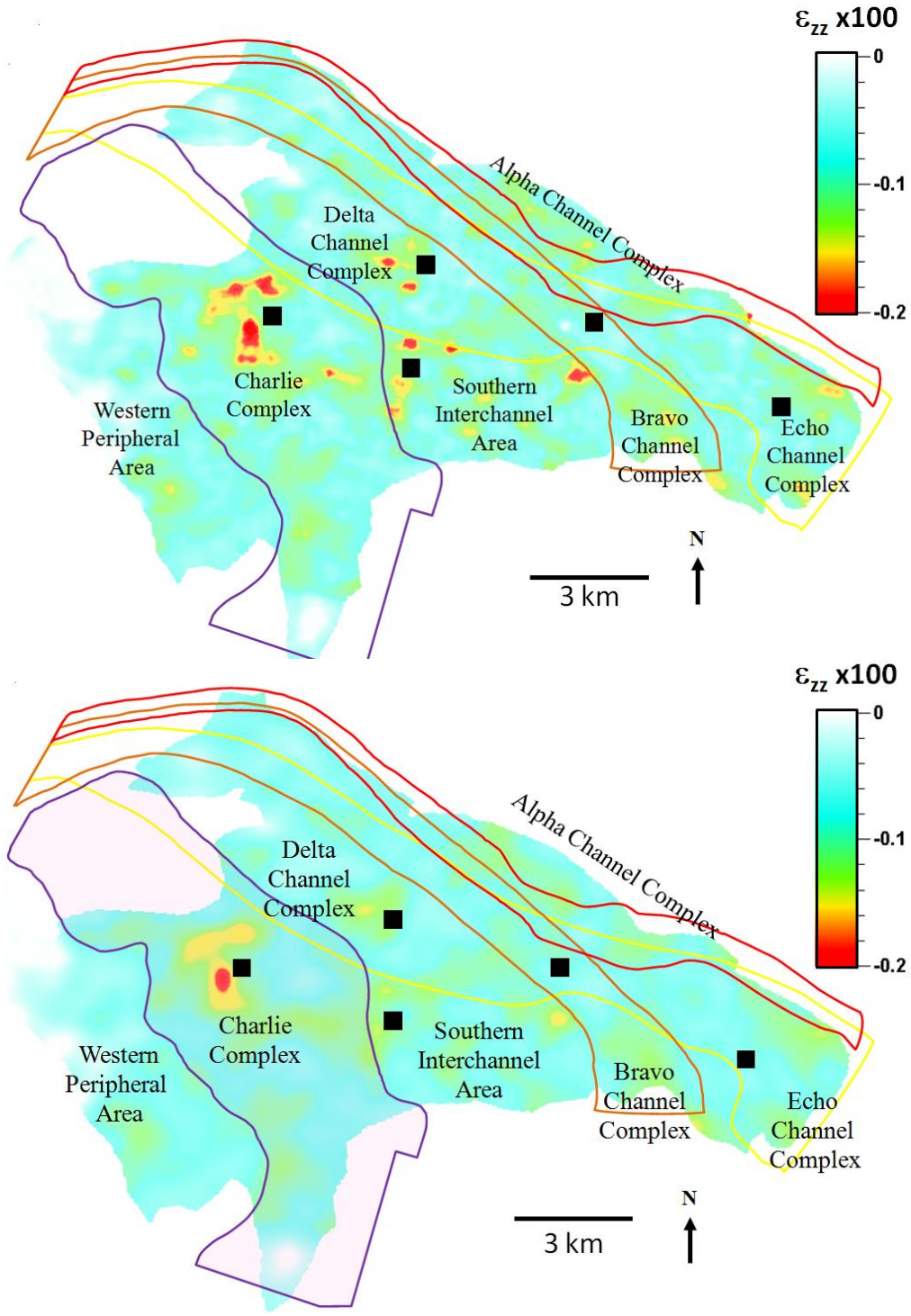

Figure 7. Computed strain, ε_{zz}, at the (a) top of the Sele regional seal and (b) base of the reservoir. The significant pore pressure decline in Charlie wells accounts for the high strain (> 0.2%) seen around the complex. Production platforms are in black squares.

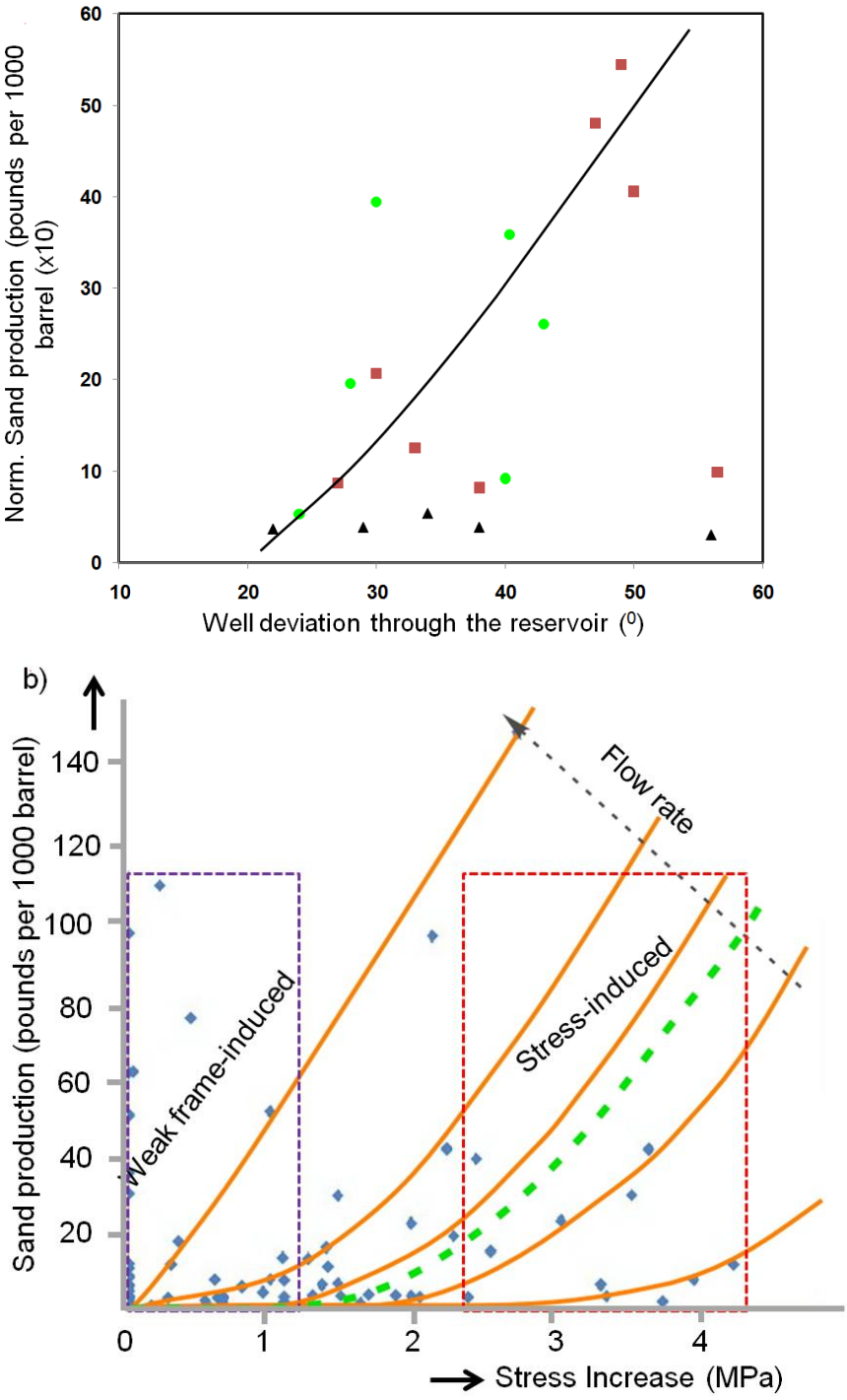

Figure 8. (a) Sand production per unit flow as a function of well deviation angle through the reservoir. (b) Average sand production increases with increase in reservoir stress. Colors in (a) represent wells from different complexes.

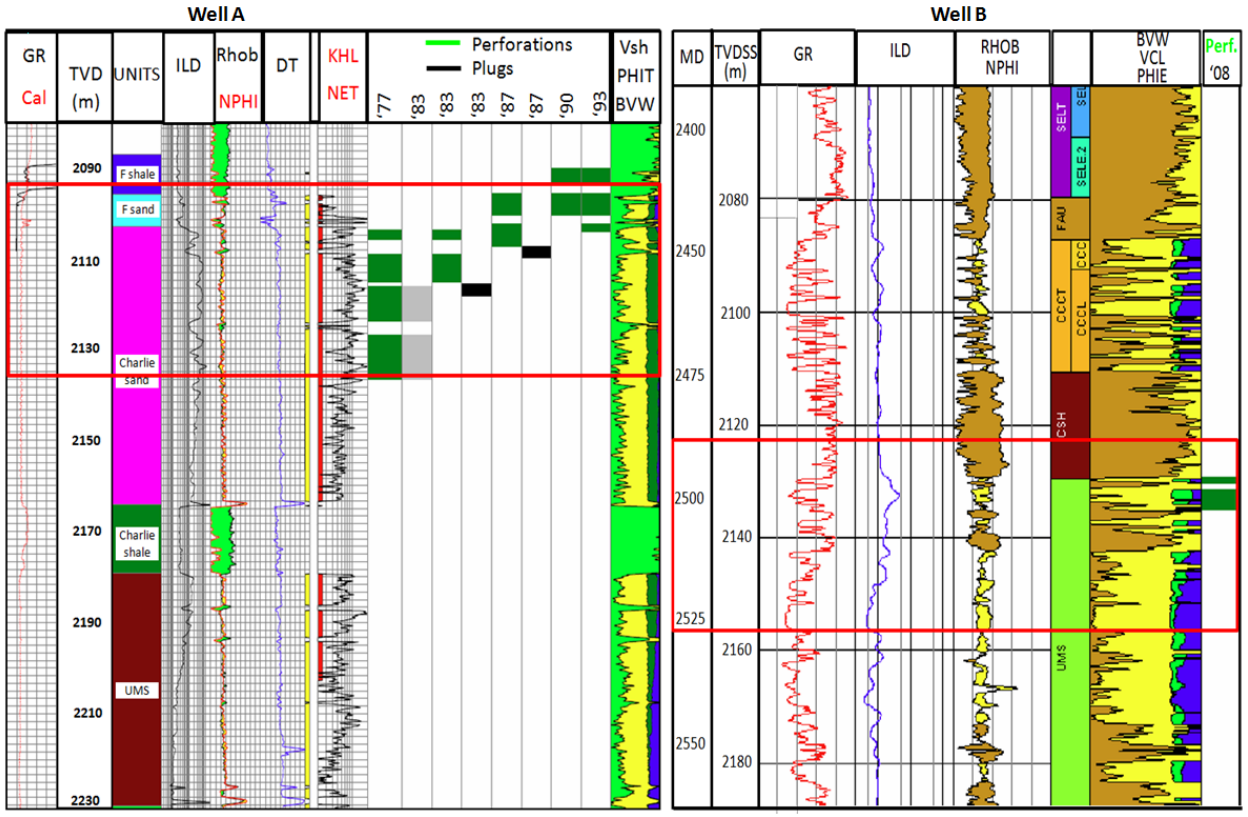

Figure 9. Logs from two high-sand producing well in Forties Field. Multiple and repeated perforation coupled with high fluid flow rate contributed significantly to the high sand production in well A, while a combination of high strain, high flow-rate and steep well deviation led to the failure of well B. The red rectangle marks the sand producing interval. KHL and BVW refer to horizontal permeability and bulk volume of water.

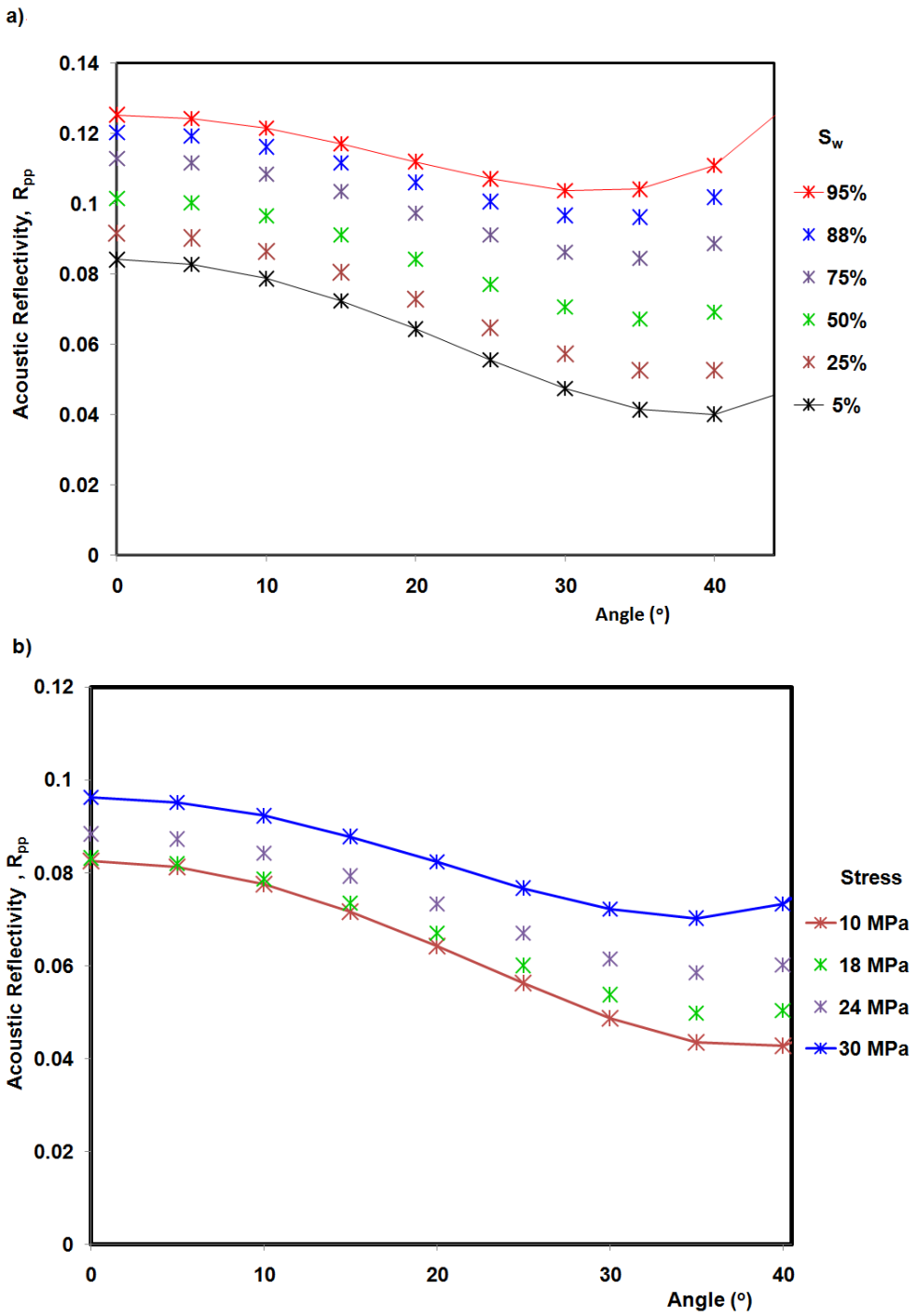

Figure 10. AVO responses to changing (a) water saturation, S_w, and (b) stress. Overburden shale velocity has been kept constant. The observed sentivities provides the bases for pressure and saturation inversion from AVO attribute difference volumes.

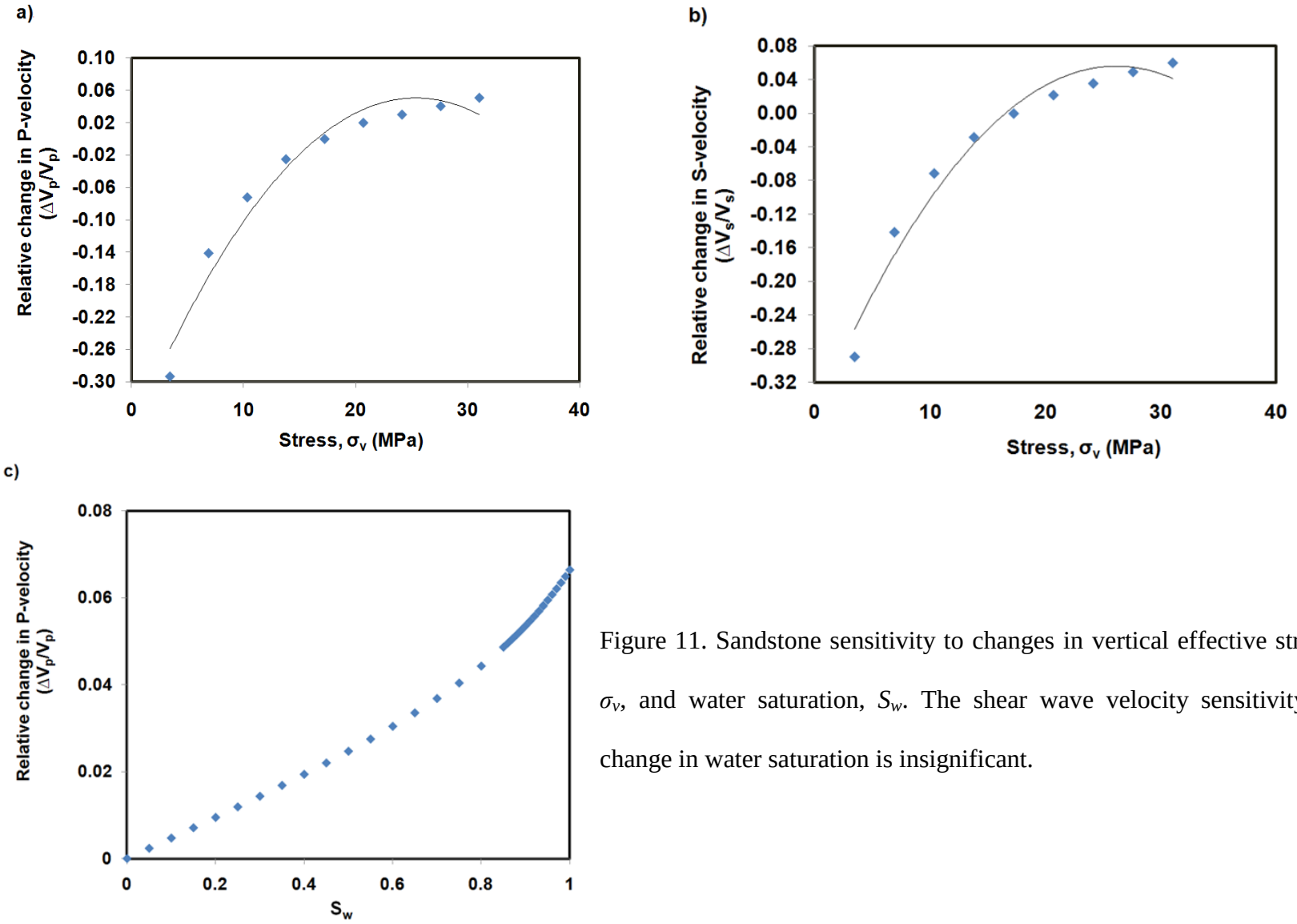

Figure 11. Sandstone sensitivity to changes in vertical effective stress, σ_v, and water saturation, S_w. The shear wave velocity sensitivity to change in water saturation is insignificant.

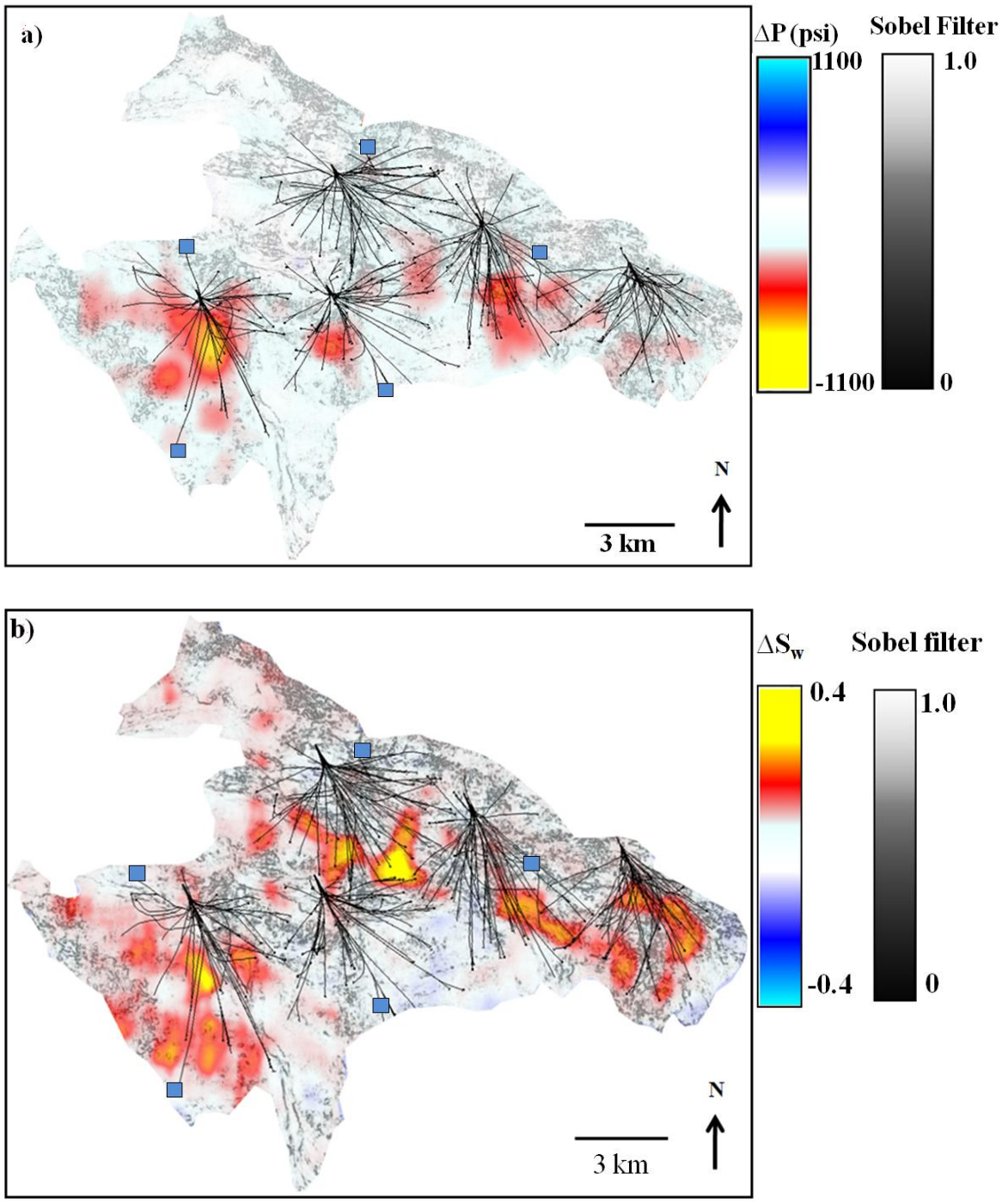

Figure 12. Time-lapse difference (1988-2005) inverted for changes in (a) pressure and (b) water saturation at the top of the reservoir using differences in AVO intercept and gradient. An edge detection attribute, Sobel filter, is shown in the background. Injector wells are shown in blue squares.

REFERENCES

Gabriels, P. W., N.A. Horvei, J. K. Koster, A. Onstein and R. Staples, 1999, Time-lapse seismic monitoring of the Draugen field: Annual International Meeting, SEG Expanded Abstracts, **18**, 2035- 2037.

Hatchell, P., and S. Bourne, 2005, Rocks under strain: Strain-induced time-lapse time shifts are observed for depleting reservoir: The Leading Edge, **24**, 1222-1225.

Hettema, M.H.H., P.M.T.M. Schutjens, B. J. M. Verboom and H.J. Gussinklo, 1998, Production-induced compaction of sandstone reservoirs: The strong influence of field stress: SPE European Petroleum Conference, SPE 50630.

Hill, P. J., and G. V. Wood, 1980, Geology of the Forties Field, U.K. Continental Shelf, North Sea, *in* Giant oil and gas fields of the decade 1968-1978: AAPG Memoir **30**, 81-93.

Landro, M., O. A., Solheim, E. Hilde, B. O. Ekren, and L.K. Strønen, 1999, The Gullfaks 4D seismic study: Petroleum Geoscience, **5**, 213–226.

Landro, M., 2001, Discrimination between pressure and fluid saturation changes from time-lapse seismic data: Geophysics, **66**, 836–844.

Landro, M., and R. Janssen, 2002, Estimating compaction and velocity changes from time-lapse near and far offset stacks: Annual International Meeting, European association of geoscientists and Engineers Expanded Abstracts, 036.

Landro, M., H. H. Veire, K. Duffault and N. Najjar, 2003, Discrimination between pressure and fluid saturation changes from marine multicomponent time-lapse seismic data: Geophysics, **68**, 1592-1599.

Landro, M., and J. Stammeijer, 2004, Quantitative estimation of compaction and velocity changes using 4D impedance and traveltime changes: Geophysics, Vol. **69**, 949-957.

Lumley, D., D. Adams, M. Meadows., S. Cole and R. Ergas, 2003, 4D seismic pressure-saturation inversion at Gullfaks field, Norway: First Break, **21**, 49–58.

McIntyre, B., T. Hibbert, D. Keir, R. Dixon, T. ORourke, F. Mohammed, A. Donald, L. Change, A. Syed and V. Biran, 2009, Managing drilling risk in a mature North Sea field: SPE Offshore Europe Oil & Gas Conference & Exhibition, SPE 124666.

Sayers, C. M., and P. M. T. M. Schutjens, 2007, An introduction to reservoir geomechanics: The Leading Edge, **26**, 597-601

Sayers, C. M., 2010, Geophysics under stress: Geomechanical applications of seismic and borehole acoustic waves: Distinguished Instructor Short Course, No **13**, 45.

Shuey, R. T; 1985: A simplification of the Zoeppritz equations: Geophysics, **50**, 609-614

Thomas, A. N., P. J. Walmsley, and D. A. L. Jenkins, 1974, Forties Field, North Sea: The American Association of Petroleum Geologists Bulletin, **58**, No. 3, 396-406.

Tura, A. and D. E. Lumley, 1999, Estimating pressure and saturation changes from time-lapse AVO data: Annual International Meeting, SEG Expanded Abstracts, **18**, 1655–1658.

Veire, H. H., H. G. Borgos and M. Landro, 2007, Stochastic inversion of pressure and saturation changes from time-lapse multi component data: Geophysical Prospecting, **55**, 805-818.

Watts, G. F. T., D. Jizba, D. E. Gawith and P. Gutteridge, 1996, Reservoir monitoring of the Magnus field through 4D time-lapse seismic analysis: Petroleum Geoscience **2**, 361–372.

Zhang, L., and M. B. Dusseault, 2004, Sand-production simulation in heavy-oil reservoirs: Society of Petroleum Engineers, No. 89037.

Acknowledgement: The authors will like to thank Apache North Sea Ltd for providing the data for this study and granting the permission to publish the results. We also thank Schlumberger and Hampson Russell for the use of their software for educational and research purposes. We are particularly grateful to Klaas Koster, Gregg Barker, Phil Rose, and Jack Orman of Apache North Sea Ltd for their tremendous support. Funding was provided by the OU AASPI consortium members.

Corresponding author: amoyedo@gmail.com

CHAPTER FOUR

4.0 SEISMIC-DERIVED GEOMECHANICAL PROPERTIES OF OVERBURDEN SHALE, FORTIES FIELD, UK NORTH SEA.

4.1 INTRODUCTION

Safe and efficient reservoir production requires understanding the geomechanical properties of not only the reservoir, but also the surrounding non-reservoir rocks (overburden and underlying strata). Drilling and well completion problems, arising from instability in the overburden, are not uncommon in deep- and ultra-deep water environment. This is due largely to rapid sedimentation and poor consolidation.

This chapter investigated overburden instability and the use of seismic-derived elastic properties to characterize zones of extreme weakness in the overburden rock of Forties Field. Adopted workflow involved laboratory measurements of rock strength and model-based inversion of rock properties.

The chapter will be submitted for the forthcoming special edition of the Leading Edge on Seismic inversion of rock properties.

SEISMIC-DERIVED GEOMECHANICAL PROPERTIES OF OVERBURDEN SHALE, FORTIES FIELD, UK NORTH SEA.

Sunday Amoyedo, Roger M. Slatt and Kurt J. Marfurt, The University of Oklahoma, USA

ABSTRACT

Rock physics-driven inversion of 3D pre-stack seismic data plays a prominent role in the characterization of both reservoir and overburden rocks. Understanding the physics of the overburden rock is required to optimize production of the reservoir and to safely guide wellbore, down-hole assembly and supporting surface facilities.

The Forties Field in-fill well drilling program is faced with severe drilling and well completion challenges. The unpredictable and highly variable shale fabrics in the overburden poses a major drilling and completion challenge in the field, where over 65% of recent wells have experienced some form of instability. While instability and subsequent failure of the overburden can be linked to the rapid decrease of the unconfined compressive strength (UCS) at inclination close to 45^0 to the bedding plane, some zones are characterized by extreme weakness regardless of the well angle through the rock. It becomes imperative to identify such zones to guide location and drilling parameters for in-fill wells in the field. In this paper, we explore the correlation between unconfined compressive strength and elastic moduli, Young's modulus and Bulk modulus, coupled with the results of simultaneous inversion to derive 3D elastic moduli calibrated to laboratory measurements to characterize the zones of extreme weakness.

INTRODUCTION

Rock physics-driven inversion of 3D pre-stack seismic plays a prominent role in the characterization of reservoir and non-reservoir rocks. Traditionally, pre-stack seismic inversion coupled with amplitude variation with offset (AVO) has been used for fluid identification and lithology discrimination (Singleton and Keirstead, 2011; Bailey et al., 2010; Hilterman et al., 2010; Zhou and Hilterman, 2010), where impedance contrast between hydrocarbon and water, sand and shale and offset-dependent seismic amplitude in hydrocarbon-bearing rocks make such identification and characterization possible. Geomechanical properties of reservoir and non-reservoir rocks (such as velocities, moduli, strength, and anisotropic parameters) are typically measured in the laboratory and consequently calibrated with well log measurements and seismic attributes for formation characterization. While laboratory measurements provide vital reservoir properties, spatial sampling is extremely limited when compared to the size of the reservoir. To overcome this shortfall in reservoir spatial sampling, vital rock properties are often inverted from 3D pre-stack seismic data. Schmid and Schmidt (2011), Gray et al., (2010) and Gray (2002) demonstrated the reliability of calibrated seismic-derived geomechanical properties of both reservoir and non-reservoir rocks. Gray et al., (2010) showed that the derivatives of simultaneous inversion coupled with estimate of seismic anisotropy can be used, with an acceptable degree of reliability, to compute the minimum, maximum and differential horizontal stresses.

Rock strength is defined by confined/unconfined compressional strength (UCS), also called the peak strength. The UCS is affected by a number of petrophysical properties including: porosity, velocity and density. Dewhurst et al., (2011) in a series of

laboratory measurements obtained a strong correlation between unconfined compressional stress (UCS) and compressional velocity, though not without some scatter . Their laboratory measurements also show a strong control of total porosity on the UCS (Figure 1a). This correlation may not be applicable to all shales. This is because of the near-uniform high total porosity (but low effective porosity) in most shales. Colwell and Frith (2006) and Carmichael (2009) further demonstrated that for poorly consolidated sediments, the Young's modulus is a good indication of the compressional stress (Figure 1b).

Forties Field, which is located in the UK sector of the North Sea, is composed of Late Paleocene sheet sands overlain by channel (Alpha, Bravo, Charlie, Delta, and Echo) complexes (Thomas et al., 1974). Porosity in the field ranges between 23 and 29% while permeability averages several hundred mD. The Forties Field in-fill well drilling program is faced with severe drilling and well completion challenges. The unpredictable and strongly varying fabrics of shale in the overburden pose a major drilling and completion challenge in the field, where over 65% of recent wells have experienced some form of instability.

Characterizing the overburden fabric will help identify the zones of extreme weakness and better guide well drilling through such zones. We use model-based simultaneous inversion of 3D seismic to characterize the overburden and identify the various fabrics of the overburden shale. We use laboratory measurement of the unconfined compressive strength (UCS) of a few competent rock samples coupled with log responses of failed wells to establish a competency threshold. We compute elastic

moduli from the results of simultaneous inversion and validate the results with well-log derived moduli.

RESERVOIR PROPERTIES OF FORTIES FIELD ROCKS

Forties Field is composed of Late Paleocene sheet sands overlain by channel (Alpha, Bravo, Charlie, Delta, and Echo) sands (Thomas et al., 1974). The reservoir, which has a cumulative thickness of about 300 m, is characterized by high porosity (23-30%) and permeability. Laboratory measurements on dry samples of Forties Field sandstone from depths ranging between 2229 and 2256 m show remarkable sensitivity of acoustic and elastic wave velocities to an increase in confining stress. Specifically, compressional velocities increase from 2560 to over 3400 m/s while shear velocities increase from under 1600 to 2180 m/s, corresponding to an increase in confining stress approaching 30 MPa. A similar velocity sensitivity is observed in the Forties cap-rock (Sele shale) when a slow tri-axial compressional stress is applied. Both compressional and shear velocities increase almost linearly with increasing stress. This velocity sensitivity can be explained by grain-to-grain squeezing, closure of micro-cracks, and a slight porosity loss. The relatively high sensitivities to stress changes recorded on Forties samples is due, in addition to the aforementioned factors, to the weak rock frame providing room for easy squeezing along grain-grain contacts. This sensitivity is further seen in the amplitude variation with offset (AVO) as both water saturation and pore pressure change.

Analysis of the impact of reservoir shaliness (volume of clay) shows a strong control of the volume of shale on both the petrophysical and geomechanical properties of the reservoir. Shale densities vary between 2.2 and 2.45 g/cm^3, while sand densities range between 2.13 and 2.3 g/cm^3 in clean water-bearing intervals. However, the compressional wave velocity is observed to be faster in the sandstone. Figure 2 is a crossplot of slowness and density from 17 wells. We observe an increase in compressional wave slowness with increasing volume of clay. This pattern can also be seen in the crossplot of the bulk modulus and neutron porosity, where incompressibility is observed to decrease as the volume of shale increases.

The Forties Field overburden Sele shale is characterized by strong anisotropy related to its layered and fractured nature. The anisotropic signature is highlighted by the variation of compressional slowness at different angles relative to the bedding plane (Figure 3). The anisotropy in the overburden causes the strength of the Sele Formation to be highly variable (McIntyre et al., 2009).

Up to date, a large number of wells have been drilled in Forties Field, only a few have dipole sonic logs in either producer or injector wells. In those wells with dipole sonic logs, the reliability of shear wave velocity measurement in the field vary considerably. A strong correlation between compressional and shear wave velocities (Figure 4) enables the modeling of shear wave velocities in wells with no or unreliable measurements. Figure 5 shows the comparison of the model prediction with actual well log measurements. The regional Sele formation is marked by a light green shading.

The inter-dependence of petrophysical and geomechanical properties of both reservoir and overburden rock provides a means to model several geomechanical properties (bulk modulus, Young's modulus, Poisson's ratio, lambda-rho and mu-rhob).

In general, we observe a strong correlation between the elastic moduli and acoustic impedance in most formations. This correlation may also be used for the direct computation of elastic modulus from acoustic impedance (Banik et al., 2010). In this field of study however, the correlation is tends to be poor in the overburden shale.

OVERBURDEN INSTABILITY AND WELL FAILURES

Forties Field, which began production in the 1970s, is characterized by a poorly-consolidated reservoir as well as by a weak overburden. The field has continued to produce through a comprehensive reservoir monitoring program. This concerted effort to keep the 'giant' alive is faced with a series of difficult drilling, well completion and severe sand production problems leading to lost production and corrosion of materials. Where possible, remedial activities cost millions of dollars per annum and often lead to total loss of wells. These losses ultimately add to production cost.

The unpredictable and strongly varying fabrics of shale in the overburden also pose a major challenge during drilling in Forties Field, where over 65% of wells drilled between 2002 and 2007 have experienced some form of instability problem (McIntyre et al, 2009). The irregular distribution of competent and weak shale across the field partly explains why one well will fail and the next will not. Figure 6 shows various

fabrics of the overburden shale ranging from competent to extremely weak rock typically encountered in the field.

Laboratory measurement of the unconfined compressive strength (UCS) of rock samples provides a means to identify different fabrics of shale based on their rock strength. Competent samples are characterized by high strength while weak fabrics have low values of UCS. For practical reasons, only a few measurements of the UCS can be made from which correlation with other petrophysical/geomechanical properties can be established. This correlation can in turn be used to compute rock strength-related parameters (elastic moduli). To obtain the compressive strength of Forties Field rock samples, some samples were subjected to a gradual increase in stress until failure. This procedure was carried out at different confining pressure (200, 400 and 600 psi). The compressive strength was calculated using

$$UCS(psi) = \frac{1450}{CSA} * Peak\ Load\ (kN), \quad (1)$$

where *CSA* is the cross sectional area in cm^2. The multiplying factor, 1450, is added to convert to *psi*.

The result of the above laboratory measurement shows a good correlation between static Young's modulus and compressive strength (Figure 7).

Apart from the unpredictable occurrence of weak overburden, Keir et al., (2009), using a series of laboratory measurements, show that the unconfined compressive strength of the Forties Field overburden also varies strongly with the angle to the bedding plane. The authors observed that the UCS decreases by almost 85% when the angle of

deviation approaches 45^0 to the bedding plane (Figure 7b). This observation suggests that wells drilled at or close to this angle through the overburden are more susceptible to collapse. The authors further showed that as the inclination angle approaches 45 degrees the correlation between the static Young's modulus and rock strength decreases significantly.

Analysis of logs in failed wells further shows that, in addition to Young's modulus, shear modulus or mu-rho can also be used to identify the weak overburden (Figure 8). The above observations form the basis for the use of elastic moduli (mainly Young's, shear moduli and mu-rho) computed using simultaneous inversion in order to map weak overburden facies in Forties Field.

PRE-STACK SEISMIC INVERSION FOR OVERBURDEN GEOMECHANICAL PROPERTIES

Seismic wave reflectivity is impacted by the geomechanical properties of the medium through which the wave propagates. The properties include compressibility, rigidity and bulk density. Goodway et al., (1997), using amplitude variation with offset (AVO), derived Lamé's parameters lambda (λ), mu (μ) and density (ρ), from which other moduli can be computed. Other products of simultaneous inversion of long offset gathers, such as Z_p, Z_s, V_p, V_s and density, provide a means to compute reservoir petrophysical properties and geomechanical properties.

The different fabrics of shale characterizing the Forties Field overburden exhibit different strength/rigidity, which in turn makes their characterization possible on seismic-derived moduli volumes.

We used a model-based simultaneous inversion to compute the elastic moduli of the Forties Field Sele Formation overburden. Maximum offset of the pre-stack gather is 3112 m or about 38 degrees for a depth of investigation between 2200 and 2800 m, which is sufficient for a reliable inversion for rock properties (Figure 9). The inversion result shows a relatively high error in the estimation of density. This margin of error is attributable to rock physics constraints i.e. weak correlation between density and velocity especially in sandstone and sandy shale intervals. Assuming an isotropic medium, we compute the Young's modulus as

$$E = \frac{9\rho\left(V_p^2 - 1.33V_s^2\right) * G}{\left[3\rho\left(V_p^2 - 1.33V_s^2\right) + G\right]}, \quad (2)$$

where ρ, V_p and V_s are density compressional velocity and shear velocity. G is the shear modulus, (and equivalent to Lame's parameter, μ):

$$G = \rho * V_s^2 = \mu \quad (3)$$

DISCUSSION OF INVERSION RESULT

The Sele Formation, which forms the regional cap rock in most North Sea fields, is composed of non-calcareous silty claystones with some thin ash layers. The Formation is characterized by lower impedance and relatively low elastic moduli compared to the Forties shale and the underlying sandstone (Figures 10a and b). Figure 11 shows the comparison between seismic-derived elastic moduli and computed moduli from well logs. The relatively lower rock strength in the overburden also varies considerably with the different shale fabrics present in the overburden. The Young's modulus extracted at the Sele Formation (Figure 12) shows a wide variation between 1.5 and 18 GPa, corresponding to very weak and competent shale fabric, respectively. Slow tri-axial compressional test at a confining effective pressure of 12.9 MPa on three samples of competent Sele Formation shows that the Young's modulus of the cap rock ranges between 11 and 19 GPa, which falls within the range of seismic-derived values.

We have defined a 6 GPa Young's modulus threshold for stability in the overburden. The threshold is based on laboratory measurements on a few samples of competent shale compared with the log responses in wells that have encountered some form of instability in the overburden. The Young's modulus map of the overburden (shown in Figure 12) indicates that the distribution of the shale fabrics is not random as initially assumed. Extreme weakness (Young's modulus less than 4 GPa and shear modulus less than 1.3 GPa-Figure 13) are observed in two zones of the overburden. These areas are marked by white polygon. Fairly weak areas are appear as cyan on the map ($4.0\ \text{GPa} < E < 6.0\ \text{GPa}$ and $1.3 < G < 2.0\ \text{GPa}$). Stable and competent areas of the overburden are in red and yellow colors.

Our inversion results and subsequent classification of the degree of competency do not take into account the 45^0 plane of weakness. This suggests that the areas exhibiting high moduli values (Young's and Shear moduli) on the inversion results are also susceptible to instability when penetrated at an angle close to the plane of weakness.

CONCLUSION

The Forties Field in-fill well drilling program is faced with steep drilling and well completion challenges. The widely varying fabrics of shale in the overburden, which might be related to the depositional process, poses a major challenge in the field, where over 65% of wells drilled between 2002 and 2007 have experienced some form of instability. Overburden shale fabrics vary from weak layered to competent shale. While instability and subsequent failure of the overburden can be linked to the rapid decrease of the (unconfined compressive strength) UCS at inclination close to 45 degrees to the bedding plane, some zones are characterized by extreme weakness irrespective of the inclination of the wellbore. Except at the plane of weakness, there exists a good correlation between laboratory-measured UCS and incompressibility (Young's Modulus). Elastic moduli (Young's and Shear moduli) from model based simultaneous inversion, calibrated to laboratory measurements, help characterize zones of extreme weakness. These zones are susceptible to collapse during drilling irrespective of the well deviation angle through the overburden.

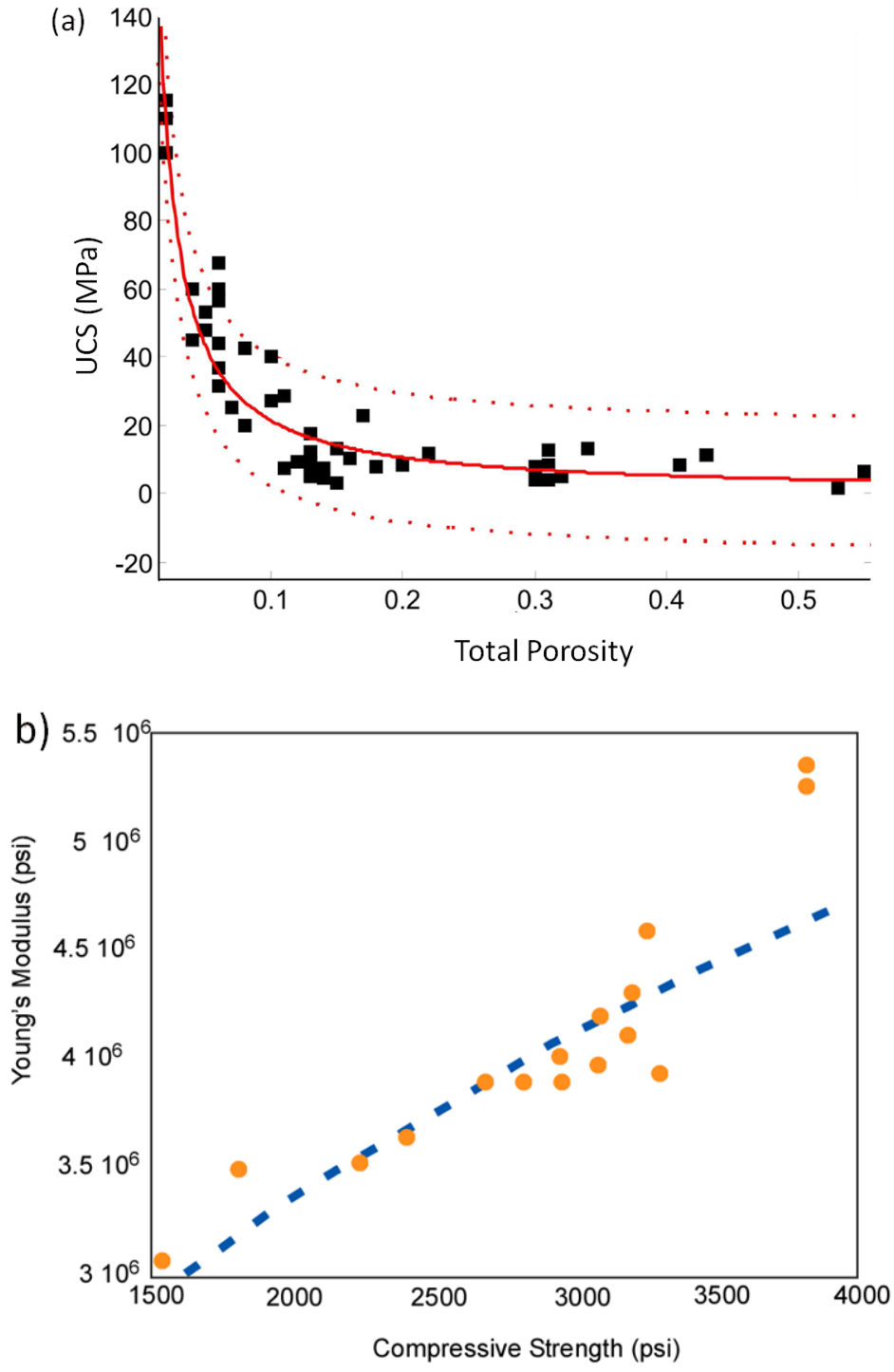

Figure 1. (a) Unconfined compressional strength (UCS) versus Total porosity (b) Young's Modulus versus compressional strength. After Dewhurst et al., (2011) and Carmichael R.P. (2009).

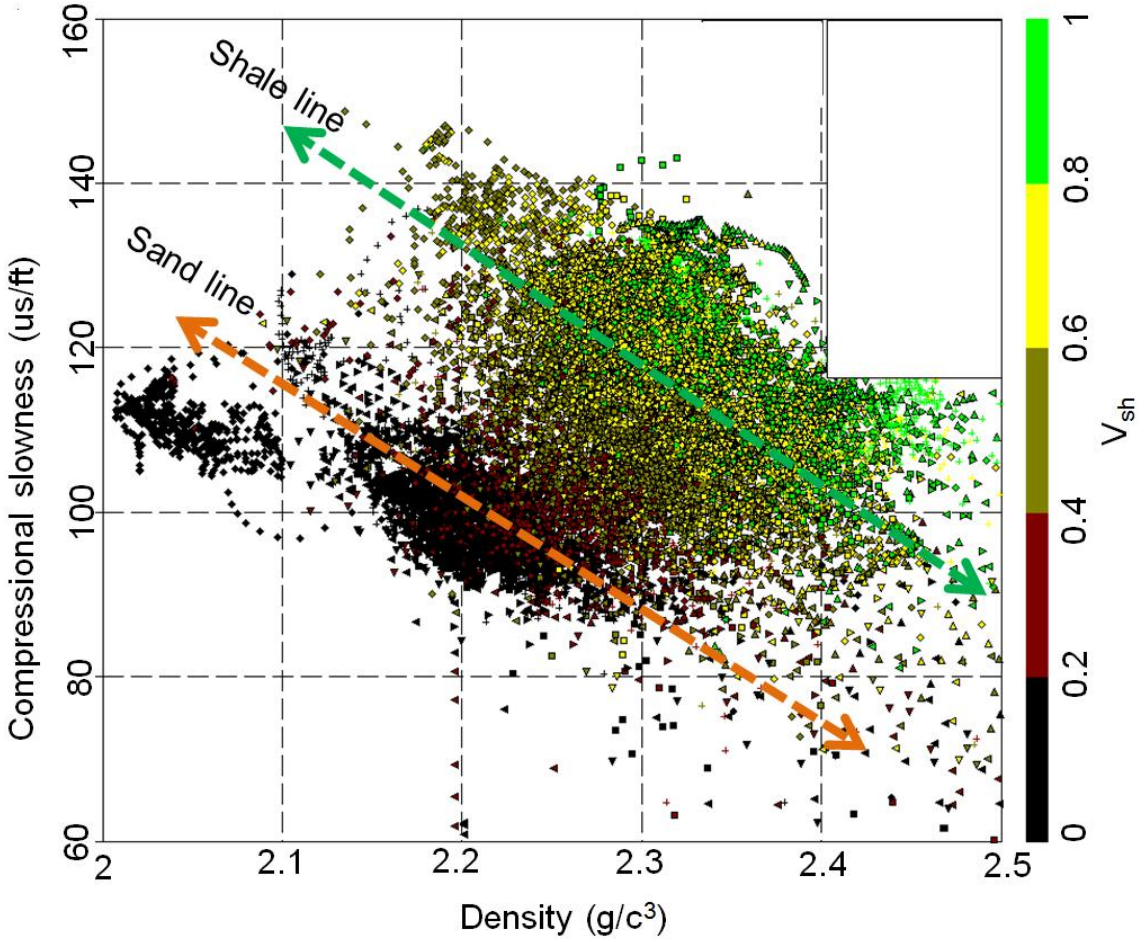

Figure 2. A plot of slowness (sonic transit time) versus density for both reservoir and non reservoir. Forties Field reservoir properties are controlled largely by the volume of shale (VSH).

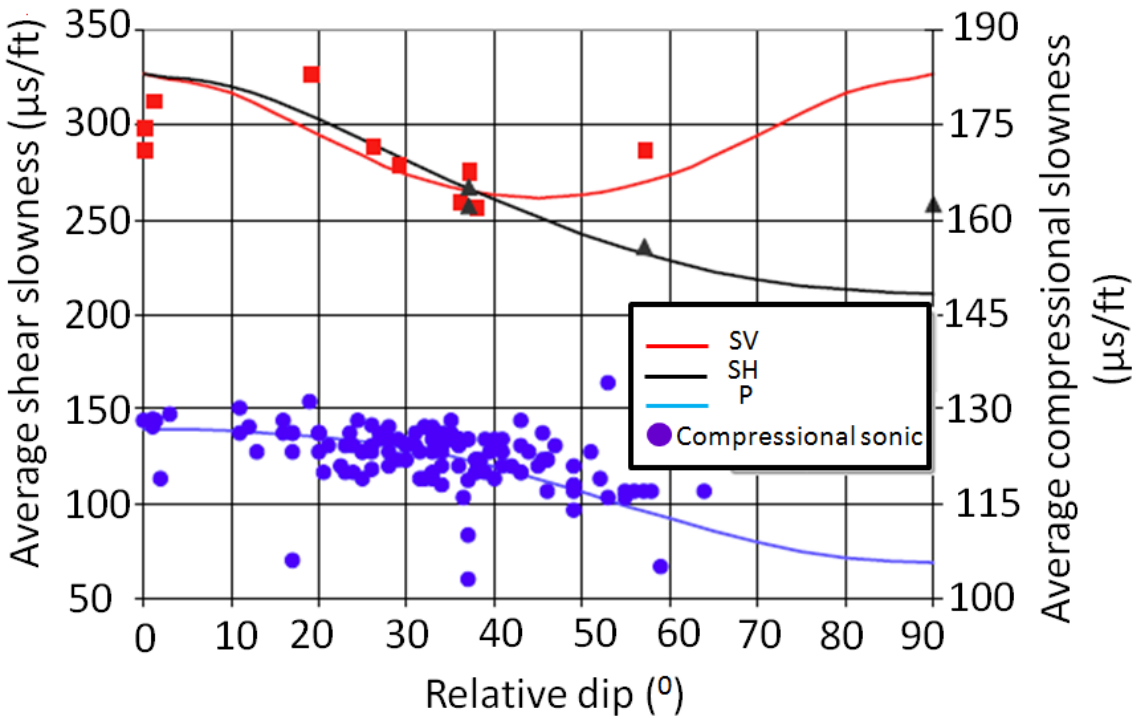

Figure 3. Primary signature of anisotropy in Forties Field overburden: Variation of slowness (sonic transit time) with dip. SV and SH refer to vertically and horizontally polarized shear wave. After McIntyre et al., (2009).

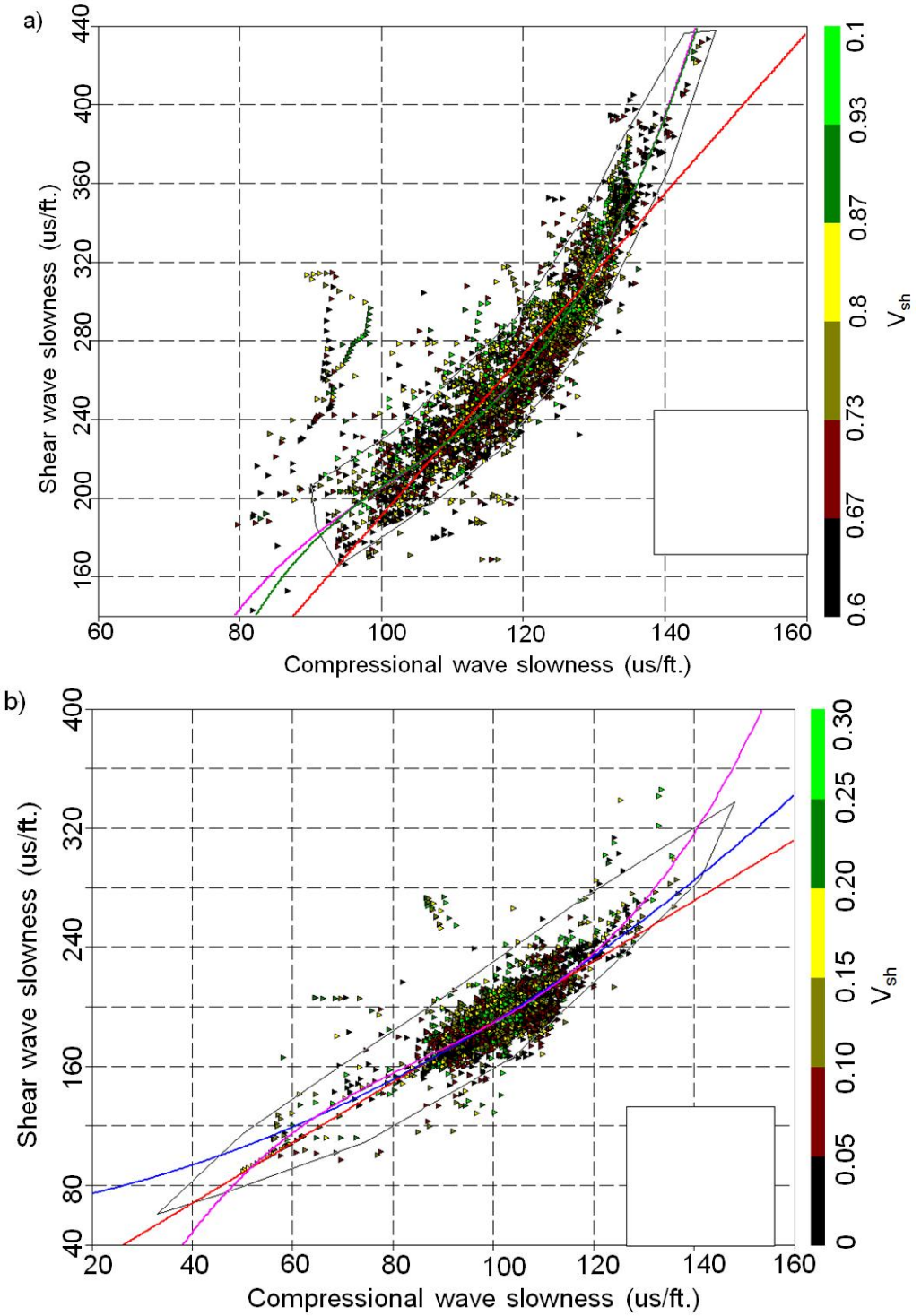

Figure 4. Cross plot of shear against compressional slowness for (a) the overburden Sele shale and (b) the reservoir sandstone. The correlation was used for the estimation of shear velocity in wells with no or poor well data.

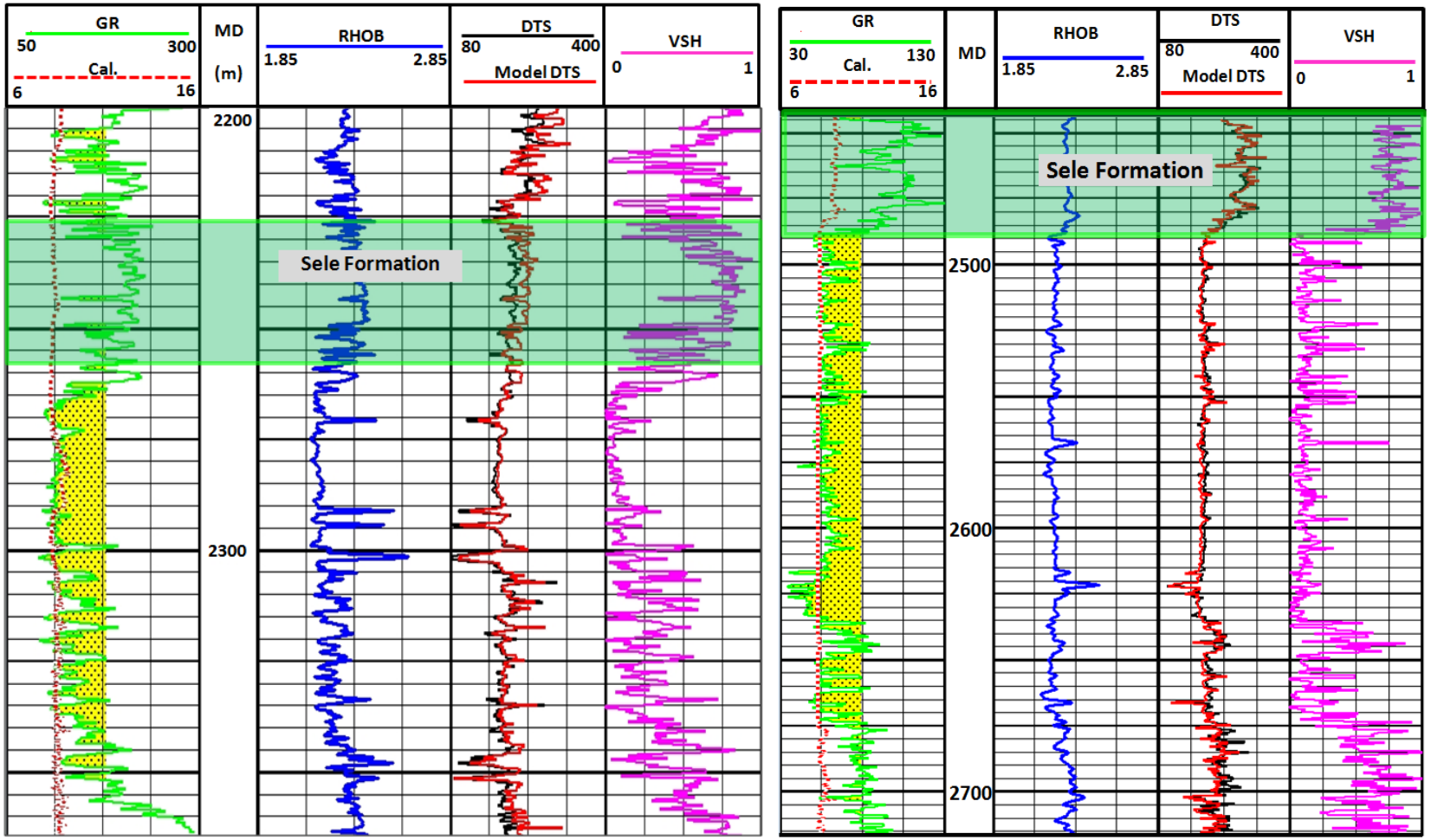

Figure 5. Typical log responses in Forties Field. Two blind wells are used to validate the modeled shear wave velocity. The actual shear velocity (DTS) and model DTS are shown in track 3 in both wells. The Sele Formation is marked with green shades.

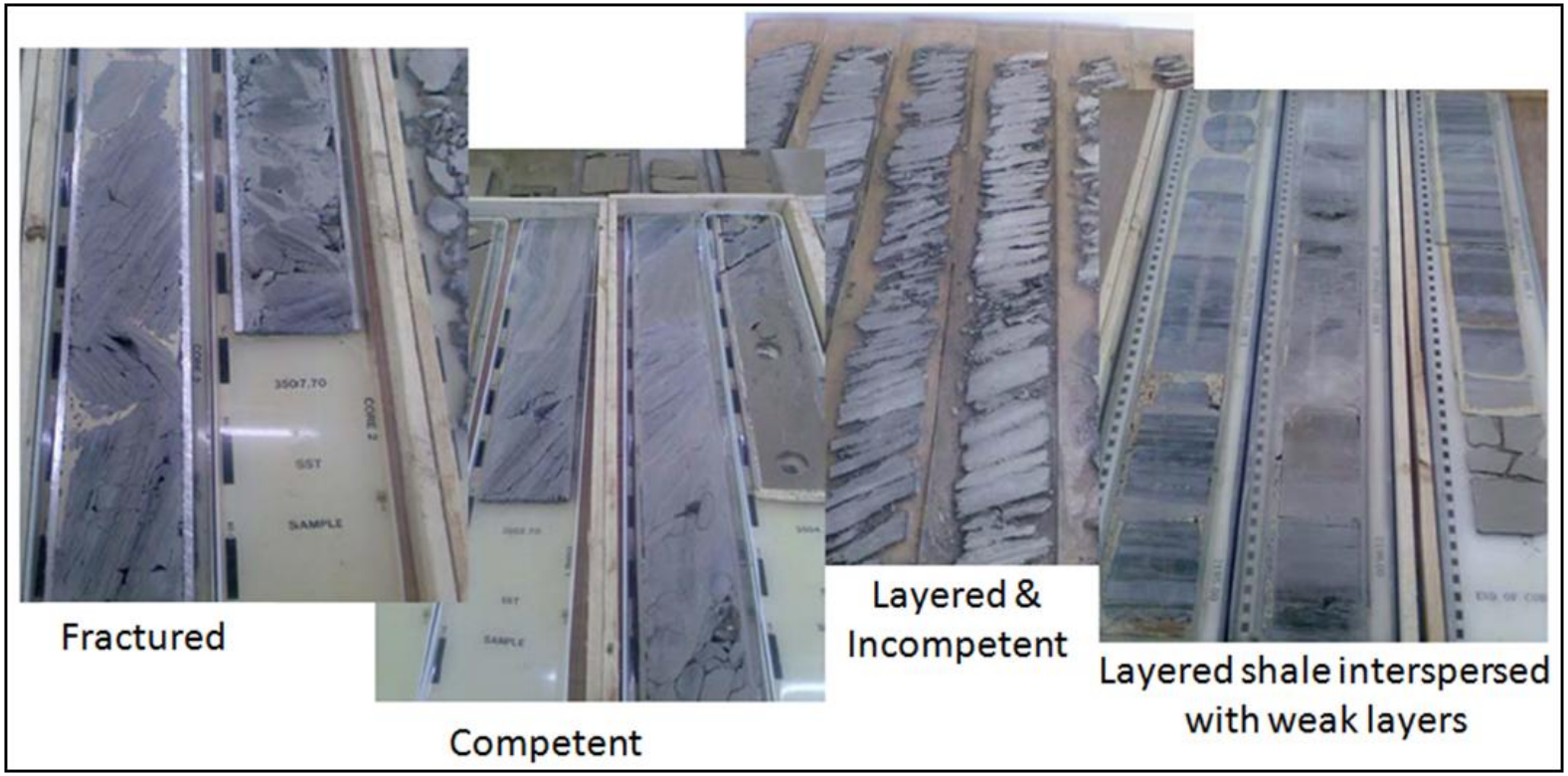

Figure 6. Images of core samples showing different overburden shale fabrics varying from competent, fractured and layered to incompetent shale. Core photos from McIntyre et al., (2009).

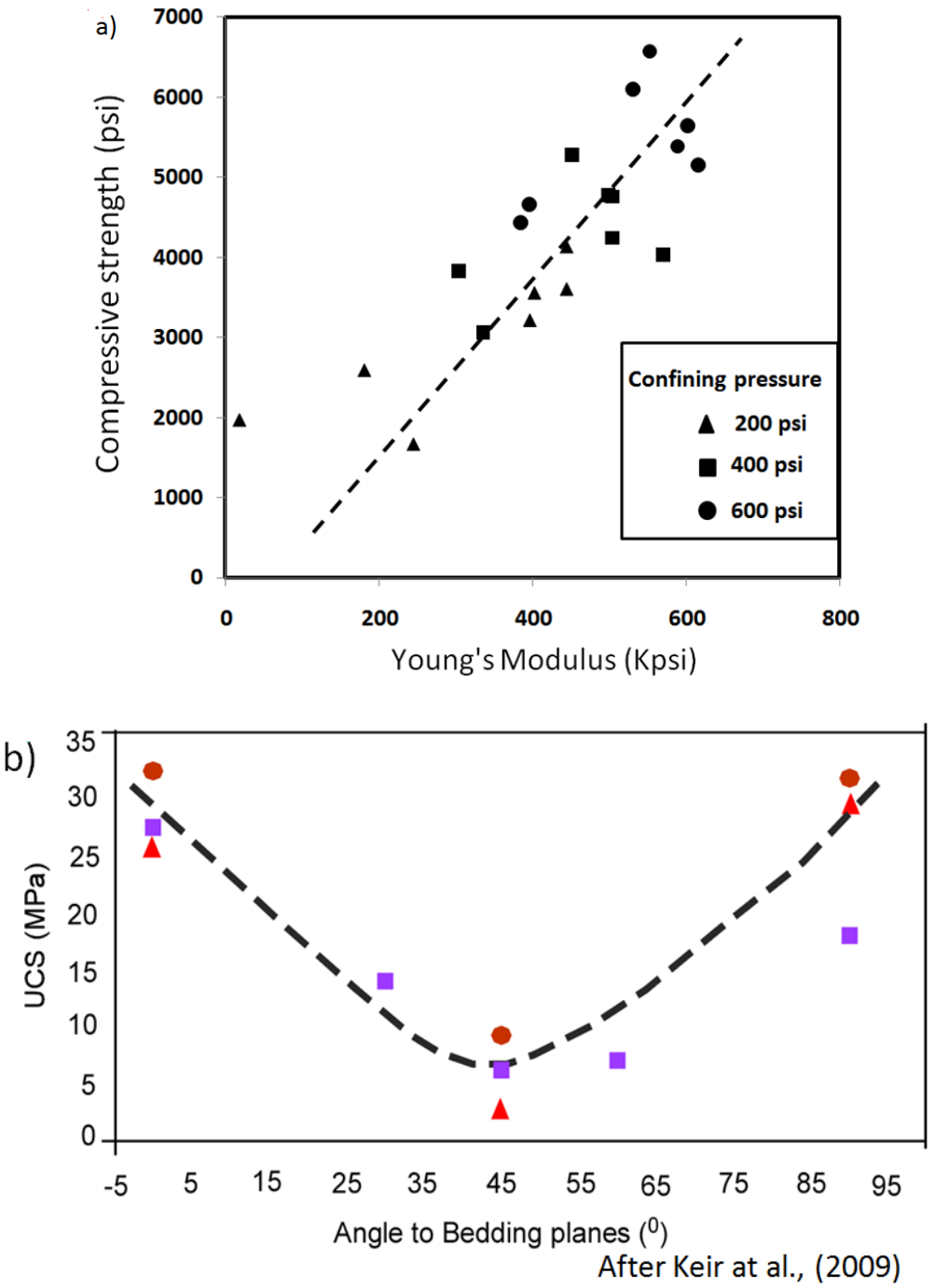

Figure 7. (a) Cross plot of compressive strength (CS) at 200, 400 and 600 psi and Young's modulus, b) plot of unconfined compressive strength (UCS) at various angles to the bedding plane. The variation of UCS with angle will severely degrade the reliability of rock strength from elastic moduli. Colors in lower diagram represent measurements from different rock samples.

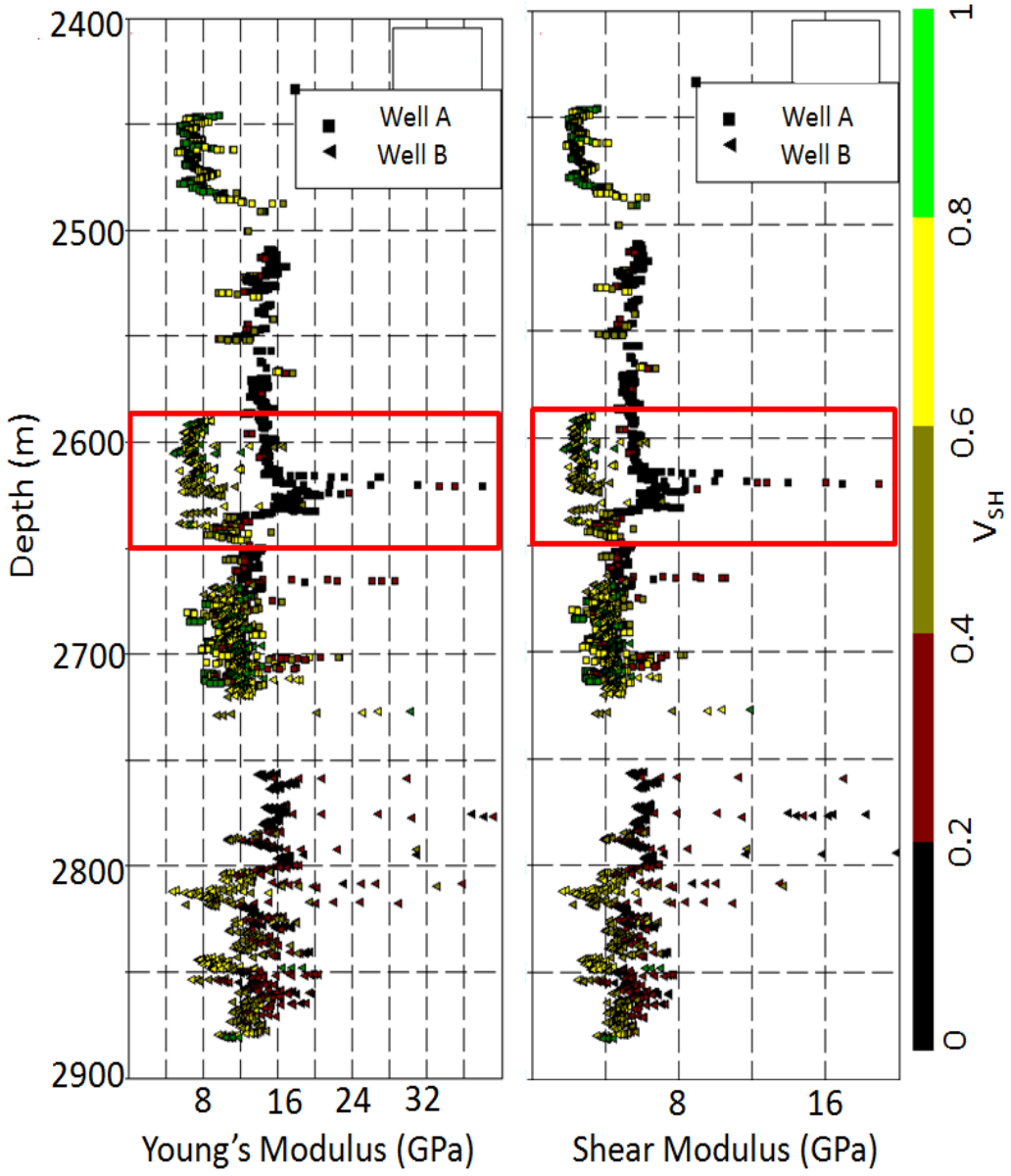

Figure 8. Elastic moduli (Young's and Shear moduli) in two wells showing competent and weak overburden Sele Formation (marked by red rectangle). The weak overburden in well B is indicated by low values of Young's and shear moduli. This pattern of deviation from normal trend has been observed in other wells that have experienced some instability in the overburden.

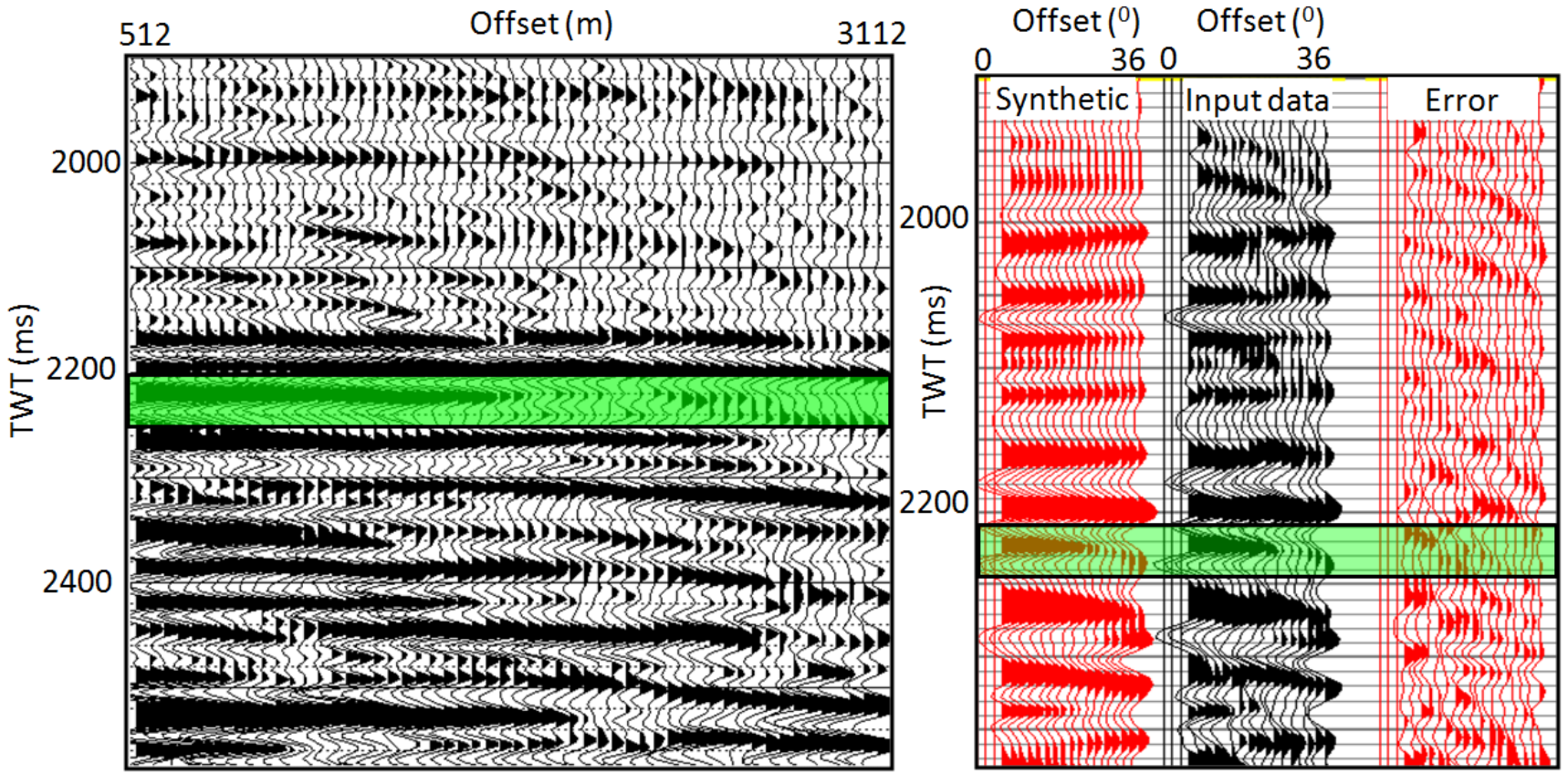

Figure 9. (a) Input CDP gather for simultaneous inversion. (b) Inversion result: comparing synthetic data with the input volume. The regional Sele Formation is highlighted by the green shading in both sections. Observe the gradual decrease of amplitude with offset in the marked zone.

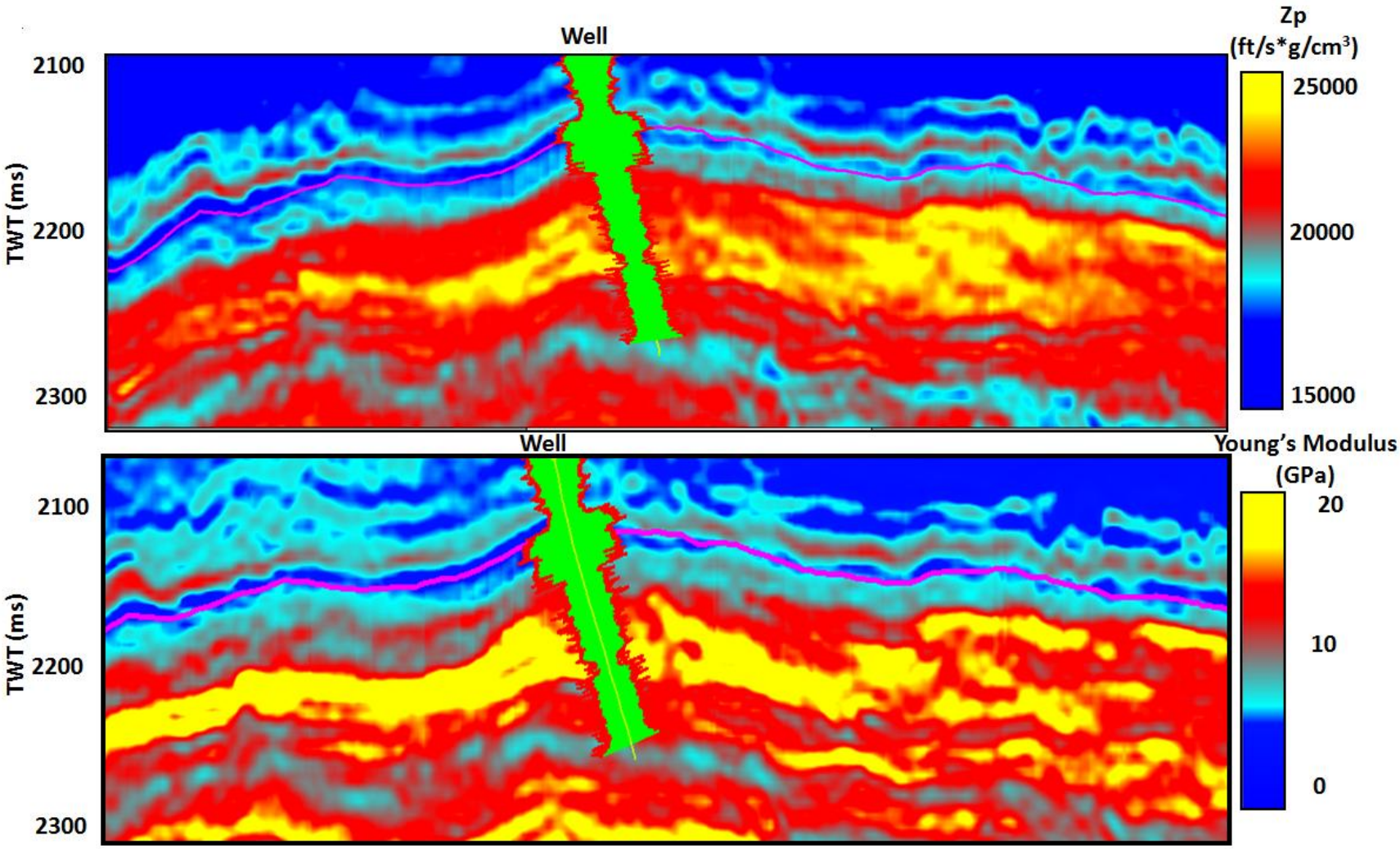

Figure 10. (a) Acoustic Impedance and (b) Computed Young's modulus. The Sele Formation is indicated by the purple pick, corresponding to low values of impedance and Young's modulus. Gamma ray log is shown along the trajectory of a well.

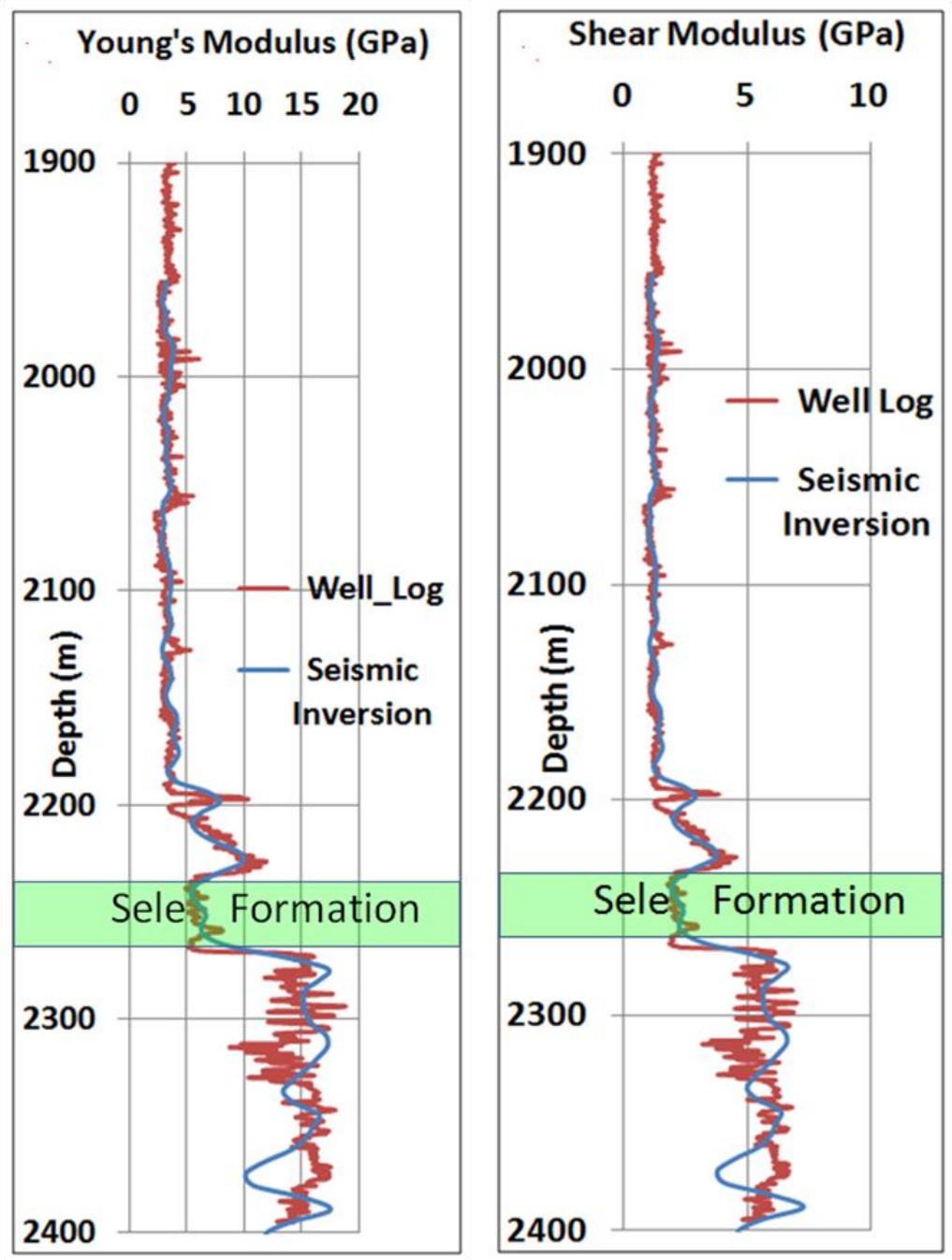

Figure 11. Comparing seismic derived elastic moduli with computed moduli from well logs. The zone of interest is marked the marked Sele Formation. Inversion parameters were optimized for the overburden and less than optimum for the reservoir.

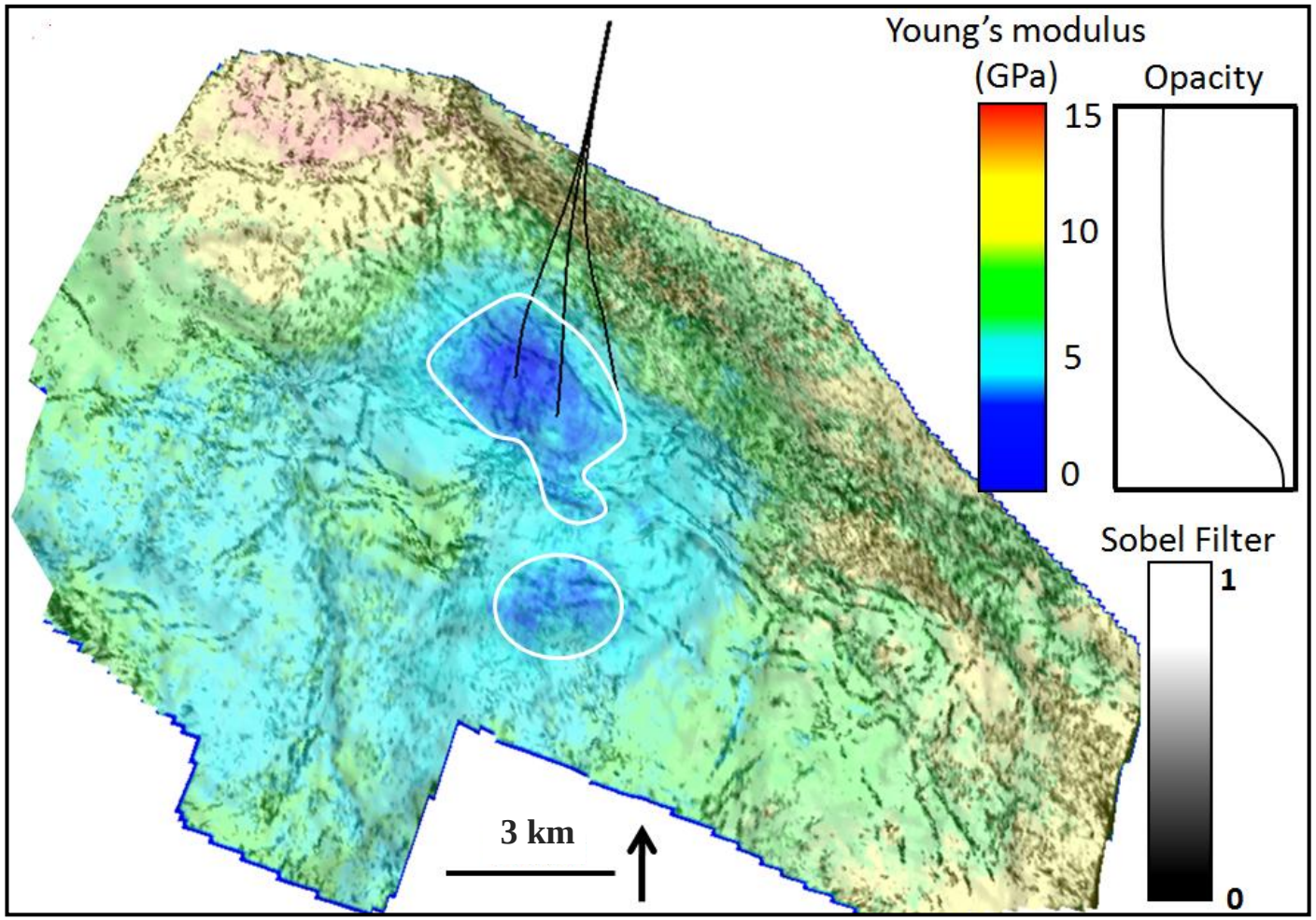

Figure 12. Young's modulus of the Sele Formation. Zones of extreme weakness are marked by white polygons. The fault network is shown in the background by an edge detection attribute, the Sobel filter.

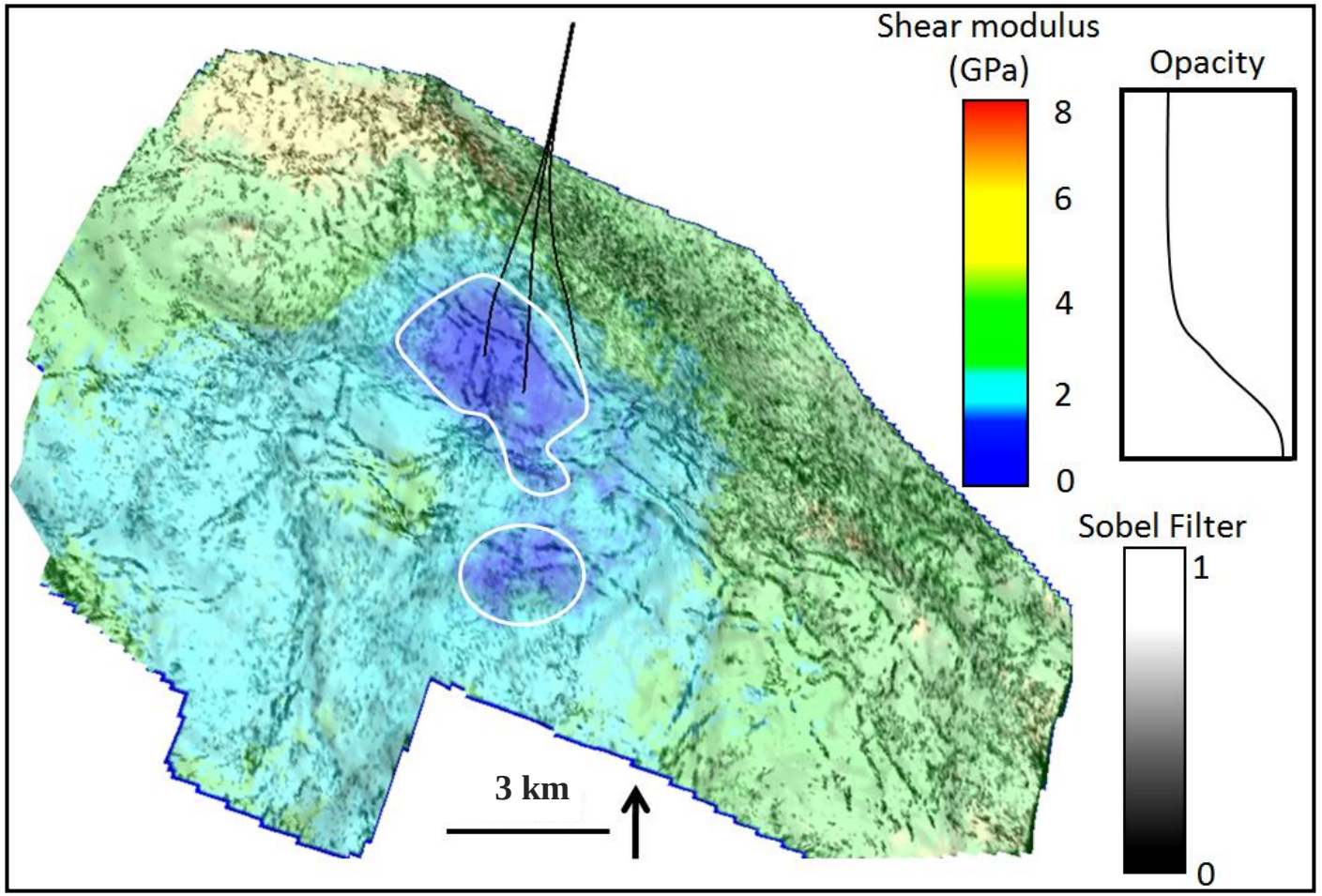

Figure 13. Shear modulus of the Sele Formation. Zones of extreme weakness are marked by white polygons. The fault network is shown in the background by an edge detection attribute, the Sobel filter.

REFERENCES

Bailey, B., F. Barclay, R. Nesbit and A. Paxton, 2010, Prospect identification using AVO inversion and lithology prediction: Petroleum Exploration Society of Australia March News letter, 22-24

Banik, N., A. Koesoemadinata and K. G. El-Kaseeh, 2010, Young's modulus from point-receiver surface seismic data: Annual internal Meeting, SEG Expanded Abstract, **29**, 2794-2798.

Carmichael, R. P., 2009, Relations between Young's modulus, compressive strength, Poisson's ratio, and time for early age concrete: Swarthmore College Department of Engineering internal report.

Colwell, M., and R. Frith, 2006, Why uniaxial compressive strength and Young's modulus are commonly poorly indicators of road roof stability-Except in the Tailgate: Underground Coal Operators' Conference, 33.

Dewhurst, D., J. Sarout, C.D. Piane, T. Siggins, M. Raven and U. Kuila, 2011, Strength Prediction and Rock Physics response in shales: 21st Annual Conference and Exhibition, Australian Society of Exploration Geophysicists.

Goodway, W., T. Chen, and J. Downton, 1997, Improved AVO fluid detection and lithology discrimination using Lamé parameters; lr, mr and l/m fluid stack from P and S inversions: Annual Meeting and Convention, CSEG Expanded Abstracts, 148-151.

Gray, F.D., 2002, Stable extraction of fundamental rock properties from seismic data: Annual International Meeting: European Association of Geologists and Engineers Conference and Exhibition, 2002.

Gray, F.D., D.P. Schmidt, and F. Delbecq, 2010, Optimize shale gas field development using stress and rock strength derived from 3D seismic data: Annual Meeting, Canadian Society for Unconventional Gas/Society of Petroleum Engineer Conference, 137316.

Hilterman, F., J.W.C. Sherwood, R. Schellhorn , B. Bankhead and B. DeVault, 1998, Identification of lithology in the Gulf of Mexico: The Leading Edge, **17**, 215-222.

McIntyre, B., T. Hibbert, D. Keir, R. Dixon, T. ORourke, F. Mohammed, A. Donald, L. Chang, A. Syed and V. Biran, 2009, Managing drilling risk in a mature North Sea Field; Annual International Meeting, Society of Petroleum Engineers Offshore Europe, 124666.

Schmid, R. and D. Schmidt, 2011, Seismic derived geomechanical properties for shale gas exploration: Annual Convention and Symposium, CSPG CSEG CWLS Expanded Abstract.

Singleton, S. and R. Keirstead, 2011, Calibration of pre-stack simultaneous impedance inversion using rock physics: The Leading Edge, **30**, 70-78.

Thomas, A.N., P.J. Walmsley, and D.A.L. Jenkins, 1974, Forties Field, North Sea: The American Association of Petroleum Geologists Bulletin, **58**, No. 3, 396-406.

Zhou, Z., F. J. Hilterman, 2010, A comparison between methods that discriminate fluid content in unconsolidated sandstone reservoirs: Geophysics, **75**, B47-58.

Acknowledgement: The authors will like to thank Apache North Sea Ltd for providing the data for this study and granting the permission to publish the results. We also thank Schlumberger and Hampson Russell for the use of their software for educational and research purposes. We are particularly grateful to Klaas Koster, Gregg Barker, Phil Rose, and Jack Orman of Apache North Sea Ltd for their tremendous support. Funding was provided by the OU Attribute Assisted Seismic Processing and Interpretation (AASPI) consortium members.

Corresponding author: amoyedo@gmail.com

CHAPTER FIVE

5.0 TIME-LAPSE (4D) GRAVIMETRY AS A RESERVOIR MONITORING TOOL: A MODELING FEASIBILITY STUDY

5.1 INTRODUCTION

Reservoir monitoring relies majorly on seismic methods and borehole measurements, there is increasing use of less-traditional techniques such as gravimetry and electromagnetics.

In this chapter I focus on the use of time lapse gravimetry as a reservoir monitoring technique. The chapter focuses on modeling gravimetry anomaly over a compacting reservoir. Furthermore, I investigate the feasibility of deployment of time-lapse gravimetry when reservoir water saturation change is significant (> 10 %).

The chapter has not been submitted yet for publication.

TIME-LAPSE (4D) GRAVIMETRY AS A RESERVOIR MONITORING TOOL: A MODELING FEASIBILITY STUDY

Sunday Amoyedo, Kurt J. Marfurt and Roger M. Slatt, The University of Oklahoma, USA

ABSTRACT

Time-lapse gravimetry continues to find increasing application in reservoir monitoring, typically in gas reservoirs and CO_2 sequestration. Little or no application to oil bearing reservoir monitoring has been reported. This is due in part to the low density contrast between oil and brine and the high acquisition cost associated with the required high density marine survey grid.

In this paper, we model the 4D gravity anomaly over Forties Field, located in the UK sector of the North Sea. The field is characterized by high porosity, poorly consolidated reservoirs, with a significant density contrast between the reservoir and the encasing shale. The Forties Field 4D gravity model results show that a significant increase in water saturation (10-15%) is required to produce a resolvable 4D gravity anomaly. We predict that time-lapse gravity anomalies can provide vital clues on reservoir compartmentalization and by-passed oil when saturation change is of the order of 10% or more. Reservoir subsidence is also observed to have a significant impact on 4D gravimetric anomaly. The models also show a decreasing resolution of compaction effects as water saturation (S_w) increases.

INTRODUCTION

The need for effective reservoir monitoring has driven the development of various techniques and tools for optimum reservoir production. Commonly adopted techniques include surface time-lapse seismic, borehole surveillance and more recently, time-lapse (4D) gravimetry. While reservoir monitoring still relies heavily on surface seismic and VSP analysis, there is an increasing use of other geophysical techniques such as gravimetry and electromagnetics, especially in the last few years. This trend is attributable to project economics, operational difficulties and project turnaround time. Relatively small gas fields are, at best, marginally economical at the current gas market, while repeatability hurdle in surface seismic also remains an eternal challenge. While certain areas of application of reservoir monitoring have no immediate economic reward, they however, still require significant investment. Such areas of application include CO_2 sequestration, monitoring subsurface breathing of volcanoes and upwelling of hot plumes, etc.). As such, techniques that are operationally less expensive and easier to implement are more attractive for such tasks. Gravimetric surveys are considered to have a wide range of applicability and relatively good cost-benefit ratio.

Recent innovations developed through collaboration between Scripps Institute of Oceanography and Statoil Research center have further advanced the use of gravimetric surveys as a reservoir monitoring tool in the marine environment. The collaboration produced the world's first remotely operated marine gravimeter (Figure 1), which has been successfully deployed in Troll and Sleipner fields, North Sea (Havard et al., 2008, Eiken et al., 2008, Zumberge et al., 2008).

Few other papers have been published on the use of a gravity anomalies for reservoir studies. Krahenbuhl et al., (2010) presented a multi-component feasibility study of the application of time-lapse gravity for CO_2 monitoring in Delhi field. Model results show a strong likelihood of imaging bulk fluid movement though expected success may decrease significantly in the thinner up-dip regions of the reservoir. Tempone and Landro (2009) describe a method for modeling 4D gravity anomaly changes for a reservoir undergoing compaction embedded in a homogenous half space with and without a rigid basement. The authors observed that compaction can account for as much as a 30-40 μGal change for a pressure depletion of 10 MPa.

Other authors have cited success in the application of time-lapse gravimetry for material balance in a depleting Troll gas field (Stenvold et al., 2008) and groundwater withdrawal in Salt Lake valley (Gettings et al., 2008).

Significant density contrast between saline water and gas (such as methane and CO_2) produces a high gravity anomaly, making gravity monitoring applicable and attractive for fluid front monitoring in gas reservoirs and CO2 sequestration. Recent advances in marine gravimeter sensitivity and improvement in repeatability to about 5 μGal (Tempone and Landro 2009; Zumberge et al., 2008) suggest that when thickness and burial are favorable, 4D gravity monitoring may be suitable for oil-water reservoir systems characterized by high porosity and a strong density contrast between the reservoir rock and the encasing shale.

In this study, we conduct a gravity monitoring feasibility study over Forties Field. The field, located in the UK sector of the North Sea, is characterized by poorly-consolidated,

high porosity reservoir rock. The density of the high-porosity, 100-200 m thick reservoir rock is significantly different than the encasing shale, which in most cases is > 150 kg/m^3 (Figure 2). Such parameters suggest 4D gravimetry may be a viable reservoir monitoring tool.

We use a cross section from a lithology indicator volume, which is derived from seismic inversion and facies classification, to model the reservoir stratigraphy in 2-D for the gravity anomaly forward modeling. We model the anomaly at constant porosity for compartmentalized and non compartmentalized reservoir units and partial drainage at different water saturation. Furthermore, we model gravity anomaly responses for a compacting reservoir while simultaneously varying the water saturation.

We observe that when water saturation change is of the order of 10% or higher, a time-lapse gravity anomaly is sufficiently large to be used in reservoir compartmentalization studies. Below this threshold, the anomaly is irresolvable at the current instrument sensitivity. Reservoir subsidence is also observed to have a significant impact on 4D gravimetric anomaly. We observe a decreasing resolution of compaction anomaly as water saturation increases.

FORWARD MODELING

A point mass of density ρ, defined by dimensions $\delta x'$, $\delta y'$, $\delta z'$ at location x' y' z' at a distance r from measurement point x, y, z, will experience a vertical gravitational attraction defined by δg_z (Figure 3). Newton's gravitational law shows that:

$$\delta g_z(x_0) = G\rho \, \frac{(z' - z)}{r^3} \, \delta x' \delta y' \delta z', \quad (1)$$

G =6.67 x 10^{-11} $m^3.kg^{-1}.s^{-2}$, defined as the gravitational constant of the earth.

Assuming that reservoir pressure has been fairly steady and no significant compaction has been recorded in the reservoir within the period of observation, we can write the observed change in gravitational attraction as

$$\delta \Delta g_z(x_0) = G\Delta\rho \, \frac{(z' - z)}{r^3} \, \delta V, \quad (2)$$

where $\Delta\rho$ is the change in density while δV is volume of the object.

For reservoir monitoring applications, we obtain the gravitational attraction by integrating over individual point masses to arrive at;

$$\delta \Delta g_z(x_0) = \sum G\Delta\rho \, \frac{(z' - z)}{r^3} \, \delta V. \quad (3)$$

Bulk density change, $\Delta\rho$ associated with fluid substitution can be written as

$$\Delta\rho = (\rho_f - \rho_{f'})\phi, \quad (4)$$

where ϕ is the porosity, ρ_f is the density of initial fluid while $\rho_{f'}$ is the density of the substituting fluid. Figure 4 shows a gradual increase in bulk density as water saturation increases for various values of porosity (ϕ).

This set of equations forms the basis for the forward modeling of gravimetric data, and assuming a perfect repeatability. While the development of remotely operated seafloor gravimeter has increased repeatability and enhanced marine gravimetry as a reservoir monitoring tool, offshore gravimetric acquisition still faces the traditional challenges encountered in a conventional gravity survey. Tidal effect, temperature variation, instrument drift etc limit the detection threshold and applicability of 4D gravimetry. With improving instrumentation and deployment, the threshold of detectability (repeatability) has improved considerably in the last few years. Fergusson et al., (2008), Zumberge et al., (2008), Tempone, et al., (2009), suggest a repeatability threshold of about 5μGal. For typical gas reservoir monitoring and CO_2 sequestration, gravity anomaly is typically well above the repeatability threshold thereby making gravimetry viable. For oil bearing reservoirs however, production induced gravity anomaly is much smaller, which makes gravity monitoring less attractive. However, a combination of poorly consolidated reservoir encased in shale with a significant density contrast between them and high porosity favor the deployment of gravimetry for production monitoring in oil bearing formations.

FIELD STRATIGRAPHY

The reservoir of the Forties Field comprises Late Paleocene submarine fan sands, mud and channel complexes. The 100 to 200 m thick Forties Sandstone can be divided into three units of roughly equal thickness. The initial fan advance is represented by the lowest unit, the Lower Main Sand, with the overlying Upper Main Sand being deposited as a fairly broad channel complex. Both units extend across the entire field and have not been further subdivided. The topmost unit, the Channel complex, which lies beneath a thick, monotonous section of gray to brown, variably calcareous and carbonaceous mudstones ranging from upper Paleocene to Holocene (Thomas et al.,1974), consists of three major sandy channel systems, the Delta/Echo, Bravo and Alpha in order of decreasing age, together with areas of inter-channel mudstone. The youngest Charlie Sand is considered a distinct unit separated from the older sands by the Charlie Shale. It lies in a different pressure compartment.

The Forties fans and channel complexes are generally very friable and characterized by excellent reservoir properties. Porosity runs as high as 35% while permeability is in the range of a few Darcys. The high recovery factor, which is in excess of 45%, bears testimony to the excellent reservoir properties of the Forties Field reservoir. A more comprehensive description of field geology and stratigraphy is given by Thomas et al., (1974) and Hill and Wood (1980). Figure 5 is a typical lithology cross section across the architectural elements of Forties Field.

Over 300 wells have been drilled in the field since the commencement of exploration and field development. While a good number of these wells have been abandoned, some have continued to produce over several years.

Forties Field cumulative production, which is supported by water injection, is in excess of 2.5 billion barrels. Reservoir pressure has been generally well maintained field-wide, though steep decreases have been recorded in the Charlie sands (Figure 6 a-b)

Reservoir production is typically associated with increase in effective stress, though the increase in stress does not necessarily lead to a significant change in porosity (Sayers, 2010). A detailed stress-porosity sensitivity analysis has been carried out in Forties Field using 8 wells. Porosity sensitivity of less than 2% is observed for a 1000 psi decrease in confining pressure (Figure 6 c). Density change due to changes in reservoir pressure is therefore considered to be minimal.

MODEL LAYOUT AND COST CONSIDERATION

Forties Field reservoir, which is oil bearing, is characterized by thickness variation ranging between 100 and 200 m. While a thicker reservoir would be preferred, the reservoir is considered to be of sufficient thickness for gravimetric monitoring of production and production effects.

A geologic cross section based on the lithology indicator cube and flattened at Sele shale representing the maximum flooding surface (MFS) was used for the gravity modeling (Figure 7). The overburden thickness of about 2128 m, is characterized by density variation from 2010 kg/m^3 just below the seafloor to 2290 kg/m^3 at the Sele Formation. The bulk density of the surrounding Forties shale is about 2330 kg/m^3 based on laboratory measurements and borehole density log readings. Saturated bulk density of the reservoir was varied between 5% and 98% water saturation.

Land-based time-lapse gravimetric survey is cost effective when compared with surface seismic and borehole surveillance. This comparative cost advantage can be diminished considerably in the offshore environment when the acquisition grid is tight, which could result in a long and expensive acquisition campaign. To enhance resolution (at the expense of acquisition cost), which is needed to detect the expected subtle anomalies due to the low contrast of density between oil and brine, we have employed a station interval of 20m. This sampling interval is significantly finer than the typical interval used in gas monitoring and CO_2 storage, which can range between 500 m and over 2000 m (Eiken et al., 2008, Zumberge et al., 2008), where the high density contrast between gas and brine gives rise to a high gravity anomaly, making a high-density acquisition

grids unnecessary. We also allow a significant aperture at the margins of the model. While being sufficiently far from the real reservoir conditions, our model has assumed a uniform porosity and by extension density and uniform drainage.

RESULTS AND DISCUSSION

In this study, we have carried out a time-lapse forward modeling of gravimetric survey of Forties Field. Figure 8 shows the sensitivity of gravity anomaly to increasing water saturation in an oil bearing reservoir. The model results show that for a 200 m thick high porosity reservoir buried at 2128 m, a water saturation increase of 15-20% is required to produce a resolvable gravity anomaly at the current instrumentation threshold of 5 μGal.

Reservoir compartmentalization, which leads to differential drainage patterns and by-passed hydrocarbons, remain the primary areas of application of reservoir monitoring. A scenario of no production from body AA (marked in Figure 9) was modeled. At low water saturation change (< 10%) in the other parts of the reservoir, the 4D gravity anomaly falls below the resolution threshold. As water saturation continues to increase(≥ 20%), we observe a relatively low gravity anomaly over the by-passed section as the anomaly grows in other sections of the reservoir. The high change in water saturation required for detection is related primarily to the small size of the body and its burial below another reservoir unit (the Charlie complex).

One of the challenges that face reservoir production is compaction. Accompanying a decrease in formation pressure is an increase in the effective stress, which could in turn lead to the onset of compaction in the reservoir and subsidence as grain to grain contact squeezing increases. We have modeled a gradual increase in reservoir subsidence and increase in water saturation in the Charlie complex, where we have a relatively higher increase in effective stress. Subsidence has been varied between 5 m and 22 m while

simultaneously increasing water saturation from 20 to 80%. Model results show a high sensitivity of 4D gravimetric anomaly to compaction and subsidence. This observation is also supported by Tempone and Landro (2009) in a model of a compacting reservoir with rigid and non-rigid basement. Our model results show that for an oil bearing reservoir, time-lapse gravity anomaly can resolve reservoir subsidence when it is greater than or equal to 5 m. This threshold is expected to reduce as overburden thickness reduces. We also observe that time-lapse gravity anomaly associated with reservoir subsidence reduces slightly as water saturation increases. Figure 10 shows a progressive decrease and flattening of the compaction anomaly with increasing water saturation.

CONCLUSION

Time-lapse (4D) gravimetry has continued to find increasing application in reservoir monitoring, typically in gas fields and CO_2 storage with little or no application yet in oil monitoring. This is due in part to the low contrast of density between oil and brine and the high acquisition cost associated with the required high density acquisition grid. This study has modeled the 4D gravity anomaly of Forties Field, located in the UK sector of the North Sea. The field is characterized by high porosity, poorly consolidated reservoirs, with a significant density contrast between the reservoir rock and encasing shale. High porosity, weakly-consolidated, homogenous and thick reservoirs characterized by shallow burial depth are considered ideal for gravimetric monitoring in oil bearing formations. Our Forties Field 4D gravity model results show that a significant increase in water saturation (10-15%) is required to produce a resolvable 4D gravity anomaly. Our model results suggest that time-lapse gravity anomaly can provide clues on reservoir compartmentalization and by-passed oil when saturation change is of the order of 10%. Reservoir subsidence is also observed to have a significant impact on 4D gravimetric anomaly. We observed a decreasing resolution of compaction anomaly as water saturation increases.

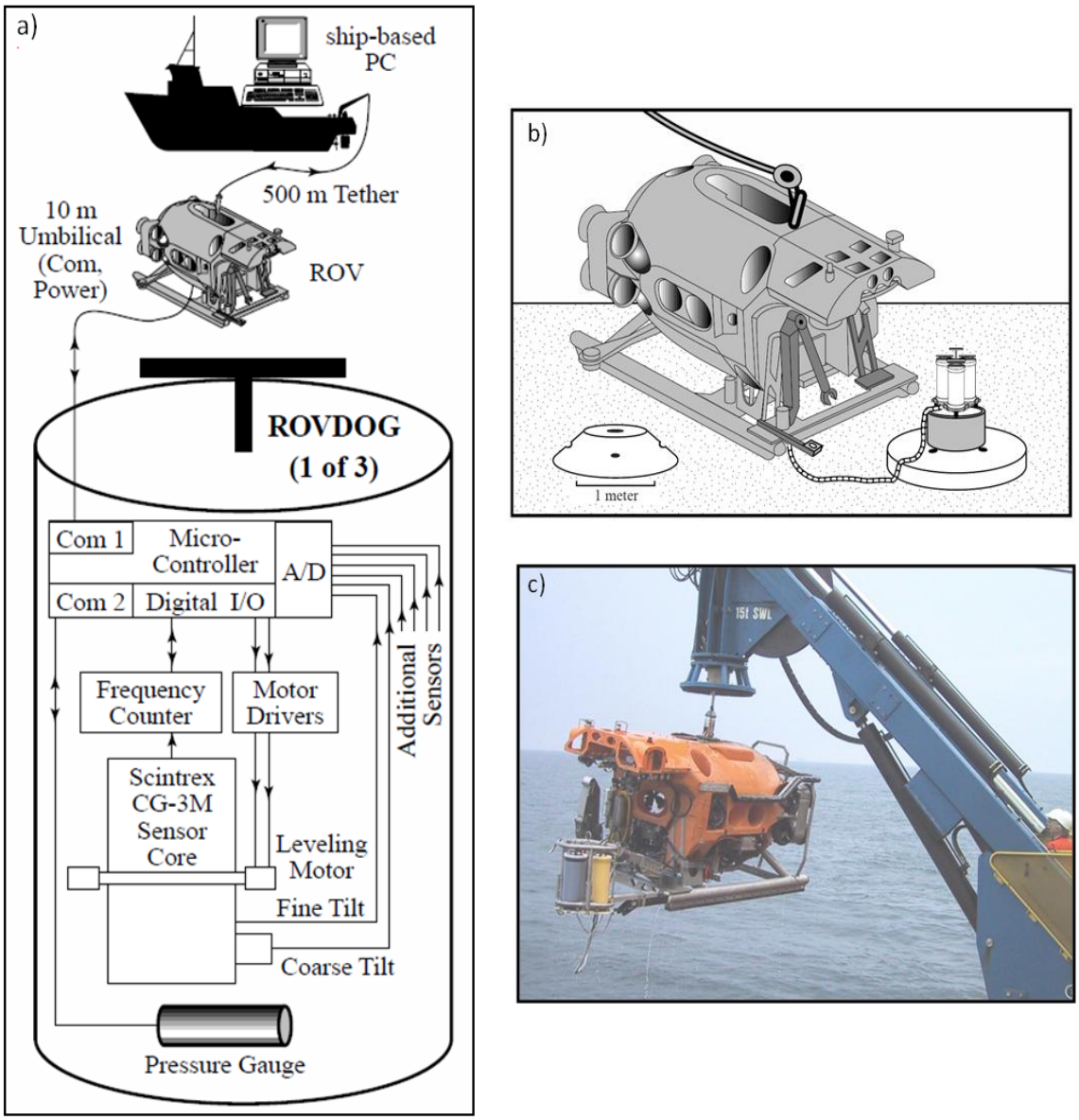

Figure 1. a) Schematic diagram of the Remotely Operated Vehicle deployed Deep Ocean Gravimeter (ROVDOG). (b) Sketch of the ROVDOG deployed at the seafloor. (c) Image of the system during recovery. (Images from: Sasagawa et al., 2003 and Zumberge et al., 2008).

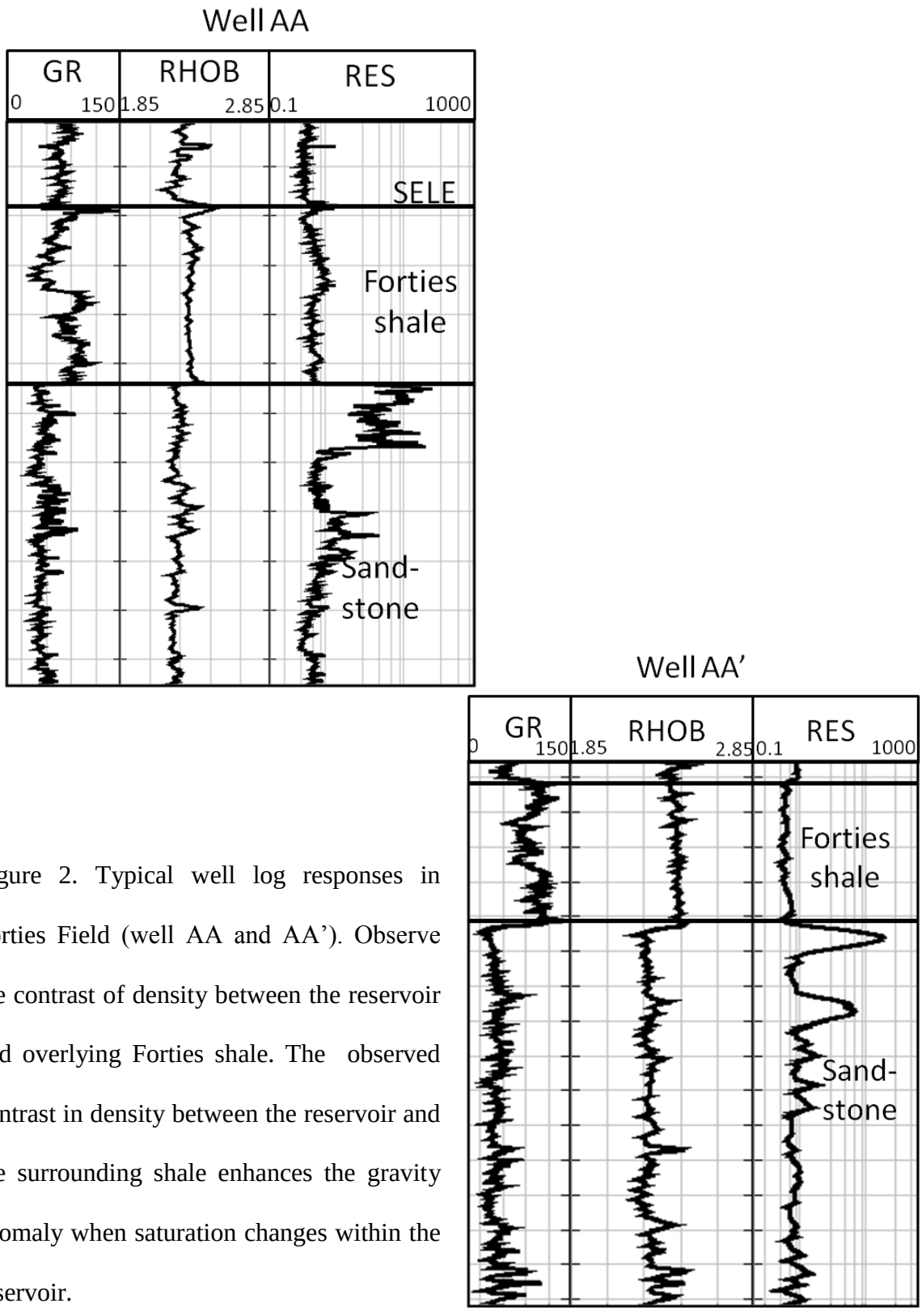

Figure 2. Typical well log responses in Forties Field (well AA and AA'). Observe the contrast of density between the reservoir and overlying Forties shale. The observed contrast in density between the reservoir and the surrounding shale enhances the gravity anomaly when saturation changes within the reservoir.

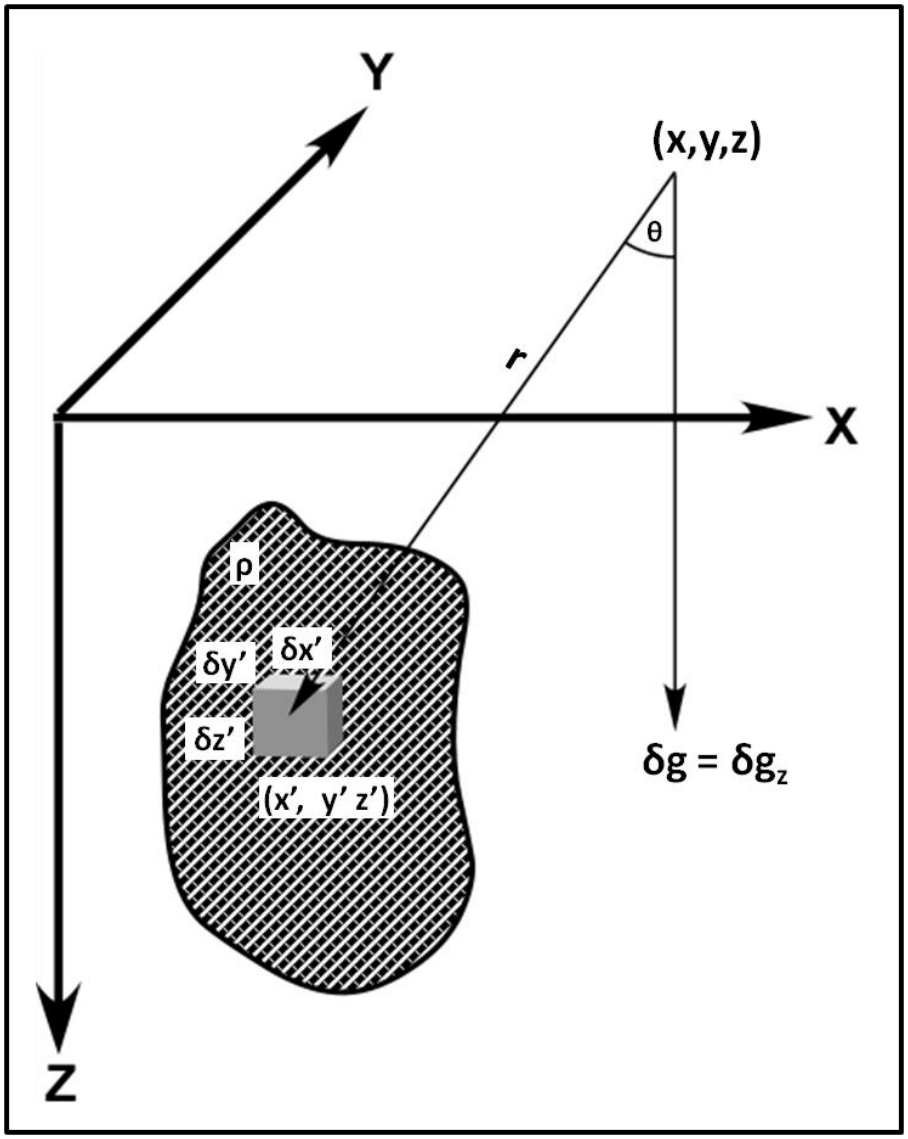

Figure 3. The vertical gravitational attraction experienced by a body is governed by Newton's gravitational second law . For reservoir monitoring purpose, we integrate the attractive force over the all point masses making up the object.

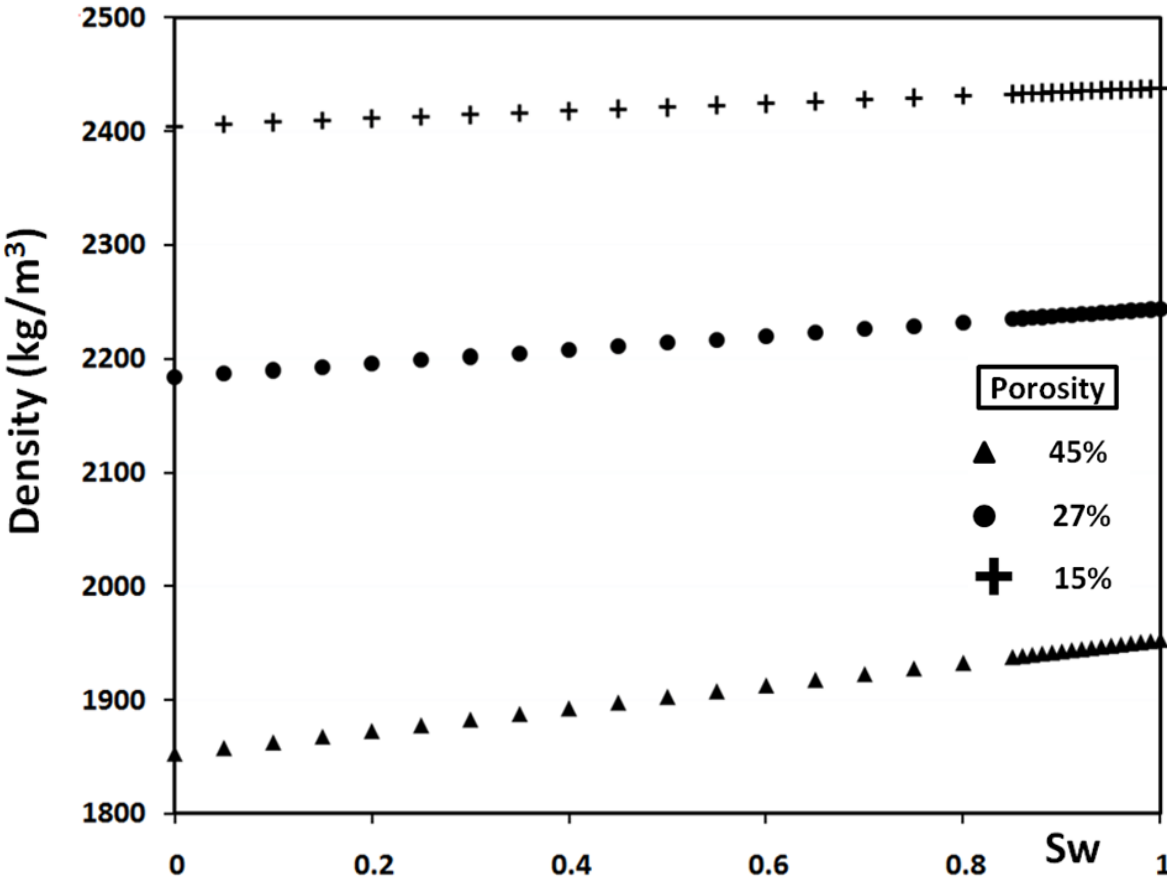

Figure 4. Bulk density increase as a function of water saturation. High porosity reservoirs produce higher changes in bulk density, which enhances gravity anomalies over the reservoir as water replaces oil.

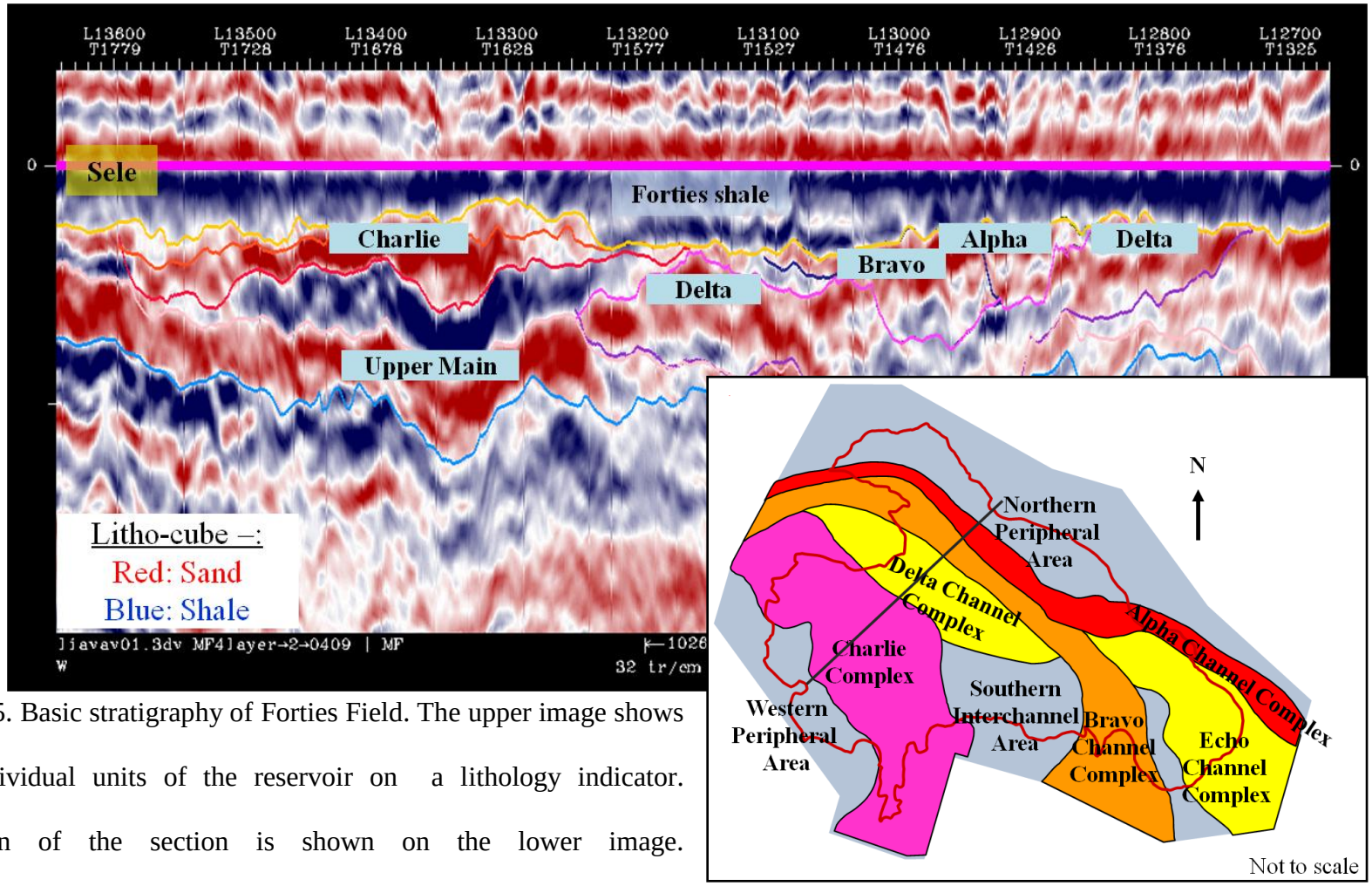

Figure 5. Basic stratigraphy of Forties Field. The upper image shows the individual units of the reservoir on a lithology indicator. Location of the section is shown on the lower image.

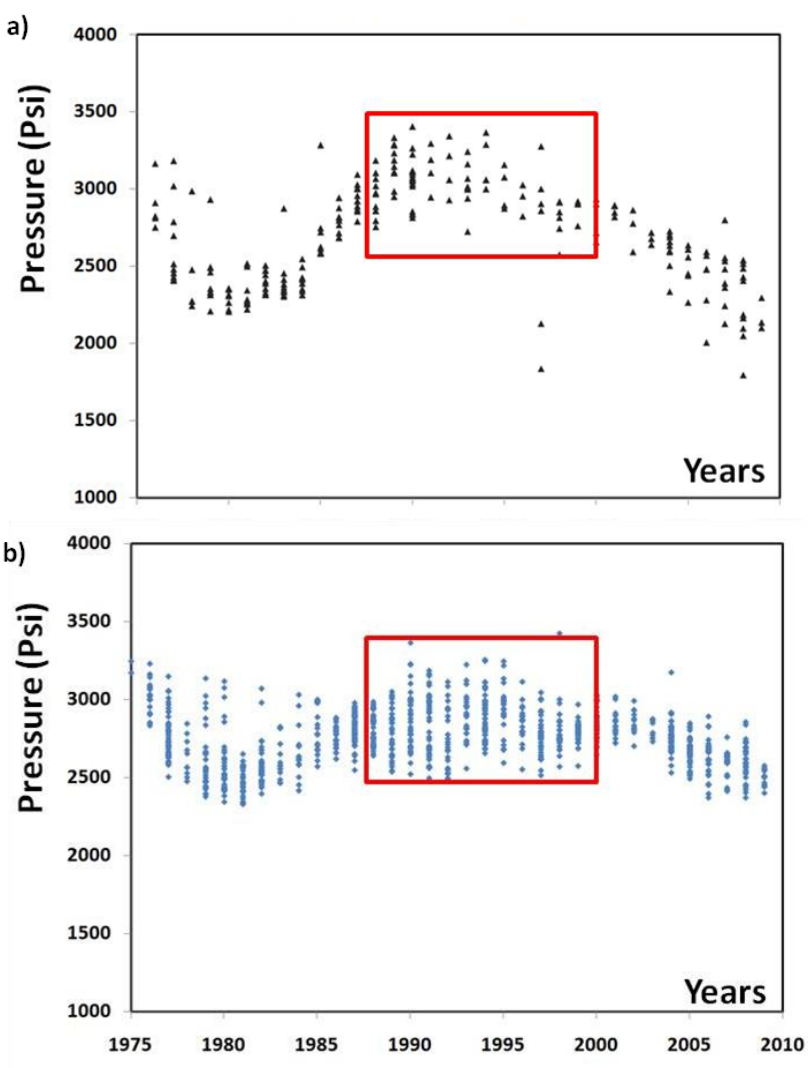

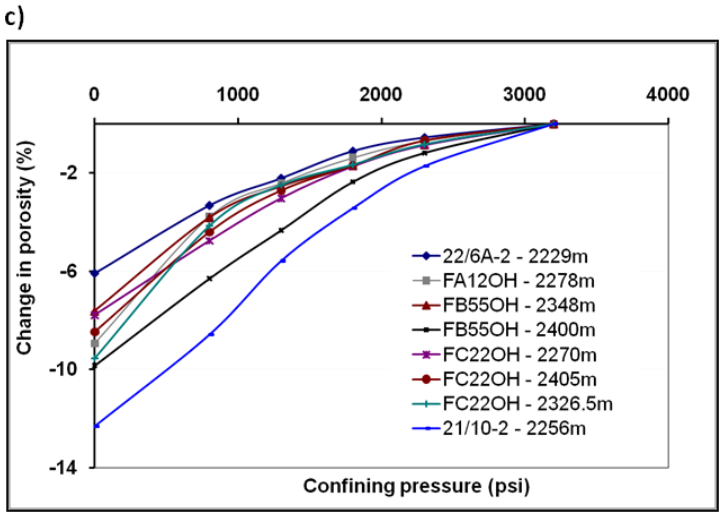

Figure 6. Forties Field pressure history, (a) for the Charlie complex and (b) the non –Charlie complexes. Observe the stronger depletion of pressure in Charlie as opposed to the near-constant pressure in non-Charlie. (c) Porosity change as a function of confining pressure. Change in porosity is assumed to be negligible in the forward modeling. Image courtesy: Apache North Sea Ltd. internal document.

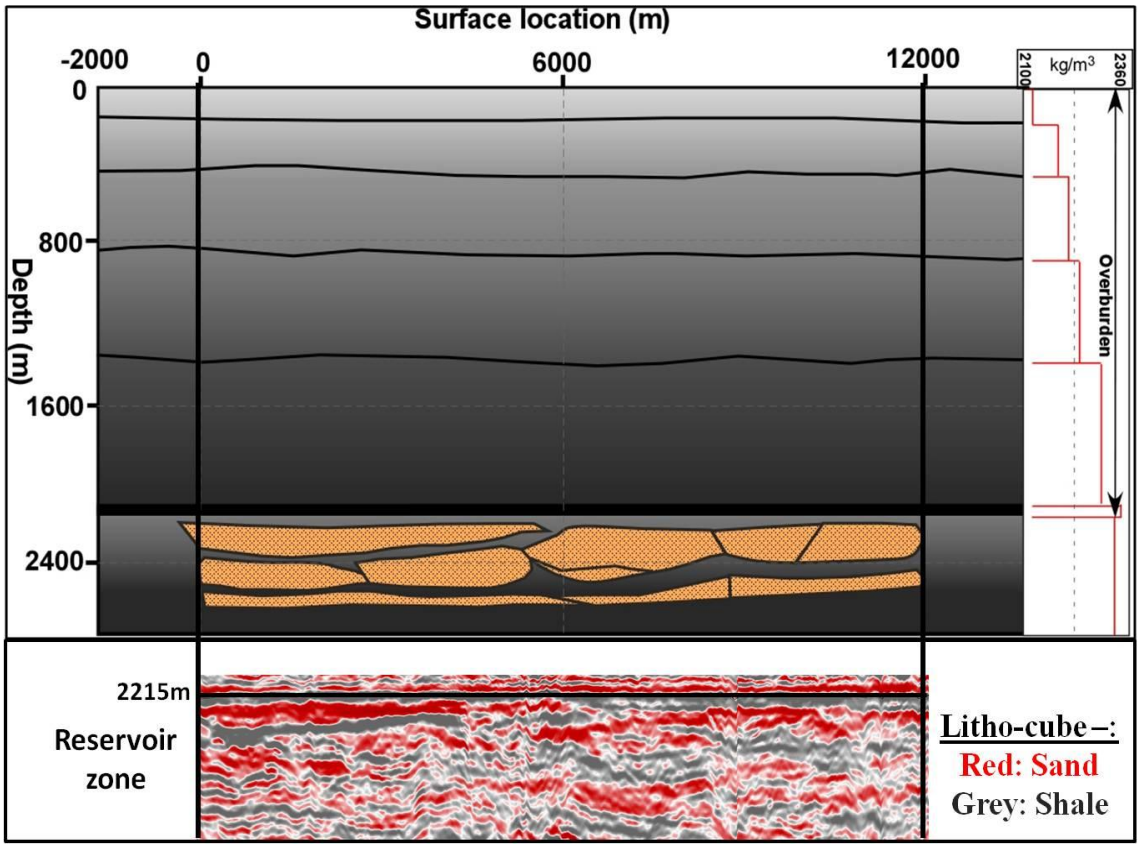

Figure 7. 2D modeling of the reservoir. Overburden density was obtained from extrapolated density logs. Lower image is a section from the lithology indicator volume that was used for the 2D modeling of the reservoir.

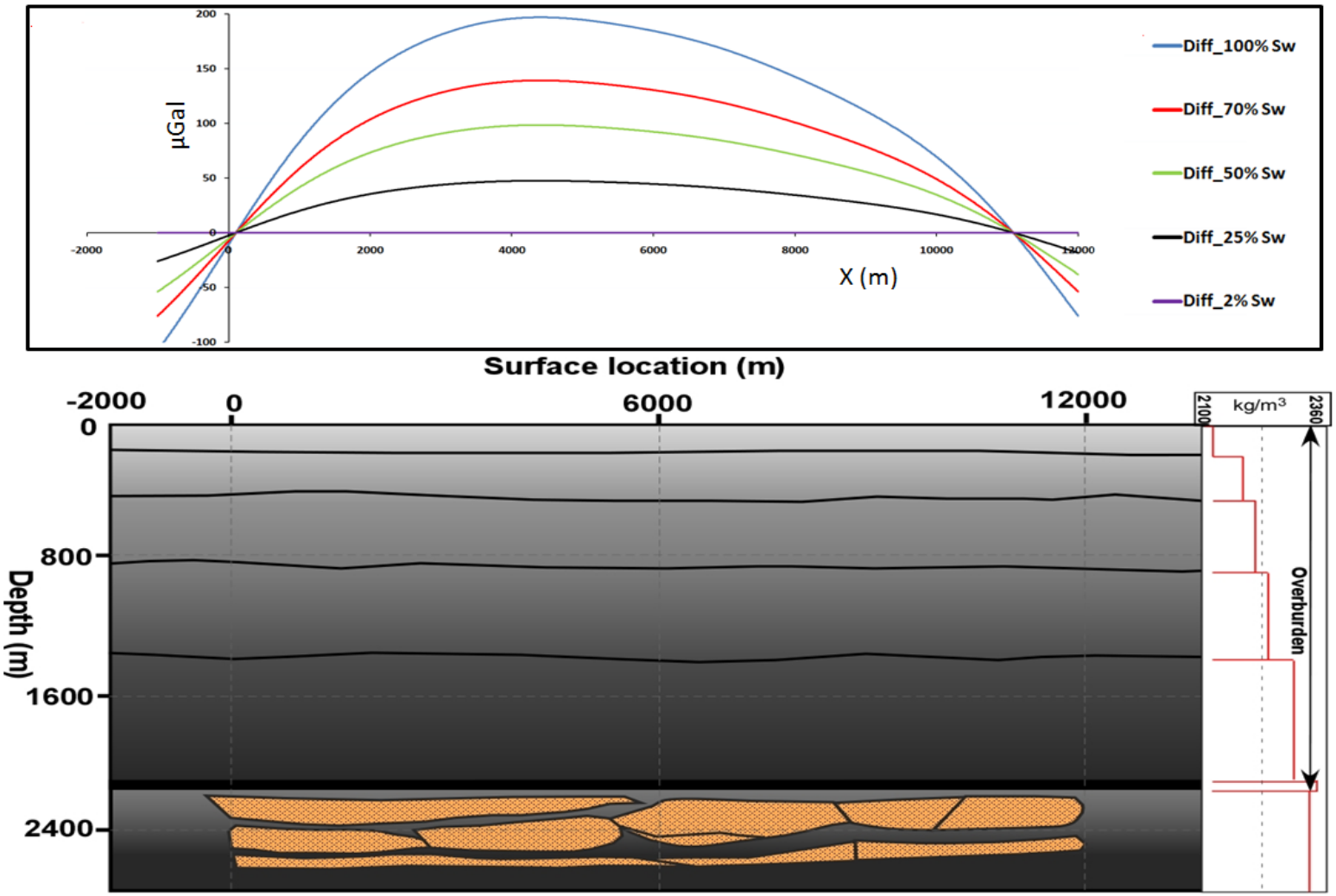

Figure 8. Gravity anomaly response over the modeled reservoir at different water saturations assuming uniform drainage.

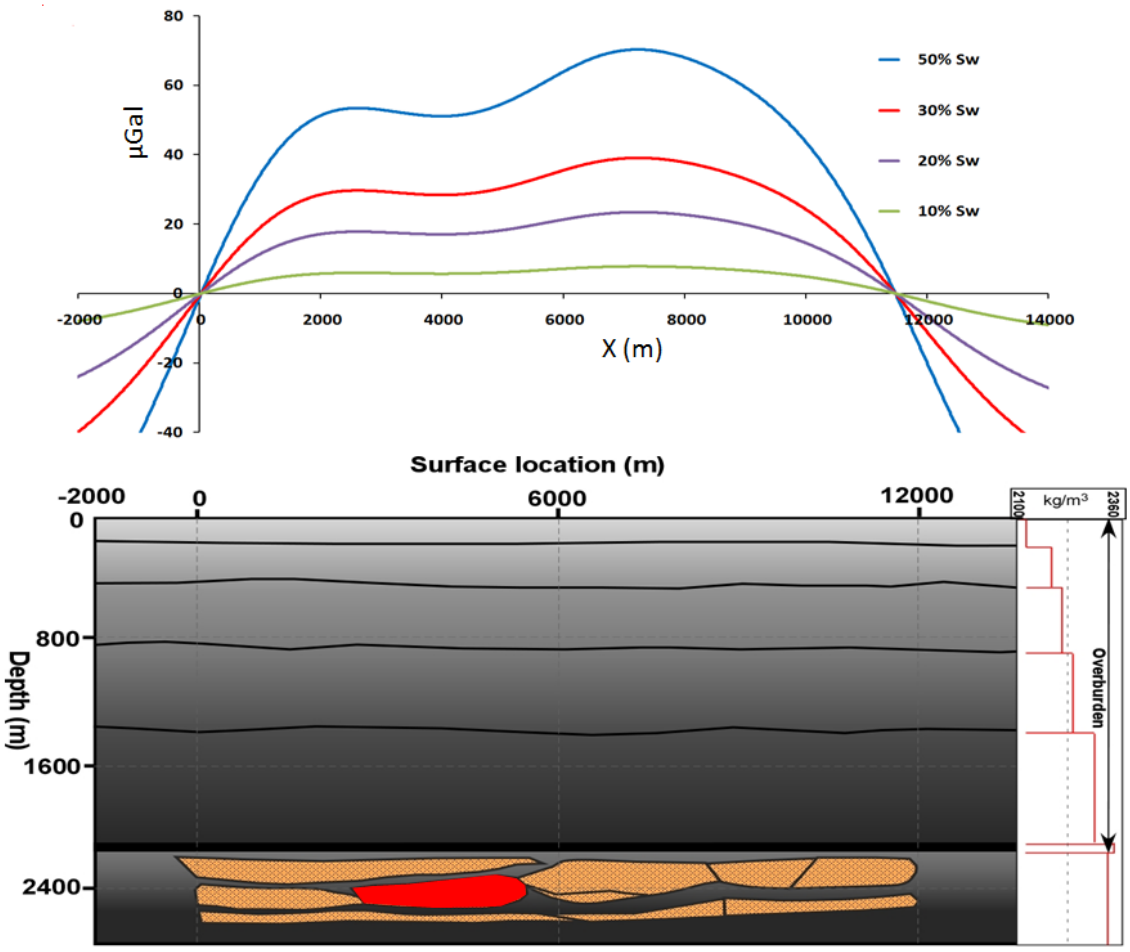

Figure 9. Gravity anomaly response over a by-passed unit of the reservoir (in red) lying below the Charlie complex. Observed that detection threshold in the gravity anomaly lies between 10 and 20 % water saturation in adjacent reservoir units.

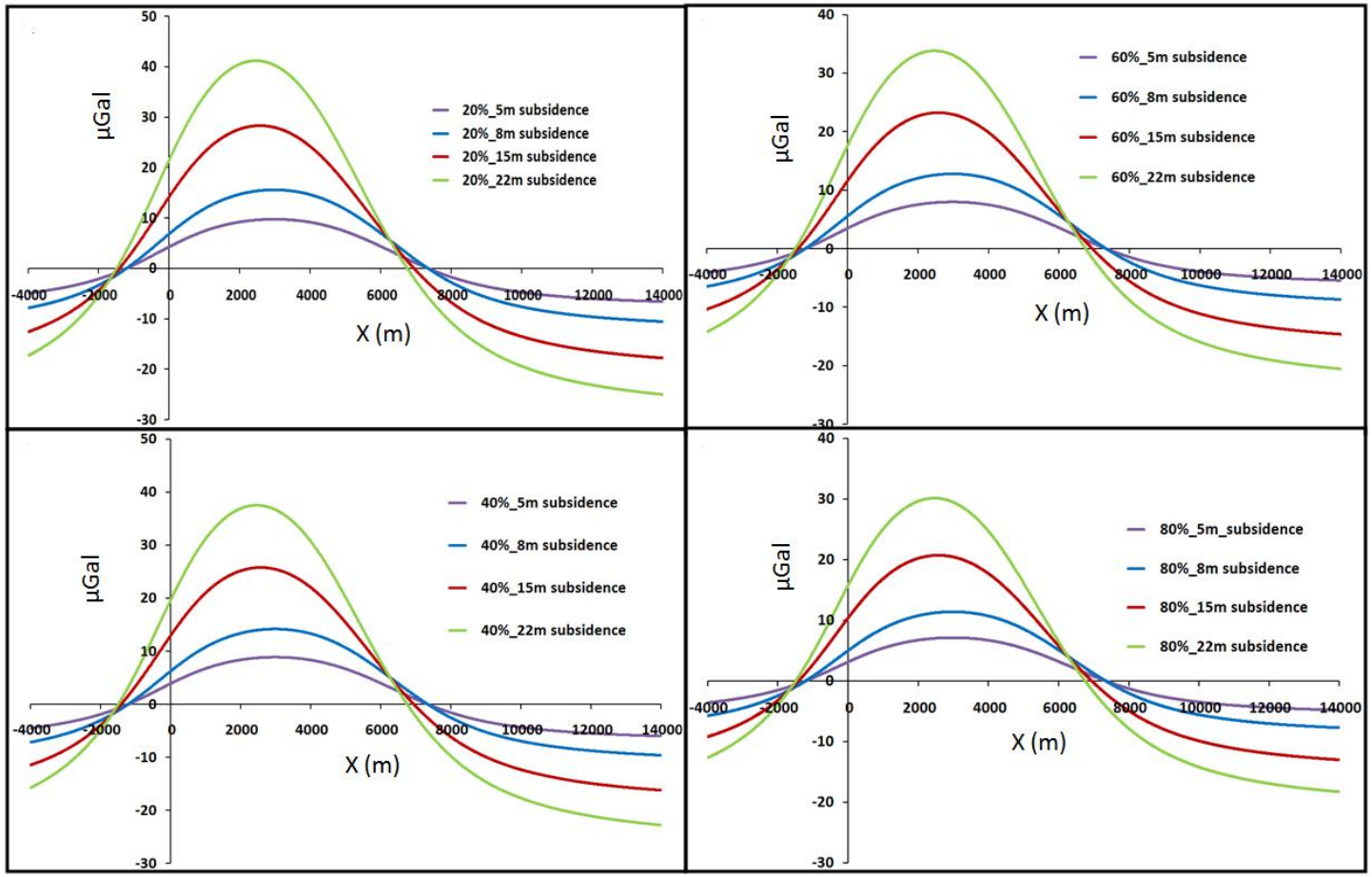

Figure 10. Gravity anomaly (Net) response over a compacting reservoir unit (Charlie complex) at various values of water saturation. We varied subsidence between 5 m and 22 m. Observe that a compaction threshold of 5m is required for detection. The water saturation in the compacting zone is the same as other units in the field.

REFERENCES

Eiken, O., T. Stenvold, M. Zumberge, H. Alnes, and G. Sasagawa, 2008, Gravimetric monitoring of gas production from the Troll field: Geophysics, **73**, WA 149- 154.

Ferguson, J. F., F. J. Klopping, T. Chen, J. E. Seibert, J. L. Hare, and J. L. Brady, 2008, The 4D microgravity method for waterflood surveillance: Part 3—4D absolute microgravity surveys at Prudhoe Bay, Alaska: Geophysics, **73**, WA163-171.

Gettings, P., D.S. Chapman, and R. Allis, 2008, Techniques, analysis and noise in a Salt Lake Valley 4D gravity experiment: Geophysics, **73**, WA 71-81.

Havard, A., O. Eiken and T. Stenvold, 2008, Monitoring gas production and CO2 injection at the Sleipner field using time-lapse gravimetry: Geophysics, **73**, WA 155-161.

Krahenbuhl, R. A, Y. Li, and T. Davis, 2010, 4D gravity monitoring of fluid movement at Delhi Field, LA: A feasibility study with seismic and well data: Annual International Meeting, SEG Expanded Abstract, **29**, 4210-4214.

Sayers, C.M., 2010, Geophysics under stress: Geomechanical applications of seismic and Borehole acoustic waves: 2010 Distinguished Instructor Series, No. **13**, 50-51.

Tempone, P. and M. Landro, 2009, Estimation of changes in gravity anomaly due to a compacting reservoir: Annual International Meeting, SEG Expanded Abstract, **28**, 3790-3794.

Sasagawa, G. S, W. Crawford, O. Eiken, S. Nooner, T. Stenvold and M. A. Zumberge, 2003, A new sea-floor gravimeter: Geophysics, **68**, 544-553.

Stenvold, T., O. Eiken and M. Landro, 2008, Gravimetric monitoring of gas-reservoir water influx- A combined flow- and gravity-modeling approach: Geophysics, **73**, WA 123-WA 131.

Zumberge, M., H. Aines, O. Eiken G. Sasagawa and T. Stenvold, 2008, Precision of seafloor gravity and pressure measurements for monitoring: Geophysics, **73**, WA 133-141.

CHAPTER SIX

6.0 CONCLUSIONS AND RECOMMENDATIONS

6.1 GENERAL CONCLUSION

Sand production remains a source of concern in both conventional and heavy oil production. Factors such as reservoir consolidation, well deviation angle through the reservoir, perforation size, depth of penetration of perforation, grain size, capillary forces associated with water-cut, flow rate and more importantly reservoir strain resulting from pore pressure depletion contribute to reservoir sanding. Understanding field-specific sand production patterns in mature fields and poorly consolidated reservoirs is vital in guiding remedial activities and identifying sand-prone wells.

The Forties Field, located in the UK sector of the North Sea, seismic study using 1988 and 2000 seismic surveys reveals an increased stress associated with pore pressure changes in the Charlie complex. The high time lag in the overburden shale above the Charlie sandstone suggests a significant increase in the reservoir stress. Reservoir strain analysis shows that the magnitude of the production-induced strain, part of which is propagated to the base of the reservoir, is of the order of 0.2%, which is significant enough to impact the geomechanical properties of the reservoir. We observe a correlation between sand production and time-lapse effect. Results of sand production analysis in Forties Field shows that in addition to poor reservoir consolidation, high well angle of deviation through the reservoir and high flow rate (which are the well known factors) reservoir strain due to pore pressure depletion, contributes significantly to sand production. For poorly consolidated reservoirs, maintaining reservoir pressure at

or close to initial condition does not only help sustain hydrocarbon production, it also serves as a sand production management tool.

Knowledge of reservoir saturation variation is vital for in-fill well drilling, while reservoir stress variation provides a useful guide for sand production management, casing design, injector placement and production management. We show that the reservoir response to increase in stress and our ability to effectively use time-lapse seismic as a reservoir pressure monitoring tool derive from rock sensitivity to water saturation and pressure changes. Time-lapse (4D) differences inverted for saturation and pressure effects, and calibrated by well and production data, provides an additional tool for reservoir pressure monitoring. We propose an amendment to the use of AVO attributes to account for the effect of porosity change. This is particularly important in highly compacting carbonate reservoirs.

While instability and subsequent failure of the overburden in many mature fields can be linked to the rapid decrease of the (unconfined compressive strength) UCS at certain inclination angle to the bedding plane, however, some zones might be characterized by extreme weakness irrespective of the inclination of the wellbore. Good correlation between laboratory-measured UCS and incompressibility (Young's Modulus). Elastic moduli (Young's and Shear moduli) from model-based simultaneous inversion, calibrated to laboratory measurements, help characterize zones of extreme weakness. These zones are susceptible to collapse during drilling irrespective of the well deviation angle through the overburden.

Time-lapse (4D) gravimetry has continued to find increasing application in reservoir monitoring, typically in gas fields and CO2 storage with little or no application yet in oil monitoring. High porosity, weakly-consolidated, homogenous and thick reservoirs characterized by shallow burial depth are considered ideal for gravimetric monitoring in oil bearing formations. Taking a field example from Forties Field 4D gravity model results, we show that a significant increase in water saturation (10-15%) is required to produce a resolvable 4D gravity anomaly. Our model results suggest that time-lapse gravity anomaly can provide clues on reservoir compartmentalization and by-passed oil when saturation change is of the order of 10%. Reservoir subsidence is also observed to have a significant impact on 4D gravimetric anomaly. We observed a decreasing resolution of compaction anomaly as water saturation increases.

6.2 RECOMMENDATIONS

Insufficient field record of sand production is a major setback for an effective sand analysis. Records of sand produced are at best insufficient, where they even exist. Understanding field-specific sand production patterns will require a good record of sand production for each well, which most operators don't keep at the moment. Putting in place a robust and up-to-date database of weekly or monthly sand production will be of great benefit. This will guide sand management efforts, especially in mature reservoirs.

Inverting for pressure and saturation from seismic is still an evolving science. Most currently adopted algorithms and workflows cannot account for the effect of porosity change in time-lapse difference, which could be dominant in carbonate and poorly consolidated reservoirs. Active study to further enhance existing tools for inverting changes in saturation and pressure as well as porosity is required.

Most geomechanical studies have focused principally on the reservoir zone(s) with very little known about the physics of the overburden rock. This lack of attention to the overburden has resulted in a knowledge gap between the reservoir and non-reservoir. While rock physics driven- simultaneous inversion of long offset seismic data will provide some measure of elastic geomechanical properties of overburden rock, there still exists the need for calibration through laboratory measurements. Reducing the knowledge gap between the reservoir and overburden is vital to efficient reservoir development.